Dissecting the cellular and molecular mechanisms of leukaemia cell migration to and localization within the testis in childhood ALL

DISSERTATION

zur Erlangung des akademischen Grades
doctor rerum naturalium
(Dr. rer. nat.)

im Fach Biologie
eingereicht an der

Lebenswissenschaftlichen Fakultät
der Humboldt-Universität zu Berlin
von
M.Sc. Tessa Skroblyn

Präsidentin der Humboldt-Universität zu Berlin
Prof. Dr.-Ing. Dr. Sabine Kunst

Dekan der Lebenswissenschaftlichen Fakultät
Prof. Dr. Dr. Christian Ulrichs

Gutachter/innen:
1. Prof. Dr. Ana Pombo
2. Prof. Dr. Johannes Schulte
3. PD Dr. Uta E. Höpken

Datum der Abgabe im Prüfungsamt: 21.05.2021
Tag der mündlichen Prüfung: 27.10.2021

Table of contents

I. Abbreviations

°C	Degree celsius
7-AAD	7-amino-actinomycin D
A --	
AF	Alexa Fluor
ALL	Acute lymphoblastic leukemia
AML	Acute myeloid leukemia
APC	Allophycocyanin
APC-Cy	Allophycocyanin/cyanin
Arg1	Arginine 1
B --	
BCP	B-cell precursor
BM	Bone marrow
BSA	Bovine serum albumin
BTB	Blood-testis-barrier
C --	
CAF	Cancer-associated fibroblasts
CCL	CC-chemokine ligand
CCR	CC-chemokine receptor
CD	Cluster of differentiation
cDNA	Complementary deoxyribonucleic acid
CM	Conditioned medium
CNS	Central nervous system
CRISPR	Clustered regularly interspaced short palindromic repeats
Ct	Cycle threshold
CXCL	CXC-chemokine ligand
CXCR	CXC-chemokine receptor
D --	
DLBCL	Diffuse large B-cell lymphoma
DMEM	Dulbecco’s Modified Eagle’s Medium
DMSO	Dimethyl sulfoxide
DNA	Deoxyribonucleic acid
E --	
E. coli	*Escherichia coli*
EFS	Event-free-survival

Et al.	Et alii
F --	
FACS	Fluorescence-activated cell sorting
FCS	Fetal calf serum
FITC	Fluorescein isothiocyanate
FSC	Forward Scatter
G --	
GFP	Green florescent protein
GOI	Gene of interest
H --	
HCl	Hydrogen chloride
HEPES	4-(2-Hydroxyethyl)-piperazin-1-ethan-sulfonic acid
I--	
i.p.	Intraperitoneal
i.v.	Intravenously
Ig	Immunoglobin
IL	Interleukine
IL7R	Interleukine 7 receptor
IMDM	Iscove's Modified Dulbecco's Media
INF-g	Interferon gamma
IVIS	*In vivo* imaging system
K --	
KO	Knock-out
M --	
M-CSF	Macrophage-colony stimulating factor
M-CSFR	Macrophage-colony stimulating factor receptor
MACS	Magnetic-activated cell sorting
MFI	Mean fluorescence intensities
MHC	Major histocompatibility complex
MM	Multiple myeloma
Mmp9	Matrix metallopeptidase 9
MNCs	Mono nuclear cells
mRNA	Messenger RNA
MSC	Mesenchymal stem cell
N--	
NOD	Non-Obese Diabetic

ns	Not significant
NSG	NOD.Cg-Prkdcscid Il2rg tm1 Wjl/SzJ
O --	
OD	Optical density
P --	
P-Value	Probability-value
P/S	Penicillin-Streptomycin
PE	Phycoerythrin
PB	Pacific Blue
PBS	Phosphate buffered saline
PDX	Patient-derived xenograft
PE-Cy7	Phycoerythrin-cyanin
PerCP-Cy5.5	Peridinin chlorophyll protein complex/cyanin
PFA	Paraformaldehyde
pH	Potential of hydrogen
Ph	Philadelphia chromosom
PModS	Peritubular factor that modulates Sertoli cell function
PTC	Peritubular myoid cells
Puro	Puromycin
Q--	
qRT-PCR	Quantitative Real Time Polymerase Chain Reaction
R--	
RNA	Ribonucleic acid
rpm	Rounds per minute
RPMI 1640	1640 Roswell Park Memorial Institute
RT	Room temperature
S --	
SCID	Severe combined immunodeficiency
SD	Standard deviation
SEM	Standard error of the mean
sgRNA	Single guide ribonucleic acid
SMA	Smooth muscle actin
SSC	Side scatter
T--	
TAM	Tumour-associated macrophages
TGCT	Testicular germ cell tumour

TGF	Tumour growth factor
tMφ	Testicular macrophages
TME	Tumour microenvironment
Tris	Tris(hydroxymethyl)aminomethane
Tween 20	Polysorbate 20

II. Tables

III. Figures

IV. Zusammenfassung

Die pädiatrische Akute Lymphatische Leukämie ist heutzutage sehr gut behandelbar. Trotzdem ist die Prognose im Falle eines Rezidives nach wie vor schlecht. Isolierte und kombinierte Knochenmarkrezidive stellen 70% aller pädiatrischen ALL Rezidive und sind schwer zu behandeln. Die häufigsten extramedullären Orte für Rezidive sind das zentrale Nervensystem und der Hoden. Um ein Rezidiv im Hoden zu verhindern, ist es nötig die zellulären und molekularen Vorgänge, welche für die Infiltration und für das Überleben der Zellen eine Rolle spielen, zu verstehen. Dafür wurde Patientenmaterial hinsichtlich seiner Expression bestimmter Oberflächenmolekülen analysiert. Verglichen wurden Proben von Patienten mit verschiedenen Rezidiv-Arten. Um die funktionellen Aspekte der Hodenphysiologie auf die Leukämiezellmigration und -lokalisation zu untersuchen wurde ein PDX-ALL Mausmodel mit Hodenbeteiligung etabliert. Um potenziell involvierte Chemokin-Chemokinrezeptor-Achsen zu identifizieren, wurden 55 Knochenmarksproben von Patienten untersucht. Die Expressionsmuster der Rezeptoren wurde mittels Durchflusszytometrie analysiert. Dabei wurde festgestellt, dass CXCR4 meistens sehr hoch exprimiert wird, unabhängig vom Rezidiv-Typ. Deshalb wurde anschließend der Einfluss der CXCR4-CXCL12 Achse in *in vitro* Versuchen mit Hilfe primären Hodenstromas untersucht. Um den Einfluss bestimmter Hodenzellsubpopulationen zu untersuchen, wurde die Isolation von Hodenmakrophagen, Sertoli Zellen und Peritubulären Zellen aus der Maus etabliert und ihr Einfluss auf ALL Zellen untersucht. Dabei wurde festgestellt, dass Hodenmakrophagen bei Tumorkontakt ihren Phänotyp zugunsten einer tumorfördernden Subpopulation verändern. Zu guter Letzt wurde ein adaptives PDX-ALL Mausmodel mit Hodenbeteiligung entwickelt. Dabei wurden die Hoden von vorpubertären Mäusen bevorzugt infiltriert. Die Bedeutung der CXCR4-CXCL12 Achse für die Hodeninfiltration wurde in einem *in vivo* Versuch validiert. Während Knochenmark und Milz nach einer anti-CXCR4 Gabe kleine ALL Populationen aufwiesen, war der Hoden komplett Tumor-frei. Das Mausmodel kann für Versuche genutzt werden, um weitere Signalwege zu identifizieren, welche in die Hoden gerichtete Migration und das Überleben der Zellen involviert sind. Ein erster Schritt sind Einzelzellsequenzierungen von Tumor infiltrierten Mäusehodenmaterials, welche momentan durchgeführt werden. Auffällige Signalachsen können mit diesem adaptiven Model validiert werden, um potentielle Angriffspunkte für zukünftige Therapien zu identifizieren.

V. Abstract

Advancing therapy strategies led to event-free-survival increase of paediatric acute lymphoblastic leukaemia (ALL). Relapses that occur despite efficient treatment are often drug resistant and come with poor prognosis. Isolated and combined bone marrow (BM) relapses account for 70% of all relapse cases and are difficult to treat. Extramedullary sites for relapse are the central nervous system (CNS) and the testis. To prevent testicular relapse, the molecular and cellular factors responsible for the infiltration and survival need to be discovered. Therefore, primary patient material was analysed with regard to differential expression of molecules relevant for adhesion, proliferation and survival on leukemic cells from BM. Secondly, to analyse functional aspects of testis physiology on leukemic cell migration and localisation an adoptive PDX-ALL mouse model with testicular involvement was established. To identify potential chemokine-chemokine receptor axes responsible for the leukaemia cell migration towards the testis, a characterization of 55 patient BM samples was performed. The expression pattern of chemokine receptors on BM derived leukaemia cells of patients with combined testis and CNS relapse as well as patients with isolated BM relapses were compared by flow cytometry. In this process CXCR4 was identified to be highly expressed on patients cells, regardless of the subclass of relapse. Subsequently, relevance of the CXCR4-CXCL12 axis was intensively studied *in vitro*. Therefore, primary testicular stroma cultures were available, which provided a useful tool to examine testis directed migration. To study the impact of certain testis cell subpopulations, isolation of testicular macrophages, Sertoli cells and peritubular cells was established and their impact on ALL cell survival was analysed. The macrophages were found to alter their phenotype upon ALL cell contact towards a tumour favourable subtype. Most importantly, a murine adoptive patient-derived xenograft (PDX)-ALL cell transfer model with testicular involvement was established. Testes of pre-puberty mice were preferentially infiltrated, which reflects clinical observations. Blocking CXCR4 with an antibody validated relevance of the CXCR4-CXCL12 signalling axis. While BM and spleen were still infiltrated by PDX-ALL cells the testis showed no infiltration in anti-CXCR4 treated animals. The mouse model will be useful to identify and validate further signalling pathways, participating in testis directed migration and survival. A first step in finding new pathways are ongoing single cell analyses of tumour infiltrated mouse testis material. Signalling axes can be validated with this novel adoptive PDX-ALL mouse model to reveal possible targets for future therapies.

1. Introduction

Leukaemia is the most prevalent type of malignancy in children, accounting for 30% of cancers in patients aged 0-18 years[1]. There are two main subtypes of leukaemia in childhood; acute myeloid leukaemia (AML) and acute lymphoblastic leukaemia (ALL)[2]. AML accounts for about 18% of paediatric leukaemia cases[3] and develops through a mutation in the myeloid lineage of progenitor cells **(Figure 1)**. These mutations lead to an increase of defective myeloid progenitor cells and to a decrease of mature blood cells, like platelets, erythrocytes, granulocytes and monocytes[4].

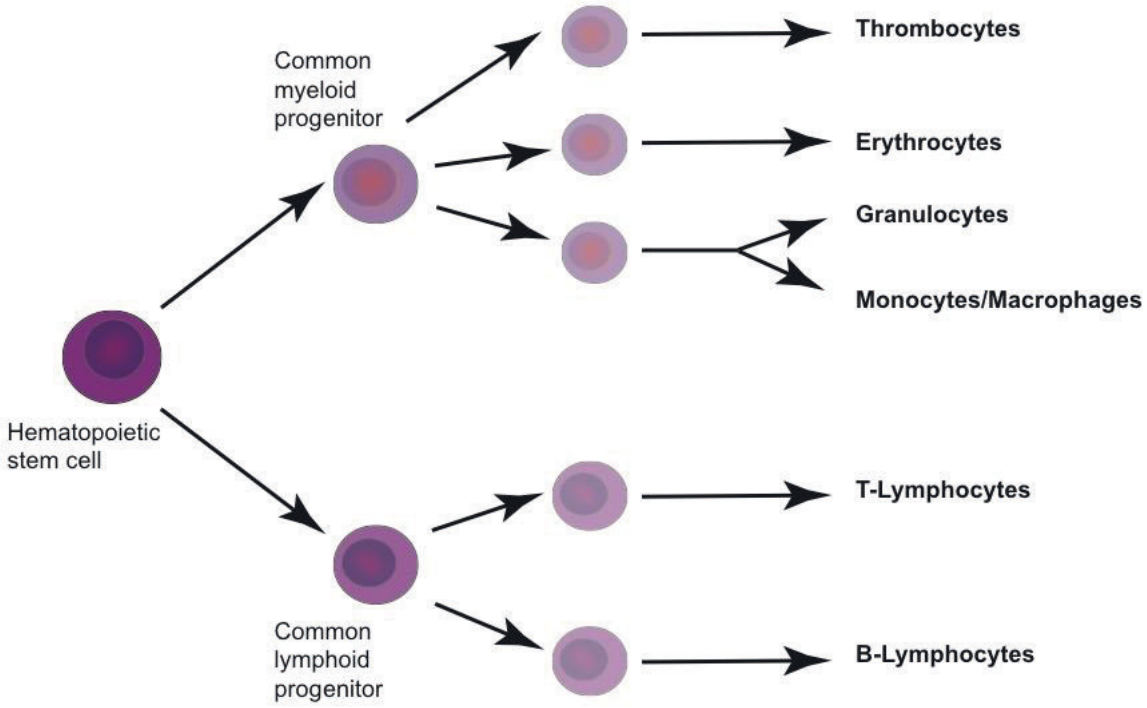

Figure 1: Development of the hematopoietic system. All mature cells from the different hematopoietic lineages develop from a common stem cell. This pluripotent cell divides and generates myeloid and lymphoid progenitors that differentiate further to mature hematopoietic cells, such as erythrocytes, granulocytes or T- and B-lymphocytes.

However the most common type of childhood cancer is ALL, responsible for approximately 80% of all childhood leukaemia cases[5]. Based on the immunophenotype ALL can be distinguished in B cell precursor (BCP) and T-cell ALL, but with up to 80 % BCP-ALL is by far the main type in paediatrics[6]. Both types are derived from mutations in the lymphoid lineage **(Figure 1)**, which leads, as in AML, to a decrease of mature hematopoietic cells[7]. This thesis focuses mainly on paediatric BCP-ALL.

1.1 Paediatric acute lymphoblastic leukaemia

1.1.1 Epidemiology and Symptoms

ALL is at about 80% the most common type of leukaemia during childhood and adolescence. The German Childhood Cancer Registry records 500 newly diagnosed cases in children less than 15 years per year in Germany. ALL can be observed in people of all ages, however most cases occur during childhood[8]. More than 60% of ALL patients are children and the incidence is highest between the age of 2-5 years[5,9]. Studies in the United States also found variations between ethnicities; Hispanic children have the highest incidence, while Afro-American children are least affected[3].

Symptoms of ALL and other leukaemia subtypes are not very specific. They usually develop quickly within a few weeks and are caused by an increase of malignant cells in the bone marrow (BM) and infiltration of other organs. ALL cells suppress the production of functional hematopoietic cells and many symptoms are caused by the resulting lack of these mature cells[8]. In total more than 90 clinical signs are described in children diagnosed with leukaemia. Frequent observed symptoms are hepatomegaly, splenomegaly, pallor, fever and infections. But also bruising, bleeding tendency and bone and/or joint pain are common[10].

1.1.2 Genetic of ALL

Paediatric ALL is classified in either precursor B-cell or T-cell subgroups, depending on the expression of certain lineage markers on the cell surface or intracellular in the cytoplasm. A special case is a malignancy of mature B-cells, a so-called Burkitt's lymphoma or leukaemia. Mutations that trigger ALL development often occur in genes relevant for normal leukemogenesis. This leads to a notable differentiation of B- or T-cells and therefore to a lack of mature functional leukocytes[11].

ALL is not caused by a single gene modification but can be triggered by many different genetic alterations, such as aneuploidy, chromosomal rearrangements (e.g. fusion genes), copy number alterations (deletions, amplifications) or sequence mutations[11,12]. Paediatric ALL genomes contain only few mutations at the time of initial diagnosis but the number increases at the time of relapse[13]. Some genetic alterations are already detectable in neonatal blood and entail a predisposition but only a second mutation will lead to a clinical manifestation of ALL **(Figure 2A)**[11,14]. Chromosomal translocations play a crucial role in ALL development. Translocations can either lead to the relocation of oncogenes in regulatory regions of other genes or they cause fusion genes. These chimeric genes encode for proteins that show functions of both proteins they are derived from[11]. *ETV6-RUNX1* is, with

25%, one of the most common fusion genes in paediatric BCP-ALL. This translocation is associated with testicular relapses[15].

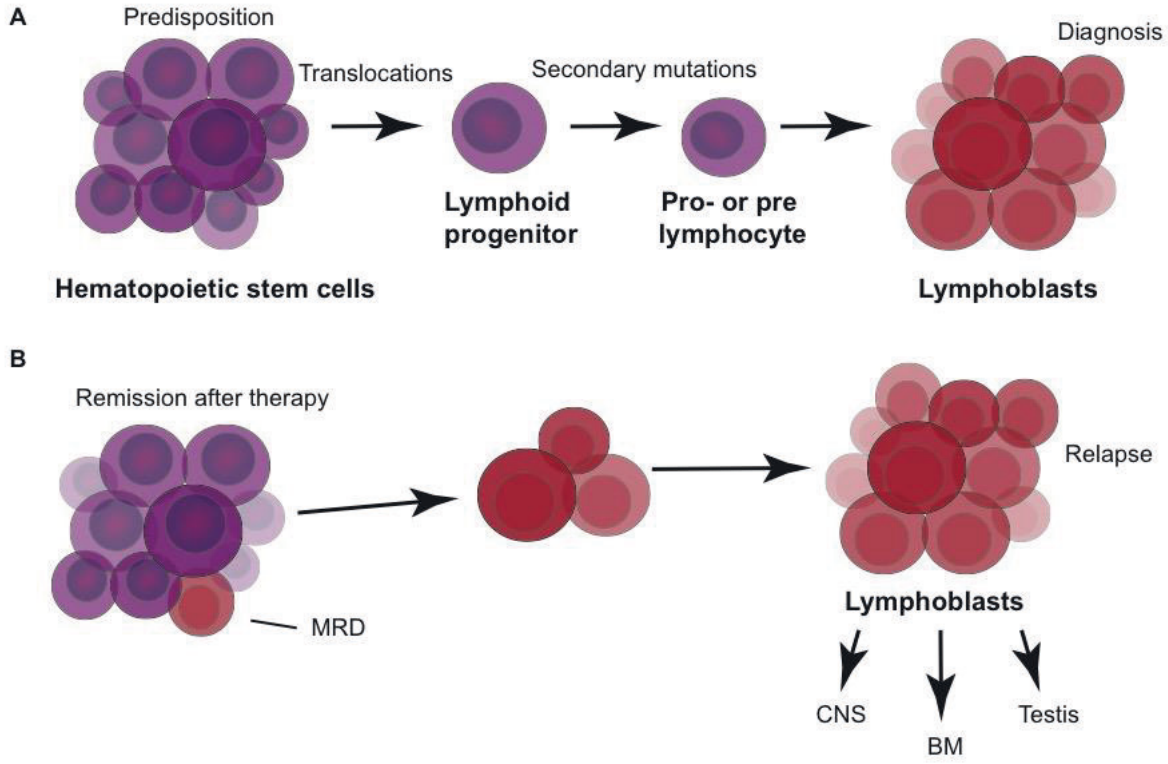

Figure 2: Acquisition of mutations contributing to the development of initial and relapse ALL. **(A)** Inherited variants or gained germline mutations determine a predisposition to ALL. Lymphoid progenitors gain lesions, often translocations, and secondary mutations lead to an arrest in lymphoid development, resulting in leukaemia. **(B)** The patient reaches remission after the induction therapy. Commonly the ALL is heterogeneous at initial diagnosis and in some cases some clones resist the initial treatment. These cells remain in the patient as a minimal residual disease (MRD) and cause a relapse at a later time point. Figure adapted and modified from Stephen et al., 2015[11].

Prognosis after treatment is strongly associated with the type of genetic alteration. While hyperdiploidy is related to an excellent prognosis, hypodiploidy is a negative prognostic factor[16,17]. The fusion gene *ETV6-RUNX1* is associated with a favourable outcome, other fusion genes such as *MLL* or *BCR-ABL1* have a high-risk profile[11,18,19]. In most patients, ALL populations are polyclonal and initial therapy erases the clones that proliferate strongly. However, sometimes a few clones are chemoresistant and might lead to a relapse at a later time point **(Figure 2B)**[11].

1.1.3 Treatment

Prior to the first description of a temporary remission of acute leukaemia by chemotherapy in 1948, ALL was considered incurable and patients died soon after diagnosis[20]. Today, paediatric ALL has an overall survival rate of about 90%, compared to 10% in the 1960s. Improvements in multi-agent chemotherapy regimens and consideration of clinical features of

the patients as well as biological characteristics of the leukaemia cells contributed to the success story in ALL treatment[11]. Therapy regimens are well defined and consist of four phases[5,21,22]:

(1) Remission induction therapy, aiming to reduce the amount of blasts rapidly, approximately four to six weeks

(2) Consolidation/intensification and re-induction, elimination of residual ALL cells in patients that reached remission by morphological criteria

(3) Extra-compartment therapy, targets leukemic subpopulations of the central nervous system (CNS)

(4) Maintenance period, aiming to stabilize remission and to suppress drug-resistant clones

During induction therapy about 98% of patients reach remission by the systemic application of a glucocorticoid, vincristine and L-asparaginase and sometimes anthracycline[5]. Dexamethason is discussed as an alternative to glucocorticoid, since its associated with a stronger anti-leukemic effect, better CNS control and lower relapse rates, but also with increased side effects[23]. After achieving remission consolidation/intensification is necessary, otherwise patients relapse within months[22,24]. Most regimens use high-dose methotrexate in combination with 6-mercaptopurine and/or asparaginase. The re-induction is a repetition of the initial remission induction and early intensification phases[22]. The CNS-directed therapy decreases CNS-originating ALL relapses from more than 50% in the 1960s to less than 5% currently. Therapy includes cranial irradiation, chemotherapy and the use of CNS penetrating drugs. Maintenance therapy includes two to three years of treatment from initial diagnosis. It includes daily oral doses of 6-mercaptopurine and weekly methotrexate[5,25]. Improvements in treatment have increased the event-free survival (EFS) up to 85%, however long term effects have been observed too[11]. Some components of the chemotherapy cause cardiac late effects, neuropsychologic and endocrinologic effects while cranial irradiation is associated with the development of secondary brain tumors[26,27].

Despite the huge advances within the last decades, 10-15% of paediatric ALL patients experience a relapse during and after initial treatment[11,28], and prognosis for these patients is still poor[29,30]. Leukemic clones in relapse tend to be resistant to conventional drugs more frequently than at initial diagnosis and ALL cells cannot be eliminated with usual treatment regimens. Alternative options for these patients are stem cell transplantation but also chimeric antigen receptor T cell therapy gains importance[31].

1.2 Testicular relapse of acute lymphoblastic leukaemia

Patient specific characteristics improved the chemotherapy regimens and increased the EFS of ALL to 85%[11]. Despite these impressive advances of therapeutic options some patients are still facing treatment failure. The majority of these patients suffer from tumour relapse, either in the BM and/or in a non-hematopoietic extramedullary site[32], of which the CNS and the male gonads are most frequently involved. While testicular infiltration with ALL cells is only reported in few cases in adults, paediatric patients show testicular involvement at relapse in up to 20% of the cases[33,34]. At the time of testicular relapse manifestation paediatric patients have a median age of nine years and are usually entering puberty (*ALL-REZ BFM* Trials, data unpublished). It is probable that the infiltration of the testis happens before the children reach sexual maturity, but tumour cell expansion starts frequently with testicular maturation. The site of relapse is, together with the time until relapse and the immunophenotype of the tumour cells, the most important prognostic factor. Even though patients with an isolated testicular relapse have the best prognosis among relapses, a combined relapse of BM and this extramedullary site decreases the EFS of the patients significantly. The standard therapy of an ALL-testis relapse includes an orchiectomy or intensive irradiation, which drastically reduces the life quality of the patients. Optimized systemic frontline therapies lead to a decrease in the number of patients challenged with testicular relapse, however the time and mechanisms of ALL cell migration before and survival within this relapse site is still unclear[35–37].

1.3 Testis anatomy and function

The testis is the site of sperm cell generation (spermatogenesis) and the synthesis of sex steroid hormones (steroidogenesis)[38]. It is a structurally complex organ, consisting of many different, highly specialised cell types some of which form the blood-testis-barrier (BTB). The structure and certain cell types contribute to the immune privilege status of the testis[39]. The following chapter will highlight some of the testis characteristics, which create a niche for ALL cells and favour relapses in paediatric patients.

1.3.1 Anatomy and physiology of the testis

The mammalian testis is a paired oval organ surrounded by the tunica albuginea, a capsule of connective tissue **(Figure 3)**[40]. Inside the capsule the testis is organised into conical lobules, each consisting of the seminiferous tubules and the interstitial space[41]. The seminiferous tubules are long loops that lead with both ends into the rete testis[42]. Fluids

secreted by the seminiferous tubules are collected in the rete testis and delivered to the epididymis via the excurrent ductal system[41].

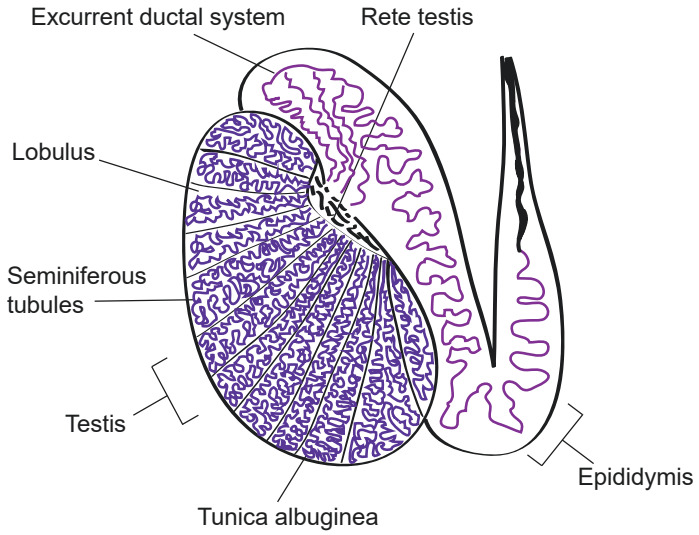

Figure 3: Schematic view of a longitudinal section of the testis and epididymis. The seminiferous tubules (deep purple) are arranged within the lobules of the testis. Secreted fluids are transported via the rete testis into the excurrant ductal system (light purple) of the epididymis. Figure adapted from Holstein et al., 2003[41].

Each seminiferous tubule is structured into the germinal epithelium and the surrounding peritubular tissue. The germinal tissue is organized in different zones that contain different stages of sperm cells and their progenitors[43]. The structure of the seminiferous tubules is supported by the Sertoli cells, a somatic cell type unique to the testis **(Figure 4)**[44] . These so called “nurse cells” were first described by Enrico Sertoli in 1865 and are essential for testis formation and spermatogenesis[45]. Sertoli cells provide mechanisms that allow the transport of micronutrients, such as iron, across the BTB and thereby support germ cell development[46]. Despite their function as “nurse cells”, Sertoli cells take part in signalling in the testis by binding follicle stimulating hormone and testosterone[45]. They also produce the chemokine CXCL12 which plays a major role in the organisation of spermatogonial progenitor cells within the seminiferous tubule[47]. The CXCL12 expression level in the neonatal mouse testis is relatively low but increases dramatically in the adult testis[48]. However, studies in marmoset testes revealed an opposite result. Here CXCL12 expression decreased during testicular maturation[49]. While the role of CXCL12 in the organisation of the testicular stem cell niche is unquestioned, the expression pattern of this chemokine during testicular development seems still unclear.

Leydig cells in the interstitial space, a testis specific cell type first described by Franz von Leydig in 1850, produce the latter. These cells contribute via androgen production to the male genital development and secrete increasing levels of testosterone[50].

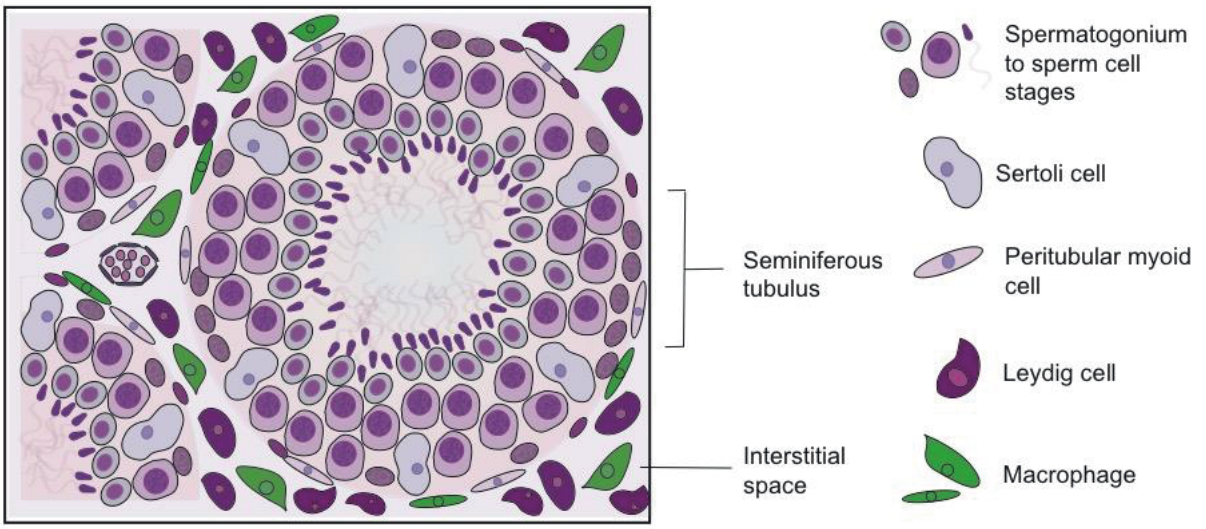

Figure 4: Schematic presentation of a testicular section visualizing the seminiferous tubules and the interstitial spaces. The seminiferous tubules are surrounded by peritubular myoid cells, which have a contractile function. Sertoli cells are located within the seminiferous epithelium and support the germ cell progenitors in their orientation within the tubules. Leydig cells and macrophages inhabit the interstitial space both are involved in steroidogenesis. Blood vessels are exclusively found within the interstitial space.

They are supported in this function by residual testicular macrophages (tMφ), which represent the most common immune cell type in the testis[51,52]. Despite providing factors for Leydig cell development, regeneration and steroidogenesis tMφ maintain an immunopriviledged environment in the testis, by the production of immunosuppressive cytokines and only low expression of proinflammatory cytokines[53,54]. Two tMφ subpopulations that can be distinguished by their morphology and localisation have been identified. While the interstitial tMφ develop from embryonic progenitors, peritubular tMφ migrate from the BM into the testis in the prepuberty period. While the interstitial tMφ, as the Leydig cells, are spread throughout the interstitial space, the peritubular cells are in close contact with the seminiferous tubules[52]. Another cell type that surrounds the tubules are the peritubular myoid cells (PTCs). They were first described by Regaud in 1901 and are found in all mammalian species. Further studies from Rosen-Runge in 1958 identified contraction of the seminiferous tubules but only in 1958 Clermont described the PTCs to be responsible for this phenomenon[55,56]. All these unique cell types form a niche that seems to favour ALL cell survival.

1.3.2 Blood-testis barrier

The concept of a BTB goes back to the early twentieth century, when it was observed that injected dyes failed to stain the testis and the brain[57]. These observations led to the idea of the BTB, a term first introduced by Chiquoine in 1964[58–61]. Other mammalian blood-tissue barriers, such as the blood-brain barrier, are mainly formed by a tight junction-permeability barrier between endothelial cells of the vessels[62,63]. In contrast, tight junctions between Sertoli cells form the BTB in mammalian testes. The seminiferous tubules do not contain any blood vessels, lymph vessels or nervous cells, which are all found in the interstitial space[57]. The seminiferous tubule is the location of spermatogenesis, which consists of a series of cellular events. Spermatogonial stem cells differentiate via spermatocytes, spermatids and spermatozoa into sperm cells that are released into the rete testis. In order to provide a suitable environment for this process, the BTB has two major functions. On the one hand it restricts the entry of substances (e.g. water, ions, nutrients, hormones, toxicants) into the apical compartment of the seminiferous epithelium, the place of post-meiotic cell development. On the other hand, the BTB provides an immunological barrier. During some stages of sperm cell development progenitors express auto-antigens on their surface, that lead to strong autoimmune reaction when injected in other parts of the body[64–66]. To avoid the production of antibodies against these antigens in the testis, part of the differentiation process takes place behind the BTB and therefore within an immune-privileged environment. This is crucial to prevent autoimmune reactions, which leads to male infertility[57]. The BTB terminates at the rete testis[39]. Some forms of autoimmune orchitis are therefore primarily observed in the testis rete[67]. In young children spermatogonial stem cell maturation is still inactive. The formation of the BTB is therefore initiated when boys reach puberty and a protection of the sperm cell progenitors gains relevance[68].

1.3.3 The testis as an immune privileged site

The concept of immune privilege was first introduced in the mid-20th century. It was based on the observation that immunogenic tissues and also tumours survive in certain areas of the body longer than expected or could not be eliminated at all by the immune system. Therefore it was assumed that some anatomical sites are specialised in a way that allows the suppression of a normal immune response [69]. Probably, the immune privilege of certain tissues is an evolutionary mechanism to protect vulnerable processes in the body in order to avoid a loss of function of these sites. In the context of the testis this protection means maintenance of reproductive capability[70–72]. The immune privilege of the testis is based on structural features but also cellular components. A structural element of the testicular immune privilege is the BTB[39]. Beside this barrier many other testicular components were considered to contribute to the immune privilege of the testes, including the lower

temperature of the scrotum, the impaired lymphatic drainage, Leydig cells, spermatogenesis and germ cells, as well as hormones produced[73]. However, the hypothermic condition was soon found to be irrelevant for the immune privilege. Placing the testis into the abdominal cavity did not affect the ability of the testis to protect transplanted cells. Additionally, the lymphatic drainage system of the testis was found to be fully functional[74,75]. Beside that the selective depletion of either Leydig cells or germ cells did not interfere with the immunoprotection of transplanted cells within the testis[74,76–78]. All these findings brought the focus back to Sertoli cells. While these nurse cells are already a main player in maintaining the immune privilege by providing the BTB, it was shown that Sertoli cells when cultured *in vitro*, secrete factors, which inhibit proliferation of both B- and T-cells[79]. By now many cytokines, pro- and anti-inflammatory, were found to be produced by Sertoli cells and there is some evidence that the immunoprotection provided by these cells is depending on a complex interaction between several immune-modulating molecules[80–83]. One example of this complexity is the interaction of Fas ligand and TGF-ß, both expressed by Sertoli cells[83]. While the exclusive expression of Fas ligand was shown to be insufficient to suppress an immune reaction in a colon carcinoma model, co-expression of Fas ligand and TGF-ß led to successful engraftment of the tumour cells[84]. However, Sertoli cells are not the only cell type contributing to the immune suppressive status of the testis. The interstitial space is, beside Leydig cells, populated with immune cells, mainly macrophages. These tMφ secrete immunosuppressive cytokines, such as IL-10 and TGF-ß, and contribute to the immunoprivileged environment of the testis[52]. Beside macrophages, other immune cells occur in very small populations in the testis. Dendritic cells, natural killer cells and different subsets of T-cells are present in interstitial space. Regulatory T-cells isolated from rat testis were shown to suppress T cell proliferation *in vitro* and secrete TGF-ß. These observations suggest that other immune cells, alongside tMφ are involved in maintaining the immune privilege of the testis[38].

1.4 Tumour Microenvironment

The tumour niche consists of cellular and non-cellular compartments that form the so-called tumour microenvironment (TME). Cellular players include many cell types such as fibroblasts, adipose cells and immune cells, but also the blood and lymphatic vessel system contribute to the TME[85]. These stromal elements are described as having important nurturing functions, supply tumour cells with growth factors and cytokines and are involved in neoangiogenesis[86]. The following chapter will highlight some cellular and molecular players of the TME and their role in tumour progression.

1.4.1 Immune and inflammatory cells

The main function of immune cells is to maintain tissue homeostasis, removal of damaged cells and protection against invading pathogens[87]. However, despite their function as guardians some immune cells are associated with immune suppression. Prominent examples for such cells are regulatory T-cells, myeloid-derived suppressor cells and certain subsets of macrophages[88–90]. The immunosuppressive function of these cells is crucial for tissue homeostasis, but in the context of cancer, they can promote tumour progression[88]. Only the macrophages will be discussed in detail.

Tumour-associated macrophages

Macrophages are part of the innate immune system and originate from BM precursors. They provide a first line defence mechanism against pathogens and activate the adaptive immune response by antigen presentation[91]. Macrophages are the most diverse cells of the hematopoietic system and can be found in all organs and tissues. Depending on their localization macrophages execute different functions and play a role in development, homeostasis, tissue repair and immunity[92]. To meet all these diverse functions macrophages are able to polarize in different subgroups. The classical-activated macrophages are classified as M1 and take part in immune response against pathogens or cancer cells. However the second alternative-activated subgroup is classified as M2 and is immune suppressive, favouring tissue repair and promoting tumour progression[93]. Depending on the cytokines present in a given environment macrophages polarize either towards M1 or M2 status. The activation status in turn influences downstream events, that either promote or suppress an immune response **(Figure 5)**. Macrophages that infiltrate tumour tissue or populate the TME are defined as tumour-associated macrophages (TAMs). These TAMs are a crucial component of the TME and affect tumour growth, angiogenesis, immune regulation, metastasis and chemoresistance[94]. It is assumed that circulating blood monocytes, derived from BM stem cells are the major source of TAMs. However also resident macrophages, originating from progenitors of the yolk sac can be recruited into the TME where they support tumour progression[94–97]. In order to maintain this tumour supportive status TAMs acquire an anti-inflammatory M2-like phenotype, which is partly shaped by the TME itself[98]. In lung adenocarcinoma and breast cancer it was observed that patients with a strong accumulation of macrophages in the TME have a poor prognosis compared with patients with fewer macrophages[99,100].

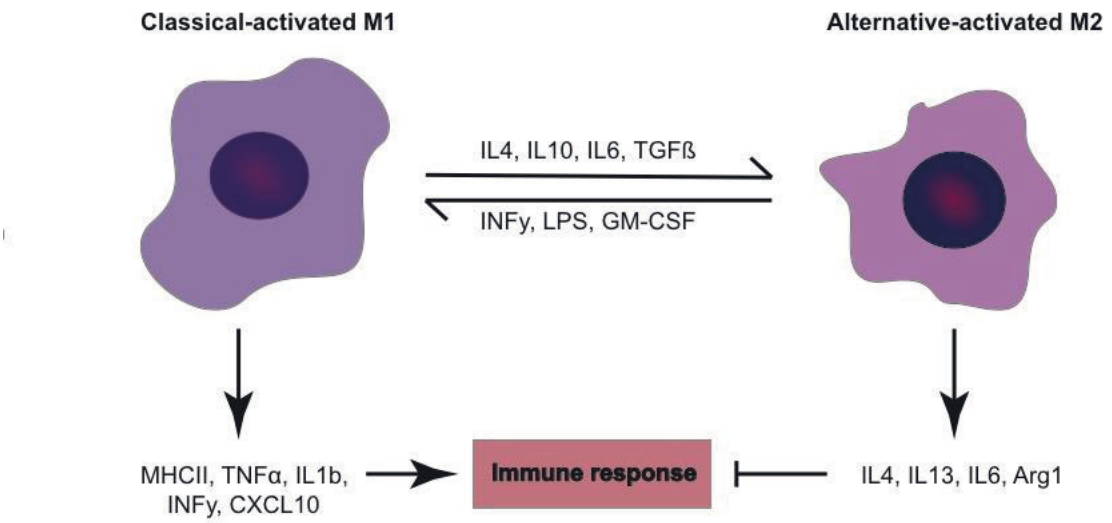

Figure 5: Macrophage polarisation towards classical-activated (M1) and alternative-activated (M2) subgroups. M1 macrophages are activated by various factors, including cytokines and LPS, a membrane component of bacteria. After activation M1 macrophages express molecules relevant for antigen presentation, as well as cytokines that support an immune response. Alternative-activated M2 macrophages are activated by cytokines such as IL4, IL10, IL6 and TGFß. They secrete cytokines that suppress an immune response. Figure adapted from Lin et al., 2019[94].

While TAMs were already widely studied in various solid cancers, their role in ALL is still poorly understood. First studies suggest an interaction of leukemic cells with TAMs, resulting in tumour progression[101]. A murine T-ALL model was used to study the tumour-TAM interaction in BM and spleen. TAMs in BM and the spleen were found to differ significantly from each other. The splenic macrophages had a stronger effect on T-ALL proliferation compared to the BM TAMs[102].

1.4.2 Chemokine signalling in tumour progression

Chemokines, a group of chemotactic cytokines, are soluble proteins that recruit cells from the immune system to the site of injury or infection[103]. Some of these chemokines have homeostatic functions and are produced constitutively others are produced exclusively under inflammatory condition[104]. However, despite their role in inflammation also other mechanisms were found to be mediated by chemokines such as haematopoiesis, angiogenesis, germ cell migration or embryonic implantation[105–107]. Many studies found evidence of a chemokine-mediated tumour progression. While chemokines are usually expressed by the different components of the TME, tumour cells often overexpress certain chemokine receptors[108–111]. The influence of some chemokines on cancer progression is already intensively studied. CCL2, the ligand of CCR2 and CCR4, was identified to promote invasion and metastasis in several tumour entities such as ovarian cancer, myeloma, breast and cervical cancer[112–115]. The homeostatic chemokine receptors CCR7, CXCR4 and CXCR5 are involved in the migration of leukaemia or lymphoma cells into secondary lymphoid organs where tumour

cells are provided with a growth-promoting niche[86,116]. An overview of different chemokine receptors and the tumours they are involved in is provided in **Table 1**.

Table 1: Chemokine receptors involved in the progression of different tumour entities.

Receptors	Tumour
CXCR2	Breast cancer, pancreatic tumour, ovarian and prostate cancer, skin tumour, colon and gastric cancer
CXCR4	Lung cancer, brain tumour, breast cancer, pancreatic tumour, ovarian and prostate cancer, AML, CLL, lymphomas, colon and gastric cancer
CXCR5	B cell non-Hodgkin's lymphoma, diffuse large B cell lymphoma
CCR1	Breast cancer, colon and gastric cancer, multiple myeloma
CCR2	Pancreatic tumour, ovarian and prostate cancer
CCR4	Lung cancer, renal carcinoma, skin tumour, colon and gastric cancer, T cell malignancies
CCR5	Colon and gastric cancer
CCR7	Ovarian and prostate cancer, colon and gastric cancer, T-ALL

One of the most frequently discussed mediators for tumour progression and invasiveness is the CXCR4-CXCL12 axis. While CXCR4 is only expressed in low levels in many healthy tissues, it is often over-expressed by various tumour entities[117]. It is expressed in lung carcinoma, breast cancer, colorectal and gastric cancers but also in multiple myeloma and paediatric ALL[109,117,118]. A high expression of CXCR4 is associated with chemotaxis, invasion, angiogenesis and proliferation[119]. In the context of ALL, CXCR4 over-expression is described to be associated with extramedullary organ infiltration[109]. On the other hand, CXCL12 is important for the maintenance of the BM stem cell niche and is expressed in high levels by BM mesenchymal stem cells (MSCs)[120]. Inhibiting CXCR4 leads to a reduction of ALL cell growth and was shown to recover the drug response in chronic lymphoblastic leukaemia cells *in vitro*[121,122]. A mouse model of human paediatric ALL revealed a mobilisation of leukemic cells from the BM into the peripheral blood upon CXCR4 inhibition. Lacking the stromal support in the BM and also other extramedullary organs makes ALL cells prone to respond towards chemotherapeutic agents[123]. This observation was confirmed in another BCP-ALL mouse model from 2016[124]. In this study, CXCR4 was deleted by CRISPR/Cas9 gene editing in BCP-ALL cells as well as inhibited by CXCR4 antagonists, already used in the clinics (e.g. AMD3100). Both attempts led to a reduction of ALL cell migration towards the CXCL12 gradient of the BM and a restored drug response against multiple agents. These results suggest that CXCR4 is a promising candidate in treatment of chemoresistant ALL.

Within the testis Sertoli cells express CXCL12, while pre-meiotic germ cells express CXCR4 and CXCR7, the second receptor that binds CXCL12. This expression patterns indicates the relevance of this chemokine-chemokine receptor axis for the interaction between undifferentiated germ cells and Sertoli cells within the seminiferous tubules[49]. On the other hand, this signalling axis might play a similar role in testicular infiltration with ALL cells, as already described for the BM. Since chemokine receptors and their ligands are of crucial importance for tumour cell dissemination, this work focuses on their role on ALL testis infiltration.

1.4.3 Cancer-associated fibroblasts

Special subtypes of fibroblasts, the myofibroblasts, are activated during the natural process of wound healing[125]. However at the site of a tumour these cells stay permanently activated and have a significant impact on tumour cells by remodelling the extracellular matrix, angiogenesis, recruitment of inflammatory cells and stimulation of cancer cell proliferation[87,126,127]. Such activated myofibroblasts are defined as cancer-associated fibroblasts (CAFs) and present another important player within the TME[87]. Similar to TAMs, CAFs are associated with a poor prognosis for the patient in various types of cancers, such as breast cancer, prostate cancer and laryngeal carcinoma. Galectin-1, expressed by CAFs are described as supporting the development of abutting tumour cells and thereby contribute to the poor outcome[128–131]. However, understanding the biology of CAFs and their function in tumour progression led to new therapeutic possibilities in recent years. Micro RNA can be used to deactivate CAFs and thereby reverse them to normal fibroblasts[132,133]. In lung carcinoma it was shown that the tyrosine kinase inhibitor Desatinib reprograms CAFs into a phenotype similar to normal fibroblasts[134]. In adult ALL it was shown that MSCs isolated from patients adopt an activated, CAF-phenotype and prevent therapy-induced apoptosis in ALL cells. Certain drugs, such as vincristine and corticosteroids, which are already established in ALL treatment prevent MSC activation and therefore the development of CAFs[135]. These examples illustrate how a better understanding of tumour-stroma interactions can be directly translated into improved treatment options for patients.

1.5 Murine models with testicular involvement in ALL

Animal models are widely used to study tumour biology, because - in contrast to *in vitro* studies- *in vivo* models depict the complexity of an entire living organism. Within the field of ALL research a broad spectrum of murine models was established that can be categorised into syngeneic and xenograft models. While syngeneic models reflect the variety of the multiple genetic mutations that can occur in ALL, xenograft models allow a closer insight into

human ALL cell interaction with a complex, yet highly immunocompromised niche[136]. So far, most studies examining testicular infiltration with ALL cells are limited to clinical observations and do not address the pathophysiological mechanisms as potential niche specific characteristics[36,37,137–139]. A publication from 1980 describes a post-mortem survey of paediatric leukaemia and lymphoma patients[140]. In all observed cases, testis infiltration seemed to occur via the haematogenous route into the interstitial space of the testis. Attempts to develop an ALL-testis animal model with testicular infiltration were first published in 1984[141]. In this study Jackson et al. transferred a murine ALL cell line into mice and observed fatal leukaemia within 7 to 8 days. While ALL cells heavily infiltrated BM and the spleen, there was no testicular involvement observed. Only manipulation of the gonadal vascular endothelium using cadmium chloride led to tumour cell infiltration of the interstitial space of the testes. Thus, the authors considered this model to be unsuitable to examine testicular ALL infiltration and survival due to the lack of testicular penetration of circulating malignant lymphoblasts. The same group published an ALL-rat model using a murine T-ALL cell line[142]. Tumour growth was again very aggressive and had a fatal outcome in 18-21 days. In rat testis and CNS was frequently involved and a remission was achieved by carmustine treatment. Rats that were successfully treated had a relapse after up to 80 days and still showed testicular involvement. One decade later a second syngeneic rodent model was published[143]. A rat T-ALL cell line was passaged in rats and testicular infiltration was analysed by immunohistochemistry. Again, tumour progression was fast, and experiments had to be terminated the last at day 17 after transplantation. Sexually immature rats always displayed testicular infiltration with ALL cells, whereas testicular ALL cells were detectable in 42% of sexually mature rats. This finding underlines clinical observations in which testicular infiltration during ALL disease mainly occurs in paediatric patients. However, rats show a more frequent testicular infiltration in post-puberty, compared to adult men. This suggests a mechanism involved in infiltration that is still active in many adult rats. The authors suggest that physiological changes throughout puberty are responsible for the reduced infiltration in adult men in comparison to children[144]. A study in 2015 found a correlation between a high CD9 expression level and testis infiltration using the BCP-ALL cell line REH in NSG mice[145]. However, only very few REH cells were detected in the mice testis in this study, even when using cells with a very high CD9 expression. One recent study analysed the influence of cortactin expression on BCP-ALL relapse and extramedullary involvement[146]. The authors used the REH cell line and patient-derived xenografts (PDX) in NSG mice and found a correlation between a high cortactin expression and an infiltration of various organs including the testes.

None of the presented studies analysed the ALL-stroma interaction within the testis. While it was shown that human ALL cells penetrate the testis in a murine model, at least in small

numbers, a detailed analysis of cellular and molecular changes upon infiltration is still lacking.

1.6 Aims of this project

To date, only a few studies have addressed the phenomenon of testicular infiltration of tumour cells in paediatric ALL relapse patients. Most of these publications did not examine the testicular infiltration exclusively but were rather focused on the CNS relapse. Studies that only examined the testicular infiltration were performed thirty to forty years ago. None of the studies of the last decades addressed the cellular and molecular changes of the testicular TME upon ALL infiltration. Nowadays advanced techniques can be applied to expand the understanding of the underlying mechanisms. It has been shown that a comprehensive understanding of tumour-stroma crosstalk is crucial for the identification of therapy targets for several tumour entities. Therefore, a model that allows for the study of the cellular requirements and molecular pathways contributing to leukemic cell dissemination into the testis would be desirable. This thesis aims to address this issue.

1) Are homing receptors and adhesion molecules differentially expressed on leukemic cells from patients with and without testicular involvement at relapse?

In the first part of the presented work, primary patient samples were intensively analysed for their marker expression by flow cytometry. The focus was the analysis of several chemokine receptors on paediatric ALL relapse samples, but also some adhesion markers and the IL7R were included in the panel. Based on the results, migration and apoptosis assays were performed to study the relevance of the identified proteins. I*n vitro* experiments were performed using human ALL cell lines, primary ALL cells and primary human testis stroma.

2) Which cellular stromal elements within the juvenile testicle contribute to leukemic cell migration and to a leukemic-permissive survival niche?

The second part of this thesis aims to dissect the crosstalk of ALL cells with the testicular stroma. To achieve this, testicular stroma cells were isolated from mice and studied *in vitro* for their impact on ALL cell survival. The ability of ALL cells to shape their testicular microenvironment was analysed by flow cytometry and RT-PCR. TMφ and their ability to polarize into TAMs were of particular interest.

3) Analysis of the functional aspects of testis physiology on leukemic cell migration, localization and progression in an animal model for paediatric ALL.

The third part of the presented work describes the generation and characterization of a novel PDX-ALL model with testicular involvement using NSG mice. PDX-ALL cells were

transduced and expressed luciferase. This allowed monitoring of the tumour progression by non-invasive bioluminescent imaging. Infiltration of the testis and other organs was analysed by flow cytometry. The localisation of ALL cells in the testis was analysed by immunohistochemistry (IHC) staining. The established mouse model allowed the study of the relevance of the CXCR4-CXCL12 axis for testicular infiltration in ALL relapse *in vivo* by using an anti-human CXCR4 antibody.

2 Materials and Methods

2.1 Material

2.1.1 Cell lines and primary cells

The following cell lines were used (**Table 2**).

Table 2: Mouse and human cell lines.

Cell line	Source	Description	Medium
Nalm6	Dr. Stephan Mathas (MDC, Berlin)	Human pre-B cell acute lymphoblastic leukaemia (B-ALL)	RPMI 1640 + 10% FCS + 1% P/S
SEM	Dr. Cornelia Eckert (Charité)	Human B-ALL	RPMI 1640 + 10% FCS + 1% P/S
697	Dr. Cornelia Eckert (Charité)	Human B-ALL	RPMI 1640 + 10% FCS + 1% P/S
REH	Dr. Stephan Mathas (MDC, Berlin)	Human B-ALL	RPMI 1640 + 10% FCS + 1% P/S
HEK293T	American Type Culture Collection (ATCC)	Human embryonic kidney	DMEM + 10% FCS+ 1% GlutaMax + 1% P/S
M2-10B4	American Type Culture Collection (ATCC)	Mouse bone marrow stroma cell	RPMI 1640 + 10% FCS + 1% P/S
TM4	American Type Culture Collection (ATCC)	Mouse Sertoli cell	1:1 F12 medium:DMEM + 1.2 g/L sodium bicarbonate + 15mM HEPES + 5% horse serum, 2.5% FCS
EL4	American Type Culture Collection (ATCC)	Mouse T cell lymphoma	DMEM 1640 + 10% FCS + 1% P/S

The following primary cells were used (**Table 3**):

Table 3: Primary patient derived cells.

Cell line	Source	Description	Medium
PDX-ALL	Dr. Jean-Pierre Bourquin (FZK, Zürich)	B-ALL	RPMI + 10% FCS + 1% P/S
BM-MSC	Dr. Cornelia Eckert, (Charité, Berlin)	Bone marrow derived mesenchymal stem cells	IMDM + 10% Horse Serum + 10% FCS+ 1% P/S
Testis stroma	Dr. Cornelia Eckert, (Charité, Berlin)	Testis derived mesenchymal stem cells	IMDM + 10% Horse Serum + 10% FCS+ 1% P/S

2.1.2 Mouse strains

NOD.Cg-Prkdcscid Il2rg tm1 Wjl/SzJ (NSG) and C57BL/6N mice were bred and housed at the Max-Delbrück-Center for Molecular Medicine Berlin animal facility in a controlled environment (12 hours dark/light cycle, 23 °C, 55 % humidity) with food and water ad libidum at the animal facility of the Max-Delbrück-Center for Molecular Medicine, Berlin, Germany. All experiments were conducted in compliance with the institutional guidelines of the Max-Delbrück-Centrum for Molecular Medicine and approved by the Landesamt für Gesundheit und Soziales, Berlin, Germany (TVV G0373/13; G0104/16; G0088/20).

2.1.3 Human testis material

The utilisation of human testis material was approved by the ethics committee of the Charité (Campus Virchow), Berlin (application number: EA2/056/17).

2.1.4 Conjugated antibodies for mouse and human surface antigens

The following fluorophore coupled anti-mouse antibodies were used (**Table 4**). They are conjugated with allophycocyanin (APC), Allophycocyanin/cyanin7 (APC-Cy7), fluorescein isothiocyanate (FITC), pacific blue (PB), peridinin chlorophyll protein complex-cyanin 5.5 (PerCP-Cy5.5), phycoerythrin (PE) or phycoerythrin/cyanin 7 (PE-Cy7).

Table 4: Conjugated anti-mouse antibodies.

Specifity	Conjugate	Clone	Isotype	Reactivity	Source
CD45	PB	30-F11	Rat IgG2b	Mouse	Biolegend
CD45.1	PB	A20	Mouse IgG2a	Mouse	Biolegend
CD45.2	PB	104	Mouse IgG2a	Mouse	Biolegend
Ly6C	FITC	HK1.4	Rat IgG2a	Mouse	Biolegend
CD11c	PE/FITC	N418	Hamster IgG	Mouse	Biolegend
CD11b	PE-Cy7	M1/70	Rat IgG2b	Mouse	Biolegend
F4/80	APC-Cy7	BM8	Rat IgG2a	Mouse	Biolegend
CD64	PerCP-Cy5.5	X54-5/7.1	Mouse IgG1	Mouse	Biolegend
MHCII	APC	M5/114.15.2	Rat IgG2b	Mouse	Biolegend

CD54	PE	YN1/1.7.4	Rat IgG2b	Mouse	Biolegend
CD115	PE	AFS98	Rat IgG2a	Mouse	ebioscience
CX3CR1	PerCP-Cy5.5	SA011F11	Mouse IgG2a	Mouse	Biolegend

The following fluorophore coupled anti-human antibodies were used (**Table 5**):

Table 5: Conjugated anti-human antibodies.

Specifity	Conjugate	Clone	Isotype	Reactivity	Source
CD10	APC	HI10a	IgG1	Human	Biolegend
CD19	PB	HIB19	IgG1	Human	Biolegend
CD3	PB	HIT3a	IgG1	Human	Biolegend
CD45	PB	HI30	IgG1	Human	Biolegend
CCR5	PE	2D7/CCR5	IgG2a	Human	BD
CCR7	PE	150503	IgG2a	Human	R&D
CCR9	PE	112509	IgG2a	Human	BD
CXCR1	PE	42705	IgG2a	Human	R&D
CXCR2	PE	48311	IgG2a	Human	R&D
CXCR3	PE	1C6/CXCR3	IgG1	Human	BD
CXCR4	PE	44717	IgG2b	Human	R&D
CXCR5	FITC	2G8	IgG2a	Human	BD
CXCR7	PE	8F11-M16	IgG2a	Human	Biolegend
CD11a	PE	HI111	IgG1	Human	BD
CD62L	PE	GREG-56	IgG1	Human	Biolegend
CD49d	PE	9F10	IgG1	Human	BD
CD44	PE	G44-26	IgG2b	Human	BD
CD127	PE	A019D5	IgG1	Human	Biolegend
CD29	APC	MAR4	IgG1	Human	eBiosciences
CD73	PE	AD2	IgG1	Human	BD
CD90	FITC	5E10	IgG1	Human	eBioscience
CD105	PE	43A3	IgG1	Human	Biolegend
CD146	APC	541-10B2	IgG1	Human	Miltenyi

2.1.5 Unconjugated primary antibodies for *in vivo* blocking

The following unconjugated antibodies for in vivo blocking were used (**Table 6**):

Table 6: Unconjugated primary antibodies for *in vivo* blocking.

Specifity	Clone	Isotype	Reactivity	Source
CXCR4	12G5R	Mouse IgG2a	Human	R&D
IgG2a	20102	IgG2a	Human	R&D

2.1.6 Antibodies for immunohistochemistry (IHC) stainings

The following unconjugated primary antibodies for IHC staining's were used (**Table 7**):

Table 7: Unconjugated primary antibodies for IHC stainings.

Specifity	Host	Clone	Dilution	Source
Anti-human CD10	Mouse	56C6	1:20	Novus
Anti.human CD68	Rabbit	KP1	1:100	Thermo Fisher
Anti-mouse Vimentin	Rabbit	EPR3776	1:200	Abcam
Anti-mouse CXCL12	Mouse	79018	1:50	R&D

The following conjugated primary and secondary antibodies for IHC stainings were used (**Table 8**):

Table 8: Conjugated primary and secondary antibodies for IHC stainings.

Specifity	Conjugate	Dilution	Host	Source
Anti-mouse a-SMA	Cy3	1:200	Mouse	Sigma
Anti-rabbit	Peroxidase	1:100	Donkey	Jackson Immunology
Anti-mouse	Peroxidase	1:100	Donkey	Jackson Immunology
Anti-rabbit	AF 488	1:350	Goat	Life technology

2.1.7 Plasmids and lentiviral vectors

The following plasmids and lentiviral vectors were used (**Table 9**):

Table 9: Plasmids and lentiviral vectors.

Name	Description
pSpCas9(BB)-2A-Puro (PX459)	Cas9 from S. pyogenes with Puromycin resistance, and cloning backbone for sgRNA

pSpCas9(BB)-2A-GFP (PX458)	Cas9 from S. pyogenes with 2A-EGFP, and cloning backbone for sgRNA
pFU-Luc-eGFP	Lentiviral vector expressing luciferase and eGFP
pCMV-VSV-g	Eukaryotic expression vector encoding G glycoprotein of the vesicular stomatitis virus (VSV-g) (*env*)
pLP1	Eukaryotic expression vector encoding HIV-1 *gag* and *pol* genes
pLP2	Eukaryotic expression vector encodes the HIV-1 Rev protein

2.1.8 Oligonucleotides

The following oligonucleotides were used for qRT-PCR (**Table 10**):

Table 10: Oligonucleotide primer for qRT-PCR using TaqMan® probes.

Gene	Reactivity	Assay ID
B2M	Mouse	Mm00437762_m1
IL1b	Mouse	Mm00434228_m1
Mmp9	Mouse	Mm00600164_g1
IL10	Mouse	Mm01288386_m1
Arg1	Mouse	MM00475988_m1
IL7	Mouse	Mm01295803_m1
CXCL12	Mouse	Mm00445553_m1
GAPDH	Human	Hs03929097_g1
IL4	Human	Hs00174122_m1
IL6	Human	Hs00174131_m1

IL10	Human	Hs00961622_m1
TGF-ß	Human	Hs00820148_g1
M-CSF	Human	Hs00174164_m1
INFy	Human	Hs00989291_m1

2.1.9 sgRNAs for CRISPR/Cas9 mediated knock-out

The following sgRNAs were used (**Table 11**):

Table 11: sgRNAs for CRISPR/Cas9 mediated CXCR4 knock-out.

Name	Sequence
CXCR4_77_forward	caccgTACACCGAGGAAATGGGCTC
CXCR4_77_reverse	aaacGAGCCCATTTCCTCGGTGTAC
CXCR4_90_forward	caccgCACTTCAGATAACTACACCG
CXCR4_90_reverse	aaacCGGTGTAGTTATCTGAAGTGC

2.1.10 Kits

Lonza	Cell line Nucleofector Kit T
Meso Scale Discovery:	U Plex assay
Miltenyi Biotec:	Anti-PE beads
	Anti-CD19 (mouse) beads
New England Biolabs	Quick Ligation Kit
Pomega	Pure Yield Plasmid Miniprep System
	Pure Yield Plasmid Midiprep System
Qiagen:	DNA Maxi Kit
	RNeasy Micro/Mini Kit
	RNase-free DNase Set
	Gel extraction Kit
Thermo Fisher Scientific:	SuperScript III First-Strand Synthesis

SuperMix for qRT-PCR

SuperScript VILO cDNA Synthesis Kit

Bradford Assay

2.1.11 Chemical reagents and consumables

Abbott Laboratories (Chicago, USA), Addgene (Watertown, USA), Applied Biosystems (Foster City, USA), Becton Dickinson (Franklin Lakes, USA), Biolegend (San Diego, USA), Biosynth (Staad, Switzerland), C. Roth (Karlsruhe, Germany), Carl Zeiss (Oberkochen, Germany), Eppendorf AG (Hamburg, Germany), Gibco (Karlsruhe, Germany), Greiner Bio-One International AG (Kremsmünster, Germany), Jackson Immunology (West Grove, USA), Life technology (Carlsbad, USA), Merck (Darmstadt, Germany), Miltenyi Biotec (Bergisch Gladbach, Germany), Nalgene (Rochester, USA), New England Biolabs (Ipswich, USA), Omni Life Bioscience (Bremen, Germany), Peprotech (Hamburg, Germany), Qiagen (Hilden, Germany), Sarstedt (Nümbrecht, Germany), Sigma-Aldrich (St. Louis, USA), Thermo Fisher Scientific (Waltham, USA), TPP (Trasadingen, Switzerland), VWR (Radnor, USA)

2.1.12 Software

Adobe:	Illustrator ® CS6
BD:	FACS Diva ®
Caliper LifeScience:	Live Image ® 4.5
GraphPad:	Prism ® 5
Microsoft:	Office for Mac 2011
TreeStar:	FlowJo2 ®
Zeiss:	Axio Vision ® 4.5

2.2 Methods

2.2.1 Cell culture

Cultivation and cryopreservation of primary human cells and cell lines

Cells were cultured at 37°C, 5 % CO_2 and a relative humidity of 95% in an incubator. B-ALL cell lines were cultured in exponential growth phase in RPMI 1640 (Gibco) + 10 % FCS (Gibco) + 1% Penicillin/Streptomycin (P/S, Gibco) and passaged twice the week at a 1:5 ratio. Primary human bone marrow mesenchymal stem cells (BM-MSC) and testis stroma

were cultured in IMDM (Gibco) + 10% FCS + 10% Horse serum (Gibco) + 1 % P/S and passaged regarding their growth rate to ensure optimal confluence. Cells were rinsed with PBS and treated with accutase (Gibco) at room temperature (RT) until cells detached from the dish. Subsequently, cells were washed off the dish with appropriate complete medium and transferred into a 50 ml tube (Falcon). All cell suspensions were centrifuged at 350 g for 5 min before seeded into fresh culture flasks or dishes. Cells for cryopreservation were resuspended in FCS + 10% DMSO (Sigma), transferred into cryo-tubes (Greiner) and stored in cryo-containers (Nalgene) for 24 hours at -80°C, before transfer into nitrogen tanks. To thaw cells, the cryo-tube was shaked for 2 min in a 37°C water bath, the suspension was taken up in 10 ml cold medium, centrifuged and cultured as described above.

Determination of cell numbers and viability

Cell numbers were determined using CASY cells counting technology. Therefore 10 µl of a cell suspension were diluted into 10 ml CASYton (Omni Life Bioscience) and applied to the CASY counting device (Innovatis). The suspension was analysed, and the device provided cell number and viability.

Isolation of cell culture supernatant

After 72h of culture, medium was transferred into a 15 ml reaction tube (Falcon) and centrifuged at 350g for 5 min at 4°C. Supernatant was transferred into 1,5 ml reaction tubes (Eppendorf) and snap-frozen in liquid nitrogen. The supernatants were stored at -80°C.

Transient transfection

Cells were transiently transfected using calcium phosphate precipitation. HEK293T cells were seeded at a density of $8*10^5$/ 6 well and were ready for transfection after 24 hours (60-70% confluent).

Transfection mixture per well, prepared in a 15 ml polysterol tube (Falcon):

18 µg total DNA

15 µl 2.5 M calcium chloride (Sigma)

adjusted to 150µl with ddH_2O

150µl transfection buffer were slowly added dropwise to the mixture that was constantly shacked.

The solution was incubated for 10 min at RT and the DNA precipitates were dropwise added to the HEK293T cells. Medium was changed 6 h after the precipitate was added to the cells and dishes were incubated for 48 hours at 37°C.

Transfection buffer: 1 % HEPES (Sigma), 1.5 mM disodium phosphate (Sigma), 270 mM sodium chloride (Roth), 10 mM Potassium chloride (Roth), pH 6.76

Culture medium HEK-293T: DMEM (Gibco), 10% FCS (Gibco), 1% P/S, 1% glutamine (Gibco)

Production of viral supernatant

Lentiviral viruses for luciferase-transduction of PDX-ALL cells were generated by transient transfection of HEK293T cells with pFU-Luc-eGFP, pLP1, pLP2, and pCMV-VSV-G (4.5µg each) viral DNA per 6-well. Virus-containing supernatant was harvested 48 hours after transfection, filtered (0.45 µm filter) and stored at -80°C before use.

Transduction of PDX-ALL cells

PDX-ALL cells were thawed and $5*10^6$ cells in 1 ml RPMI 1640 + 10% FCS resuspended and applied to a 24 well plate (Sarstedt). Afterwards 1 ml virus-containing supernatant and 16 µl polybrene (1 µg/µl) was added to the well and the plate was centrifuged for 90 min at 2000 rpm and 37°C. The plate was incubated another 2 hours at 37°C before cells were washed three times in PBS, taken up in 250 µl cold RPMI 1640 and transplanted into two mice ($2*10^6$ cells/mouse). After five weeks mice were imaged with the IVIS system and in case of a signal scarified. BM and spleen were dissected, and cells were sorted for GFP positive cells with fluorescence associated cell sorting (FACS) using the BD Aria device. GFP positive cells were re-transplanted into mice and tumour growth monitored by IVIS imaging and blood analysis. After approximately seven weeks mice were sacrificed, BM cells were FACS sorted a second time and cryopreserved until further experiments.

Transwell migration assay

The day before performing the migration assay tissue culture inserts (Sarstedt, 5 µm pore size) are coated with 400 µl of a collagen solution (Sigma, 20µg/ml in 0.05M HCl) per insert and incubated at 4°C. Next day, the collagen solution is withdrawn, inserts are washed four times with 400 µl PBS and dried before cells are applied. While inserts are drying, 500 µl of cell culture supernatants or chemokine solutions (mouse or human CXCL12, Peprotech) are applied to 24 well plates. Each condition is performed as a triplicate. Chemokines are diluted in migration medium (RPMI + 1% BSA (Sigma) + 25 mM HEPES (Gibco)) in a concentration of 100 ng/ml. Negative control is migration medium without additional supplements. The dried tissue culture inserts are transferred onto the solution. Cells are washed twice with PBS and a cell suspension of 1×10^7/ml is prepared. 100 µl of the cell suspension is applied per tissue culture insert (1×10^6/well) and the culture dish is incubated for 4 hours at 37°C. For

some conditions, cells were treated with AMD3100 (Merck, 1 µg/ml) or DMSO (1 µg/ml) for 30 min at 37°C and washed twice prior starting the migration experiment. Afterwards inserts are removed and 400 µl of the migration medium/supernatant is transferred into a 1.5 ml reaction tube. The suspension is centrifuged at 2000 rpm for 5 min before 340 µl per tube is carefully withdrawn. Cells are counted in a Neubauer chamber and the migration factor is calculated by setting the number of cells migrated towards the chemokine solution/supernatant in ratio with the cells migrated towards the negative control.

Isolation of murine testicular stroma cells and co culture with ALL cells

Per 24 well ten C57BL/6N were sacrificed and testes transferred into a 50 ml reaction tube containing 10ml digest solution (RPMI containing 1 mg/ml collagenase II (Gibco) and 0.15 mg/ml DNaseI (Sigma)). Testes were gently disrupted prior a 30 min digest at 34°C under frequent shaking. After incubation tubes were filled with 40 ml cold PBS + 10% FCS and filtered through a 100 µm cell strainer. Suspensions were centrifuged for 5 min at 350g, the pellet taken up in 0.5 ml Medium 199 and seeded onto a 24 well dish. The cells were incubated 30 min at 34°C before rinsed 4 times with warm PBS and cultured in complete Medium 199 (10% FCS, 1% P/S) for 4 hours. Subsequently cells were washed one time with warm PBS and 0.8 * 10^6 ALL cells per well were added in reduced medium 199 (1% FCS, 1% P/S). Co-cultured macrophages and ALL cells were analysed after 20 hours by flow cytometry regarding their surface marker expression (macrophages) and their viability (ALL cells) and compared to mono-cultured cells.

Isolation of Sertoli cells and peritubular myoid cells (PTCs) from the testis

The isolation of Sertoli cells and PTCs was performed using a protocol published by Kauerhof et al, 2019[147]. Tests of eight mice were removed and transferred into sterile DMEM/F12 in a 50 ml reaction tube. Isolated testes were decapsulated in a petri dish and tubules transferred in PBS. Tubules were placed in 5 ml collagenase solution (1 mg/ml collagenase II + 6 µg/ml DNAse in DMEM/F12 (Thermo Fisher Scientific) and incubated at 34°C for 20 min and shacked 60 cycles/minute. Subsequently, 30 ml DMEM/F12 were added and the tube inverted for three times. Tubules settled for 5 minutes and the supernatant, containing the interstitial cells was discarded. Tubules were washed two times with DMEM/F12 to remove all interstitial cells. Remaining tubules were resuspended in 5 ml trypsin solution (1mg trypsin (Sigma) + 0.02mg DNAse /ml) and incubated at 34°C for 20 min and shacked 60 cycles/minute. Trypsin was inactivated with 25 ml DMEM 1640 + 10% FCS.

PTCs:

Tubules settled for 5 minutes and supernatant containing the PTCs was collected. The tubules were washed another two times and the supernatant was collected. The isolated PTCs were centrifuged at 400*g for 10 minutes, and supernatant was discarded. Cells were resuspended in 10 ml DMEM 10% FCS and filtered into new tube through a 100µm cell strainer to remove clumps. Another 10 ml DMEM 10% FCS was added, and cells were plated in a 75cm^2 flask and incubated at 37°C and 5% CO2 until confluent. When PTCs reached confluence, they were detached with trypsin and splitted into two 75cm^2 flasks (TPP).

Sertoli cells:

The tubules remaining after the PTC isolation were resuspended in 5ml hyaluronidase solution (1mg hyaluronidase (Sigma) + 0.006mg DNAse/ml). Tubules were incubated at 34ºC for 15 minutes and shacked with 60 cycles/minutes. Afterwards tubules were pipetted up and down with a 5ml pipette for 5 times. Subsequently, 20 ml DMEM-F12 was added to dilute the hyaluronidase. Cells were centrifuged at 400 x g for 3min and the supernatant discarded. The pellet was resuspended in DMEM / F12 and filtered into a new reaction tube through a 100µm cell strainer to remove clumps. Another 10ml medium were added and the suspension centrifuged at 400 x g 3min. The pellet was resuspended in 2ml DMEM + 0.1% BSA and cells counted. Sertoli cells were diluted to a concentration of 1 x 10^6/ml in DMEM + 0.1% BSA. Cells were seeded in a 24 well plate (0,5*10^6 cells per well) and incubated for 48 hours at 34°C in 5% CO_2.

2.2.2 Immunological Methods

Flow cytometry and fluorescence-activated cell sorting (FACS)

To measure surface marker expression of specific proteins, cells were thawed or detached from the culture dish and washed on time in PBS. Cells were adjusted to up to 1 x 10^6/100 µl and the Fc-receptors were blocked for 20 min at 4°C by either 5% human serum (Sigma) for human cells or purified anti-mouse CD16/32 (Biolegend) for mouse cells in FACS buffer. Afterwards cells were washed and resuspended in 100 µl FACS buffer containing specific monoclonal and polyclonal antibodies labelled with various fluorochromes. Specificity of the stainings was controlled by isotype control stainings or fluorescence minus one stainings. After staining, cells were washed twice with 150µl FACS buffer and resuspendend in 200 µl FACS buffer. To discriminate between living and dead cells 2 µl of 7-amino-actinomycin D (7AAD, Biolegend) was added per sample 10 min prior measurement. Fluorescent signals were measured using a FACS Canto II flow cytometer (BD Biosciences). And analysed using

the FlowJo software (TreeStar). FACS was performed on a FACSAriaIII (BD Biosciences. Before sorting, cells were filtered through a 70µm cell strainer (Miltenyi). Selected cell populations were collected in FCS and purity was analysed by an instant analysis by flow cytometry of part of the collected cells.

FACS buffer: PBS + 3% FCS + 5mM EDTA (Sigma)

Cell sorting by MACS MicroBeads

Mouse B-cells from the spleen were isolated by magnetic-activated cell sorting (MACS). Therefore, a single cell suspension of the spleen was prepared, and cells labelled with CD19 micro beads (Miltenyi). The positive fraction was used for further experiments. For detailed instructions see manufacturer manual. CXCR4 KO cells generated by CRISPR/Cas9 were enriched by staining cells with an anti-CXCR4 PE antibody (R&D) before labelling the cells with anti-PE beads (Miltenyi). The negative fraction was used for further culture and experiments. For detailed instructions see manufacturer manual.

Cytokine secretion assay

CXCL12 levels in human BM-MSC and testis stroma supernatants was quantified by U-PLEX assays (MSD). This technology uses an antibody conjugated with electrochemiluminescent labels binding the target analytes in a sample. These antibodies bind to U-PLEX linkers on a U-PLEX plate. For detailed instructions see manufacturer manual.

Protein quantification

Total protein concentration in human BM-MSC and testis stroma supernatants was detected by a Bradford assay (Thermo Fisher Scientific). This assay is a coomassie dye-binding assay allowing the quantification of total protein in an analyte. For detailed instructions see manufacturer manual.

2.2.3 *In vivo* experiments

Adoptive transfer of PDX-ALL cells

Cells for adoptive transfer were freshly thaw, cell suspensions were washed three times with PBS (350g, 5 min, 4°C), counted and an appropriate cell number resuspended in 100 µl cold RPMI 1640 per mouse. Cell suspensions were stored on ice until injection.

Experiments were performed with three to four- or twelve-week-old mice. Tumour cells (1 x 10^4 or 1 x 10^6 per animal) were transplanted by intravenous injection (i.v) after mice were exposed for 10 min to red light. IVIS spectrum imaging and blood analysis monitored tumour growth **(Figure 6)**.

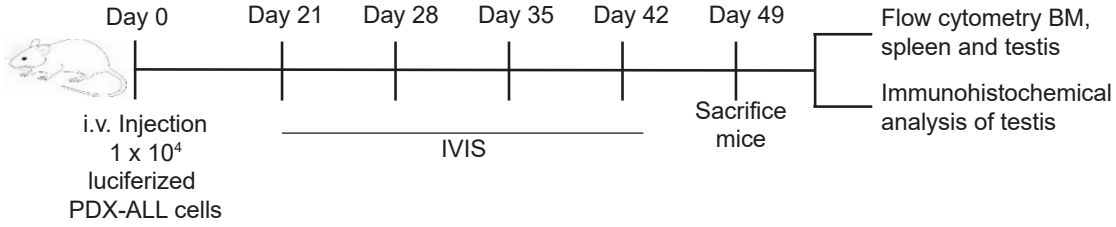

Figure 6: Experimental setup of PDX-ALL cell transplantation into NSG mice. PDX-ALL cells were i.v. injected into the tail vein. From day 21 tumour growth was monitored by IVIS imaging. Mice were scarified when ALL specific symptoms were observed, defined in the guidelines approved by Landesamt für Gesundheit und Soziales Berlin, Germany.

BM transfer

The BM of one C57BL/6N mouse was isolated and adoptively transferred into two NSG mice by i.v. injection. After three weeks NSG mice were sacrificed and the spleen and testes macrophages were analysed for their MHCII and CD64 expression.

In vivo imaging

Mice were anesthetised by isoflurane (Abbot) exposure (2.5 % isoflurane in oxygen) in a XGI-8 Gas Anesthesia Chamber (Caliper Life Science). The substrate luciferin (Biosynth)(150 µg/mouse in PBS) was intraperitoneal (i.p.) injected and after 10 min mice were placed onto the 37°C heated imaging platform of the Xenogen IVIS 2000 (Caliper LifeScience). Detector exposure times between 1 and 240 s and small binning were used to image the mice.

Determination of tumour burden in peripheral blood

Additionally, to *in vivo* imaging the tumour burden was monitored by blood analysis during later stages of the disease. Therefore, mice were anesthetised using isofluran and blood was taken retrobulbar and directly transferred to a 1.5 ml tube containing 50 µl 0.5 M EDTA to prevent clotting. Blood was taken up in 5 ml hypotonic lysis buffer for up to 5 min at RT to deplete erythrocytes. Suspensions were centrifuged for 5 min at 350g and 4°C and remaining cells were resuspended in FACS buffer and further processed for flow cytometry analysis.

Blockage of the CXCR4-CXCL12 pathway in NSG mice

PDX-ALL transplanted mice were treated i.p. twice weekly from day 4 after transplantation with either anti-human CXCR4 or anti-IgG2a antibody. In total each mouse received six antibody injections. The first three times mice were treated with 50 µg/mouse, afterwards the dose was increased to 100 µg/mouse.

Isolation of lymphoblast's from bone marrow, spleen, blood and testis

When mice displayed ALL specific symptoms, they were sacrificed and tumour cells from BM, spleen, blood and testes were examined. Blood was withdrawen from the heart using a 25 G syringe containing 50 µl 0.5 M EDTA. BM lymphoblast's were isolated by dissecting femur and tibia and flushing the BM with 10 ml ice-cold FACS buffer per bone using a 25 G syringe. The spleen and testes were gently disrupted in ice-cold FACS buffer and applied to a cell strainer (100 µm) too. Cell suspensions of the organs were centrifuged for 5 min at 350g and 4°C.

BM, blood and spleen were treated with 5 ml hypotonic lysis buffer for up to 5 min at RT to deplete erythrocytes. Suspensions were centrifuged for 5 min at 350g and 4°C and remaining cells were resuspended in FACS buffer and further processed for flow cytometry analysis or cryopreservation.

Hypotonic lysis buffer: 1.7 M Ammonium chloride (Sigma)
100 mM Potassium bicarbonate (Sigma)
1 mM EDTA

2.2.4 Histology

Fixation of spleen and testis in paraformaldehyde

For histopathology, testis and spleen were collected from all scarified mice and fixed in 4% phosphate-buffered formaldehyde (PFA, Roth) for 24 hours. Organs were removed from the PFA solution and dehydrated by an ethanol dilution series before embedding in paraffin for about 24 hours (tree exchanges of paraffin). The embedded organs were cut into 5 µm sections on a rotary microtom (HM 355S), transferred onto superfrost plus slides (Menzel) and stained with hematoxylin (Roth) and eosin (Roth) using a Thermo Scientifc Microtom HMS 740 robot-stainer.

Immunohistochemical staining

To remove paraffin and rehydrate the sections of testis and spleen was either removed by a xylol (Roth) and acetone (BD) /Tris (Sigma) treatment or by a xylol and ethanol dilution series. Afterwards sections were boiled for 5 min in citric buffer a pressure cooker before they were treated for 30 min 0,4% Triton X 100 in PBS + serum to block to block unspecific binding regions. Subsequently, the blocking solution was removed, and the sections were incubated with the antibody solution at 4°C over night. Next day, the antibody solution was removed, and sections were washed three times with TBST buffer before the secondary

antibody solution was applied for 1 hour at RT. Afterwards sections were washed three times with TNT buffer and treated for 3 min with a DAPI solution. When sections were washed a last time with TNT buffer, they were Images were prepared for imaging. Images were recorded using an AxioCam MRm (Zeiss) camera for bright field or an AxioCam MRc2 (Zeiss) camera for fluorescence images. Images were further processed with the Axio Vision 4.5 system (Zeiss).

Citric buffer:

Solution A	0.1 M Citric acid mono hydrate (Roth)
Solution B	0.1 M Trisodium citrate dehydrate (Roth)
	20 ml Solution A + 90 ml Solution B in 1000 ml distilled water

TBST buffer:	0.5 M Tris base (Roth)
	1.5 M Sodium chloride (Roth) in 1000 ml distilled water, pH 7.6,
	+500 µl Tween 20 (Roth)

2.2.5 Molecular biology

RNA Isolation, cDNA synthesis and qRT-PCR

Cells were resuspended in 350 µl RLT lysis buffer (Qiagen) supplemented with 1% b-mercaptoethanol (Thermo Fisher Scientific) and either stored at -80°C or immediately used for RNA isolation. RNA was isolated by using the RNeasy Micro or Mini Kit including the RNase-free DNase Set (Qiagen) according to the manufacturers instructions. The RNA concentrations were determined spectrophotometrically at an OD of 230 nm. For transcribing the isolated RNA into complementary DNA (cDNA), the SuperScript VILO cDNA Synthesis Kit (Thermo Fisher Scientific) or the SuperScript III First-Strand Synthesis SuperMix for qRT-PCR (Thermo Fisher Scientific) was used according to the manufacturer’s instructions. Afterwards, quantitative real-time PCR (qRT-PCR) analysis was performed by using TaqMan probes that anneal specifically, to a complementary sequence between forward and reverse primer sites. The reaction was done in 10 µl by adding 200 ng cDNA, 1x TaqMan Gene Expression Assay and 1x TaqMan Gene Expression Master Mix. Reactions were performed in duplicates using the Applied Biosystems StepOnePlus Real-Time PCR system. The expression of a gene of interest (GOI) was calculated relative to the expression of a housekeeping gene (Gapdh or B2M) by using the following formula:

Relative gene expression (GOI to Gapdh) = $2^{-[Ct(GOI)-Ct(house\ keeper)]}$

(Ct = mean value of in duplicates measured Ct (cycle threshold) value)

Generation of a Cas9-CXCR4 *knock-out* vector

The pSpCas9(BB)-2A-Puro (PX459) plasmid includes Cas9 with a puromycin resistance and a cloning backbone for sgRNA. To insert sgRNAs into the backbone, following steps were performed:

The sgRNA was annealed and frozen until further processing:

496 µl TE Buffer (0.01 M Tris-HCl, 1 mM EDTA)

2µl sgRNA forward

2µl sgRNA reverse

95°C for 5 min

RT 30 min

The Cas9 plasmid was digested with BbsI high fidelity (NEB):

1µg px459 plasmid

5µl Smart Cut

1µl BbsI

Add water to a total of 50 µl

37°C for 30 min

65°C for 20 min

DNA fragments were resolved by base pair size using an agarose gel electrophoresis (1 % agarose, 0.5 µg/ml ethidium bromide gel) run at 100 V. DNA bands with intercalated ethidium bromide were visualized with ultraviolet light excitation. Fragments with the desired base pairs size were manually extracted from the gel and DNA was isolated using a gel extraction kit (Qiagen). For detailed instructions see manual.

The annealed sgRNA fragments and the digested px459 plasmid were ligated with the Quick Ligation Kit (NEB):

1µl px459

1 µl sgRNA

2 µl T4 buffer

1 µl T4 ligase

Add water to a total of 20 µl

16°C o/n

The generated construct was used for a transformation.

Transformation

The chemically competent *Escherichia coli* (*E.coli*) strain XL10Gold cells were thaw for 30 min on ice before 200 µl of the cell suspension was added to the ligation reaction. The suspension was incubated another 30 min on ice, then they were transferred to a 42°C water bath for 90 s. Afterwards they were cooled for 2 min on ice before 800 µl Soc medium was added. The cell suspension was incubated at 37°C for 1 hour at 550 rpm. Subsequently, the suspension was centrifuged at 25°C for 2 min at 5000 rpm, the supernatant was discarded, and the pellet resuspended in the remaining medium. Afterwards, the mix was plated onto LB-agar plates containing 100 µg/ml ampicillin (Roth).

SOC medium:	2 % tryptone (Roth), 0.5 % yeast extract (Roth), 10 mM sodium chloride (Roth), 2.5 mM potassium chloride (Roth), 20 mM glucose (Roth), 10 mM magnesium chloride (Roth), 10 mM magnesium sulfate (Roth), add 1 l distilled H2O
LB medium:	1 % tryptone (Roth), 1 % Sodium chloride (Roth), 0.5 % yeast extract (Roth)
LB-agar:	1.5 % agar (Roth) in LB medium

Plasmid DNA extraction and sequencing

For small-scale DNA extraction plasmid DNA from transformed *XL10Gold* cells was extracted using the PureYield Plasmid Miniprep System (Promega). The PureYield Plasmid

Miniprep System (Promega) was used for larger scale plasmid DNA preparations. Sanger DNA sequencing conducted by Eurofins Genomics verified the plasmid sequence.

Electroporation of Nalm6 cells

Nalm6 cells were transfected with the px459-CXCR4 KO plasmid by electroporation using the Amaxa Cell Line Nucleofector Kit T (Lonza). Each reaction was performed with 2µg plasmid DNA. Electroporation was performed in an Amaxa Nuleofector II (Lonza) using the program C-005. For detailed instructions see manufacturers manual. Transfected Nalm6 cells were cultured for two days before 0.5µg/ml puromycin (Thermo Fisher Scientific) was added to the media to enrich the successfully transfected cells.

2.2.6 Statistics

Prism version 5.0a (GraphPad) was used to analyse data and to calculate the statistical significance of differences between groups. Results are presented as arithmetic means ± standard error of the mean (SEM) or standard deviation (SD). Data were either analysed by using the Student`s unpaired two-tailed t-test (normally distributed data) or the unpaired Mann-Whitney U test (non-normally distributed data). To analyse matched groups the non-parametric Wilcoxon signed-rank test was used. Values of $p<0.05$ were considered to be statistically significant and marked with one asterisk. Values of $p<0.01$ were illustrated with two asterisk and $p<0.001$ with three asterisks.

3 Results

3.1 Homing receptor expression on paediatric patient ALL samples at initial diagnosis and relapse

ALL cells express so-called homing receptors on their surface that mediate cell infiltration of cancer cells towards their niches[148,149]. The expression of certain receptors enables the population of different niches. Therefore, comparing the homing receptors of paediatric patient samples with different relapse sites might reveal differences in their expression pattern of chemokine receptors or adhesion molecules.

3.1.1 CXCR4 is the only chemokine receptor consistently expressed on paediatric ALL patients samples

Chemokine receptors are a crucial element in immune cell migration. However many tumour cell types also express these receptors and benefit from enhanced survival and homing[108]. Data for chemokine receptor expression in ALL are often inconsistent and analysed cohorts small[109,150]. In order to close this gap, a selection of chemokine receptors was analysed on a cohort of paediatric patient samples. Prior to analysing patient material, 18 chemokine receptors were tested in ALL cell lines. Promising candidates, which were expressed on these cell lines, were included into the following characterisation of primary tumour samples. Therefore, mononuclear cells (MNCs) isolated from BM samples from a cohort of paediatric relapsed ALL patients were analysed for nine chemokine receptors (CCR5, CCR7, CCR9, CXCR1, CXCR2, CXCR3, CXCR4, CXCR5 and CXCR7) using flow cytometry. Cells were first gated single and live cells and secondly on distinct surface markers (B-ALL: CD19, CD45; T-ALL: CD3, CD45) to define the lymphoblast population before the protein of interest was analysed. The cohort included MNCs isolated from BM samples from initial diagnosis and relapse and was subdivided into different relapse groups (isolated BM relapse, combined CNS relapse and combined testis relapse). In total 30 patients were analysed, most of them are represented at initial diagnosis and relapse**. Figure 7** shows representative histograms of the analysed chemokine receptors. A majority of the patients were negative for most receptors regardless of the time of withdrawing the sample or the site of relapse. CXCR1, CXCR2, CCR5, CCR9, and CXCR7 were never detected, CCR7, CXCR3 and CXCR5 were only found in a few samples spreaded throughout the groups (**Table 12**). CXCR4 was expressed at high levels in all measured samples, irrespective of the relapse site. Based on these results, CXCR4 was considered to be the only chemokine receptor, which is consistently expressed by all paediatric ALL patients.

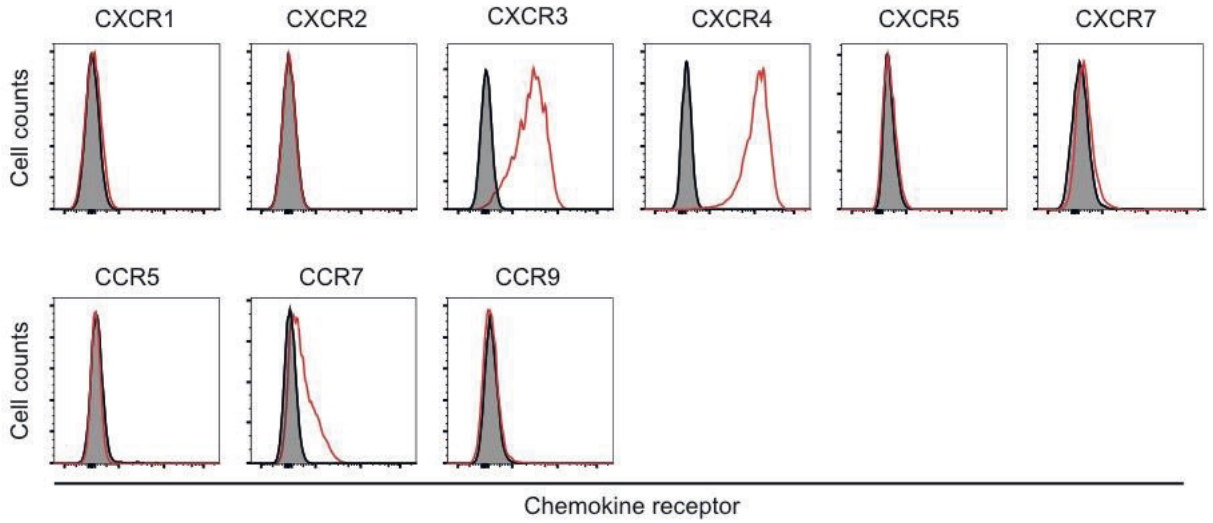

Figure 7: Representative histograms showing chemokine receptor expression on ALL patient samples. Patient samples were stained with an anti-chemokine receptor antibody or its matching isotype control. Doublets and dead cells were excluded. A representative histogram for each chemokine receptor is shown. In total 55 patient samples were analysed. Histograms display fluorescence intensity, black filled lines represent the isotype control, and red solid lines show anti-chemokine receptor staining.

Based on the results presented above, the CXCR4 expression pattern was analysed in detail. **Figure 8** displays the expression levels of CXCR4 in samples withdrawn at initial diagnosis and at relapse diagnosis. No significant difference was observed in the expression level of CXCR4 in patients with testicular involvement compared to those with CNS involvement or an isolated BM relapse (**Figure 8A**). This observation accounted for the initial diagnosis or the relapse situation. Since patient samples of the initial diagnosis as well as from relapse diagnosis were available a matched pair analysis was performed (**Figure 8B**). Nevertheless, no significant change in CXCR4 expression was found comparing initial diagnosis and relapse. These flow cytometry results indicate the relevance of CXCR4 expression for ALL cells in different tumour niches in the early stages of the disease as well as in the relapse situation.

Table 12: Chemokine receptor expression of primary ALL samples.

	CCR7		CXCR3		CXCR4		CXCR5	
	Diagnose	Relapse	Diagnose	Relapse	Diagnose	Relapse	Diagnose	Relapse
BM 1	-	-	+	-	++	+++	-	-
BM 2	-	-	-	-	+++	+++	-	-
BM 3	-	-	-	-	++	++	-	-
BM 4	-	-	-	-	+++	++	-	-
BM 5	-	+	+	-	+++	+++	-	-
BM 6	-	-	-	++	++	+++	-	-
BM 7	-	-	-	-	++	++	-	-
BM8	++	/	++		+++	/	-	/
BM 9	-	-	-	-	+++	++	-	-
BM 10	-	-	-	-	++	+++	-	-
BM 11	/	-	/	+	+++	+++	/	-
BM 12	+	-	-	-	+++	++	-	-
BM 13	-	-	-	-	+++	+++	-	-
CNS 1	++	-	-	+	+++	+++	+	-
CNS 2	-	-	-	-	+++	+++	-	-
CNS 3	-	-	-	-	++	+++	-	-
CNS 4	-	-	-	-	++	+++	-	-
CNS 5	-	-	+	++	+++	++	-	-
CNS 6	-	-	-	-	++	++	-	-
CNS/Testis	-	/	-	/	++	/	-	/
Testis 1	-	-	-	-	+++	+++	-	-
Testis 2	-	/	-	/	++	/	-	/
Testis 3	-	-	-	-	+++	++	-	-
Testis 4	-	-	-	-	++	++	-	-
Testis 5	-	/	-		+++	+++	-	/
Testis 6	-	-	+	-	+++	+++	-	-
Testis 7	-	-	-	+	+++	++	-	-
Testis 8	-	-	-	-	+	+	-	-
Testis 9	-	/	-	/	++	/	-	/
Testis 10	/	-	/	-	/	++	/	-

Chemokine receptor expression intensity was classified based on the measured MFI. MFI <200 -; MFI 200-500 +; MFI 500-2000 ++; MFI >2000 +++.

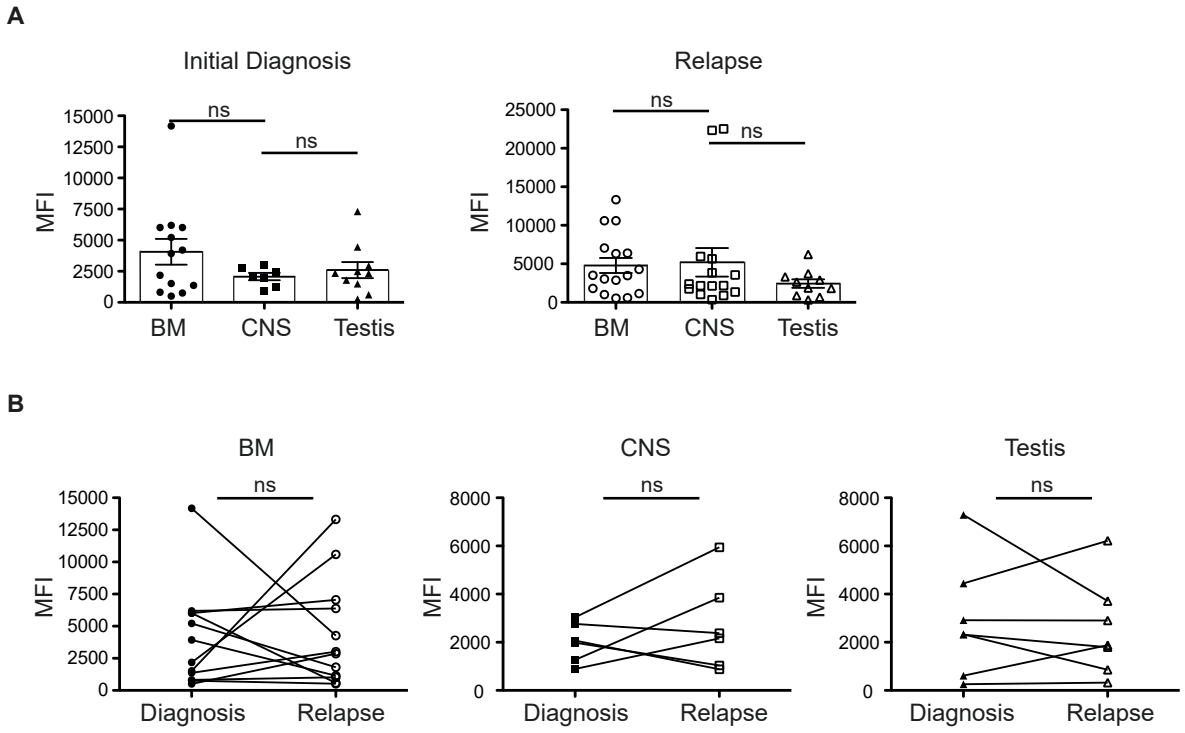

Figure 8: CXCR4 expression in BM samples, at different time points and subdivided into different relapse sites. (A) Statistically analysis of CXCR4 expression levels. Values are displayed as single measurements, p values (*p<0.05) were calculated by Mann-Whitney U test, ns=not significant, BM Diagnosis n=13; BM Relapse n=16; CNS Diagnosis n=7; CNS Relapse n=15; Testis Diagnosis n=10; Testis Relapse n=10 Values are displayed as mean ± SEM. **(B)** Matched pair analysis of samples taken at initial diagnosis and at relapse diagnosis for different relapse sits. Values are displayed as single measurements, p values (*p<0.05) were calculated by Wilcoxon signed rank test, ns=not significant, BM n=12; CNS n=6; Testis n=7, MFI= Mean fluorescence intensities.

3.1.2 IL7R is up-regulated on ALL cells of paediatric patients with testicular involvement

Despite its main function during human T-cell development, the IL7R and its ligand the cytokine IL7 are thought to take part in T-ALL progression and are considered to be associated with CNS infiltration and relapse in paediatric B-ALL[151,152]. Therefore, the IL7R was included into the analysis panel used to phenotypically characterise the patient samples. As displayed in **Figure 9A** the IL7R was expressed on ALL cells at an early stage of the disease at the time of initial diagnosis as well as in relapse samples. However, patients developing a relapse with testicular involvement had a significant higher IL7R expression compared to patients that develop an isolated BM relapse or a relapse with CNS involvement (**Figure 9B**). The IL7R up-regulation in patients evolving a testicular relapse was manifested during the initial diagnosis and was still present in the relapse samples. Nevertheless, performing a matched pair analysis revealed no significant change in IL7R expression during initial diagnosis and relapse (**Figure 9C**). While the role of IL7R expression was already

described for CNS infiltration, the presented results provide evidence for its relevance in testicular relapse.

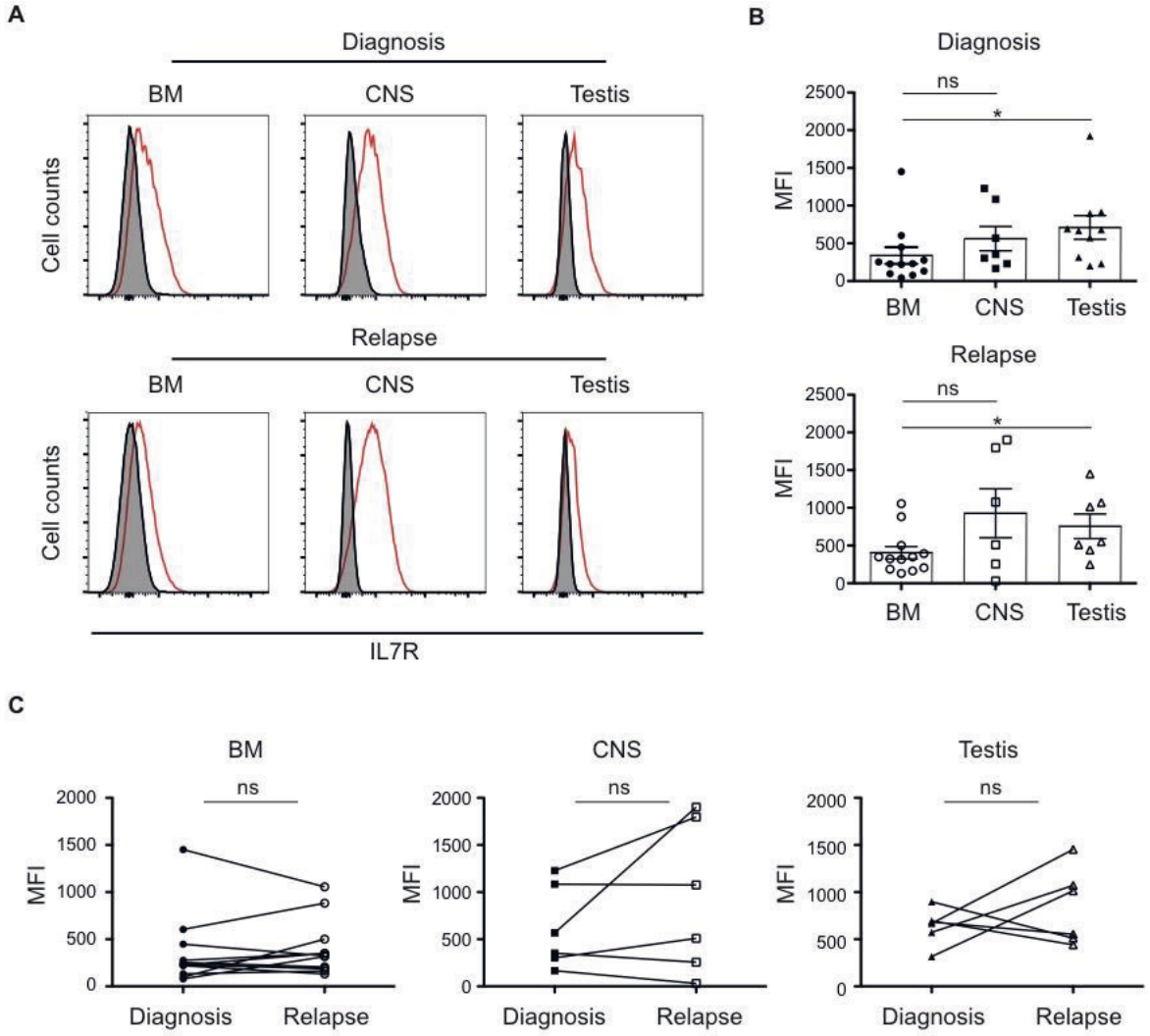

Figure 9: IL7R expression in BM samples, at different time points and subdivided into different relapse sites. (A) Representative histograms of IL7R expression during initial diagnosis and relapse subdivided into relapse sites. Patient samples were stained with an anti-IL7R antibody or its matching isotype control. Doublets and dead cells were excluded. A representative histogram for each relapse site is shown. Histograms display fluorescence intensity, black filled lines represent the isotype control, red solid lines show anti-IL7R staining. **(B)** Statistic analysis of IL7R expression levels. Values are displayed as single measurements, p values (*p<0.05) were calculated by Mann-Whitney U test, BM Diagnosis n=12; BM Relapse n=12; CNS Diagnosis n=7; CNS Relapse n=6; Testis Diagnosis n=10; Testis Relapse n=7 Values are displayed as mean ± SEM **(C)** Matched pair analysis of samples taken at initial diagnosis and at relapse diagnosis for different relapse sits. Values are displayed as single measurements, p values (*p<0.05) were calculated by Wilcoxon signed rank test, ns=not significant, BM n=12; CNS n=6; Testis n=7, MFI=Mean fluorescence intensities.

3.1.3 Adhesion molecules are similarly expressed on patient cells from all relapse groups

While chemokine receptors are important molecules to induce cell migration of haematopoietic cells and tumour cells, adhesion molecules are another central element of

cellular movement. Migration through the blood and lymphatic vessels is coordinated by adhesion molecules, which react to ligands produced by the extracellular matrix and stromal cells. These adhesion molecules play a central role during haematopoiesis by regulating interaction between haematopoietic cells and the BM microenvironment[153,154]. Frequently expressed adhesion molecules on ALL cells are CD11a, CD44 and CD49d[154]. CD44 down-regulation on B-ALL cells might be associated with the migration of leukaemia cells from BM to other organs[155]. CD11a and CD49d were described to be involved in mediation of transendothelial migration of monocytes[156]. Therefore, these molecules might be interesting candidates for ALL cell infiltration of extramedullary organs. On the other hand, CD49d is also involved in the development of cell adhesion-mediated drug resistance, which is a serious problem in relapsed ALL treatment[157]. The stated adhesion molecules were analysed in the paediatric patient samples and expression levels compared between different sites of relapse. As shown in **Figure 10** all three markers are expressed at high levels. CD44 displayed the highest expression with mean values above a MFI of 10,000. This high expression was seen in samples from initial diagnosis and relapse and no significant difference could be observed between the different relapse groups. This also accounts for CD49d with mean MFI values between 7,000 and 10,000 and CD11a, which had the lowest expression of the three markers with a mean MFI of around 2,000. As seen in CXCR4 and IL7R measurements, patient samples are very heterogeneous and also the adhesion molecule markers showed this characteristic.

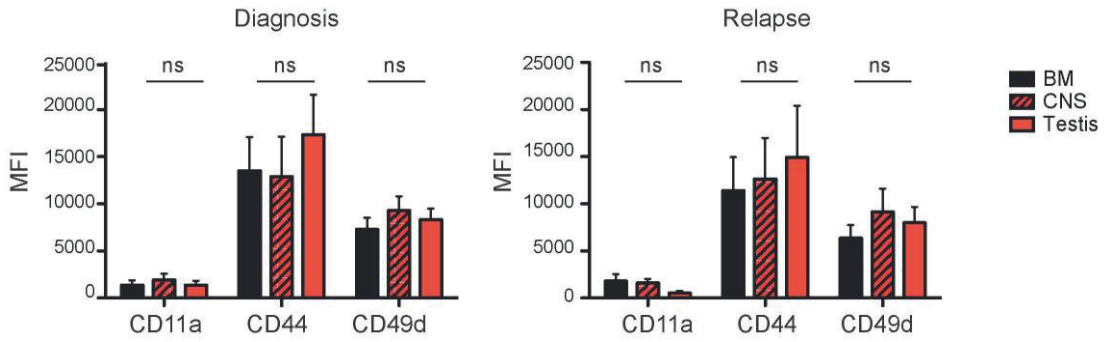

Figure 10: Adhesion molecule expression on ALL patient samples at different time points, subdivided into different relapse sites. Statistical analysis of CD11a, CD44 and CD49d expression levels. Values are displayed as mean ± SEM, p values (*p<0.05, ns=not significant) were calculated by Mann-Whitney U test, BM Diagnosis n=12; BM Relapse n=11-12; CNS Diagnosis n=7; CNS Relapse n=6; Testis Diagnosis n=10; Testis Relapse n=7, MFI= Mean fluorescence intensities.

The matched pair analysis reveals the great heterogeneity of the adhesion marker expression in patient ALL cells. Comparing CD11a expression in ALL samples from initial diagnosis and relapse showed an inconsistent regulation in all relapse groups (**Figure 11A**). While CD11a expression stayed stable in the majority of the patients some showed an up and other a down-regulation of this adhesion marker from initial diagnosis compared to

samples taken at relapse diagnosis. However, changes in expression pattern was not significant in any of the relapse groups.

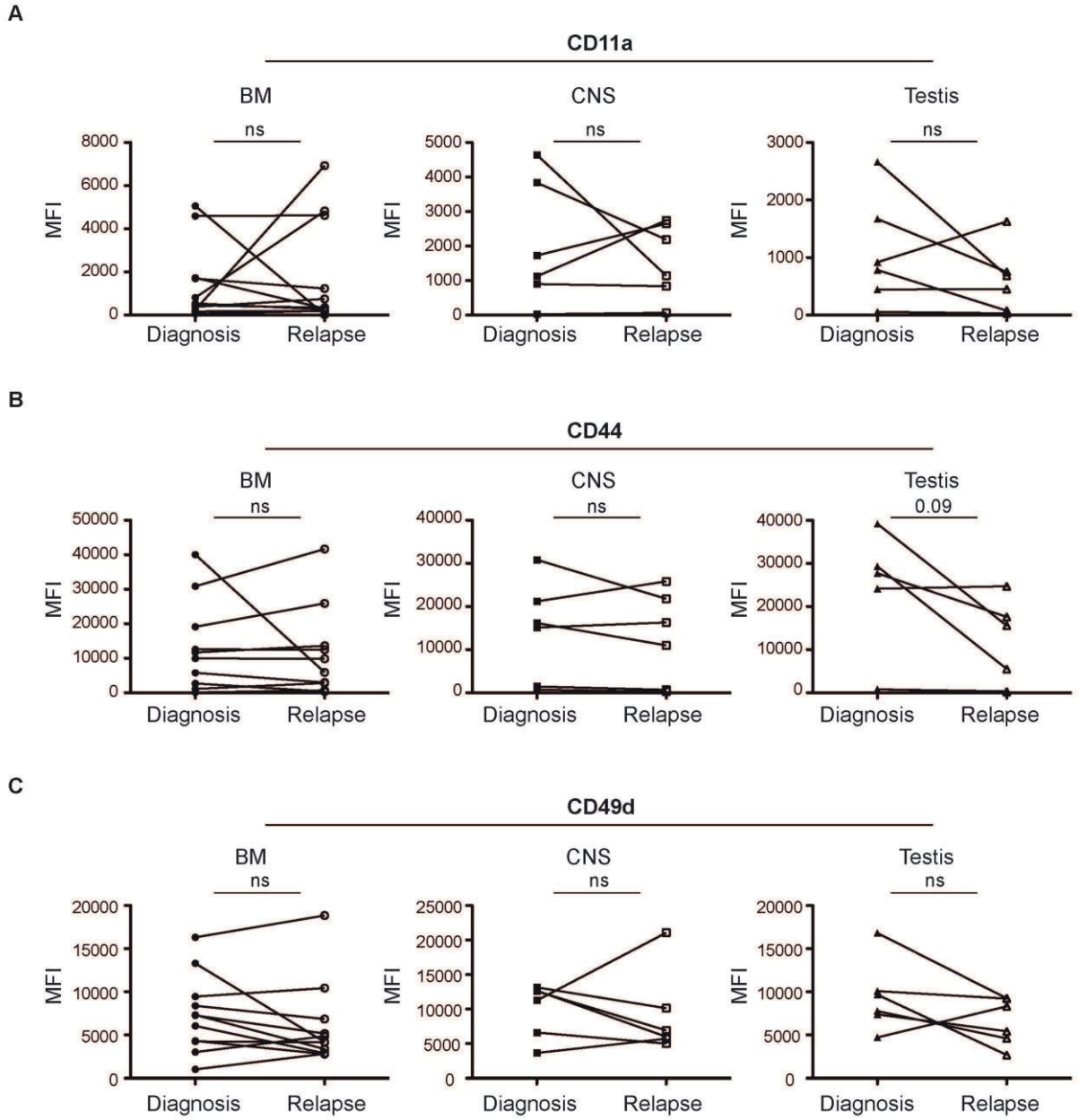

Figure 11: Matched pair analysis of adhesion molecule expression of initial diagnosis and relapse samples. (A) Matched pair analysis of CD11a expression of samples taken at initial diagnosis and at relapse diagnosis for BM, CNS and testis relapse. **(B)** Matched pair analysis of CD44 expression of samples taken at initial diagnosis and at relapse diagnosis for different relapse sits. **(C)** Matched pair analysis of CD49d expression of samples taken at initial diagnosis and at relapse diagnosis for different relapse sits. Values are displayed as single measurements, p values (*p<0.05) were calculated by Wilcoxon signed rank test, ns=not significant, BM n=10-11; CNS n=6; Testis n=6, MFI= Mean fluorescence intensities.

As displayed in **Figure 11B**, patients with an isolated BM or combined CNS relapse showed a stable CD44 expression at initial diagnosis and relapse. In contrast patients with a

testicular involvement had a tendency towards a down-regulation of CD44 in samples taken at relapse diagnosis (p=0.09). CD49d was consistently expressed in the majority of the patients and no significant changes could be observed between initial diagnosis or relapse in any of the groups (**Figure 11C**). The strong expression on all analysed patient samples throughout the different groups indicate the important role of these molecules for ALL development and migration, regardless of the relapse site. Since the expression level of the three markers is stable throughout the course of the disease, it seems an up or down-regulation is not nesseccary for the infiltration of extramedullary sites. However CD44 might be down regulated in testis relapse patients but a larger cohort would be required to get a clear picture.

3.2 Primary testicular stroma and BM-MSCs support ALL cell survival

Primary ALL cells are difficult to study *in vitro* due to a lack of suitable culture conditions. Cells get apoptotic within a few hours when kept in culture dishes, which weakens their experimental accessibility. However, in recent years many studies were published using MSCs as a feeder cell layer to cultivate primary leukaemia cells. These cells are generated mostly from patients BM samples and were described to support short- and long-term *in vitro* maintenance of ALL cells and were used for studying chemoresistance in T-ALL[158,159]. BM-MSCs secrete CXCL12 and were already used to study the migration behaviour of ALL cells *in vitro*[160].

BM and testis derived stroma cells from 15 patients were analysed for their MSC characteristics and used to study their support in ALL migration and survival within an *in vitro* co-culture system.

3.2.1 Common MSC markers are highly expressed by BM-MSCs and testicular stroma

Human MSCs are multipotent cells and can be retrieved from BM and many other tissues. To validate their homogeneity several markers are used to characterise MSCs. By now, a cell is considered to be a MSC when expressing CD29, CD44, CD73, CD90, CD105 and CD146 while being negative for CD19 and CD45[161–163]. This panel was used to characterise stromal cells derived from BM and testis of paediatric ALL patients by flow cytometry[163]. In total 15 BM and 15 testis derived stroma samples were analysed for their MSC characteristics. After having been cultured for one week, patient samples were analysed at passage 4 to 6. All markers, except CD19 and CD45 were expressed on both, BM and testis derived stroma,

though expression levels were very heterogeneous. As displayed in **Figure 12** BM-MSCs had higher expression levels of all markers, but only CD29, CD90 and CD146 were significantly higher compared to the testis-derived cells. Considering these results, stroma cells derived from either BM or testis fulfil the criteria to be considered as MSCs.

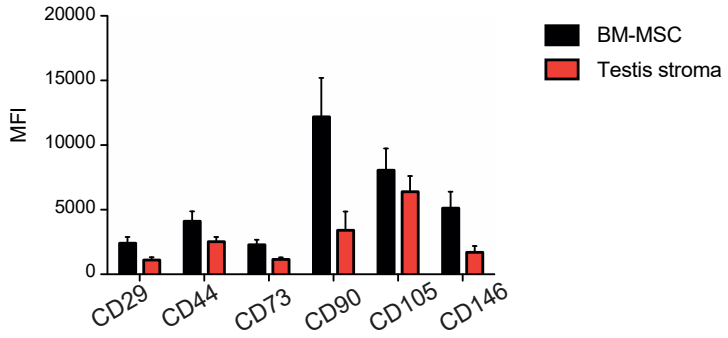

Figure 12: Characterisation of BM-MSCs and testis stroma for MSC marker expression. Representative Expression of CD29, CD44, CD73, CD90, CD105 and CD146 were analysed by flow cytometry. Prior measurement cells were cultured for about one week. Samples were at passage 4 to 6 at the day of characterisation. Values are displayed as mean ± SEM, p values (*p<0.05, ***p<0.001, ns=not significant) were calculated by Mann-Whitney U test, BM-MSC n=15; Testis stroma n=15, MFI= Mean fluorescence intensities.

3.2.2 Testicular stroma and BM-MSCs, prevent pre-apoptotic and apoptotic death of primary ALL cells in an *in vitro* co-culture

ALL cell lines provide a useful tool to perform *in vitro* functional studies. However, despite conserving their original mutations, they adapt to culture conditions and do not relay any longer on niche support[159]. Therefore, cell lines are unsuitable to study *in vitro* ALL-niche interaction. Primary ALL cells on the other hand are depending on their environment and undergo apoptosis within a few hours when kept in mono-culture. Co-culturing primary patient samples with BM-MSCs, however is thought to prevent apoptotic cell death to a certain extent[164,165]. Seven primary ALL samples were co-cultured for 48 hours with five BM-MSC donor samples and testicular stroma samples. All seven ALL samples were additionally cultured without a stroma feeder layer in mono-culture. Apoptosis was measured by flow cytometry analysis of Annexin V and 7AAD. As shown in **Figure 13** the viability of the mono-cultured primary ALL after 48 hours is highly diverse. When co-cultured with either BM-MSCs or testicular stroma primary ALL cells showed no significant difference in viability compared to the mono-cultured cells. However, while most ALL cells in mono-culture were already apoptotic after 48 hours, co-culture kept them in a pre-apoptotic state for a longer period. Both, BM-MSCs and testicular stroma led to a significantly higher percentage of primary ALL cells that were pre-apoptotic, while a significantly lower part was already apoptotic. Despite this positive effect on most primary samples, two donors had a disadvantage when cultured

with stroma cells. These samples showed the highest viability when mono-cultured. Overall, testicular stroma and BM-MSCs prevent pre-apoptotic and apoptotic death of primary ALL cells in an *in vitro* co-culture.

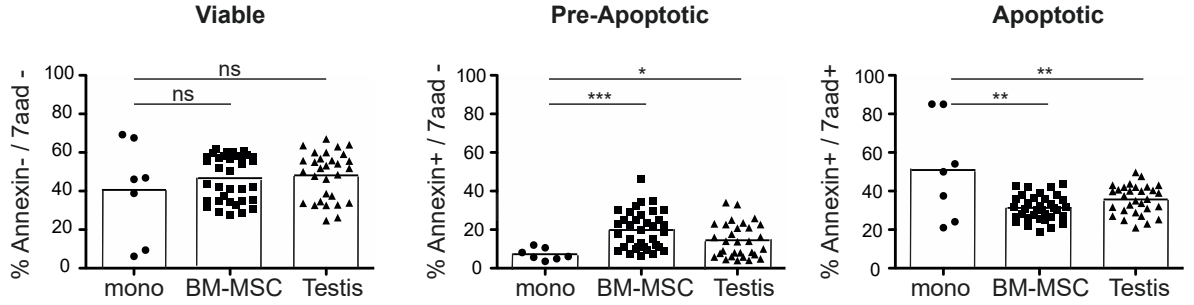

Figure 13: Co-culture of primary patient ALL samples with primary patient stroma. Cells were cultured for 48 hours at 37°C in RPMI + 1% FCS + 1% P/S. Apoptosis was analysed by flow cytometry. Values are displayed as mean ± SEM, p values (*p<0.05, **p<0.01, ***p<0.001, ns=not significant) were calculated by Mann-Whitney U test, mono-culture n=7; BM-MSC co-culture n=35; Testis stroma co-culture=35.

Another factor that might be supported by MSCs is the *in vitro* proliferation of primary ALL cells. Cell cycle phases of co-cultured primary ALL cells were analysed by flow cytometry using a propidium iodide staining. Within the S-phase cells replicate their DNA, therefore this phase indicates how many cells were actively proliferating in culture. As displayed in **Figure 14** most cells were in G1-phase regardless whether cultured with BM-MSCs, testicular stroma or without stromal support.

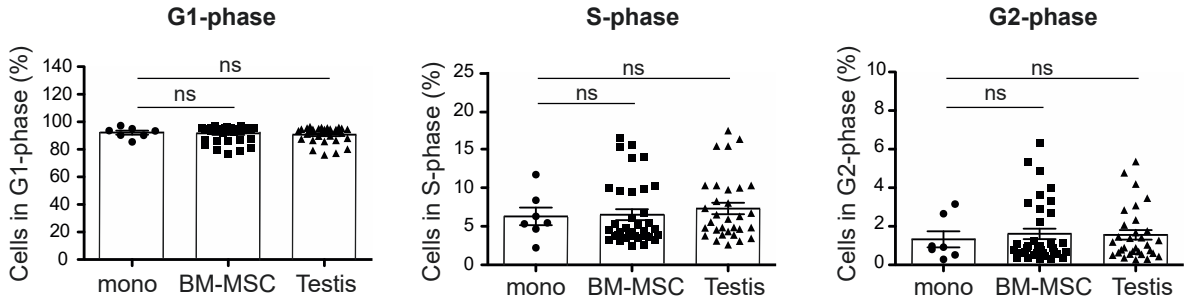

Figure 14: Cell cycle analysis of primary ALL cells in co-culture with primary patient stroma. Cells were cultured for 48 hours at 37°C in RPMI + 1% FCS + 1% P/S. Cell cycle was analysed by flow cytometry using a propidium iodide staining. Values are displayed as mean ± SEM, p values (*p<0.05, ns=not significant) were calculated by Mann-Whitney U test, mono-culture n=7; BM-MSC co-culture n=35; Testis stroma co-culture=35.

The percentage of cells that entered the S-phase varied between only 2% up to 17%. While some ALL donors seem to profit from the stroma support in most cases only about 5% of the cells enter S-phase and no significant difference can be detected between the different culture conditions. When cells successful complete the S-phase they enter the G2-phase, the

point of the cell cycle directly preceding the mitosis. Only few cells reached this stage of the cycle and as in the other phases no significant difference could be measured. Although primary patient ALL cells co-cultured with BM-MSCs or testicular stroma stayed for a longer period in a pre-apoptotic stage before being fully apoptotic, the stroma cells did not support proliferation.

3.2.3 B-ALL cell lines Nalm6 show the highest CXCR4 expression

Since primary ALL patient samples are difficult to cultivate *in vitro* different B-ALL cells lines were screened for CXCR4 expression to perform further functional experiments. The *in vitro* cell lines 697, SEM, REH and Nalm6 were selected and stained with an anti-CXCR4 antibody or it's matching isotype control and were analysed by flow cytometry. Cells were gated on single cells and dead cells were excluded by 7AAD staining. As shown in **Figure 15** all cell lines expressed CXCR4 at profound levels, however the highest expression was measured in Nalm6, while 697 displayed a moderate CXCR4 expression. Thus, Nalm6 was considered for further experiments involving the CXCR4 receptor.

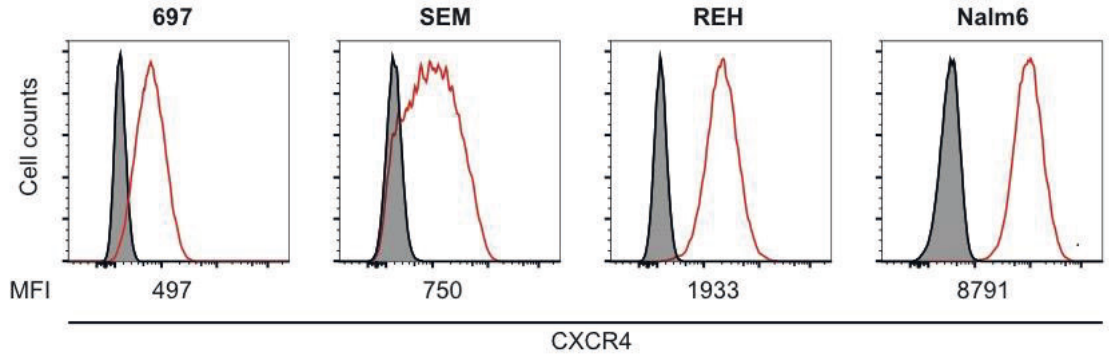

Figure 15: Flow cytometry analysis of surface expression of CXCR4 on different B-ALL cell lines. B-ALL cell lines were stained with an anti-CXCR4 antibody or its matching isotype control. Doublets and dead cells were excluded. A histogram for each cell line is shown. Histograms display fluorescence intensity, black filled lines represent the isotype control, and red solid lines show anti-CXCR4 staining. MFI= Mean fluorescence intensities.

3.2.4 CXCL12 is secreted by testicular stroma and BM-MSCs

BM-MSC and testicular stroma cells were cultured for 72 hours in reduced medium (IMDM + 1% FCS + 1% P/S) either in mono- or in co-culture with Nalm6 cells. The medium was isolated and centrifuged for 10 min at 1200 rpm. The supernatant was quick-frozen in liquid nitrogen and stored by -80°C prior analysis. After thawing the supernatants of 10 BM-MSC and 10 testis stroma samples they were analysed for their total protein yield using a Bradford assay and for the CXCL12 level using the U-Plex technology by MSD. The U-Plex assay is a sandwich immunoassay based on electrochemiluminescent labelling. As shown in **Figure 16** all tested samples contained high yields of CXCL12, and most samples showed increasing

levels when co-cultured with Nalm6 cells. Due to the high variability between the samples, no significant difference was observed between BM-MSCs and testicular stroma cells neither in mono-culture or co-culture.

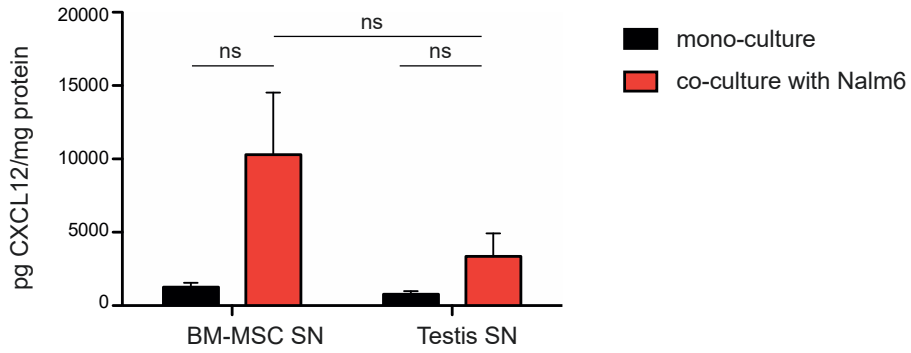

Figure 16: CXCL12 secretion of BM-MSCs and testicular stroma. The patient cells were cultured for 72 hours in reduced medium (IMDM + 1% FCS + 1% P/S) either in mono- or in co-culture with Nalm6 cells. The supernatants were analysed by the U-Plex technology of MSD. Measured CXCL12 levels were normalized to the total protein content measured by Bradford assay. Values are displayed as mean ± SEM, p values (*p<0.05, ns=not significant) were calculated by Mann-Whitney U test, BM-MSC n=10; Testis stroma n=10.

3.2.5 AMD3100 inhibits Nalm6 migration towards stroma cell supernatant

As shown in **Figure 16** BM-MSCs as well as testicular stroma cells secrete CXCL12. Culture supernatant from 11 BM-MSC and testicular stroma cell cultures was used to perform transwell migration assays with the CXCR4 expressing B-ALL cell line Nalm6. AMD3100, an antagonist strictly confined to CXCR4[166] was used to block CXCR4 mediated migration towards the culture supernatant. As displayed in **Figure 17** Nalm6 migration can be triggered by 100nM human recombinant CXCL12. Migration towards the chemokine is approximately 60-fold higher compared to medium without additional CXCL12.

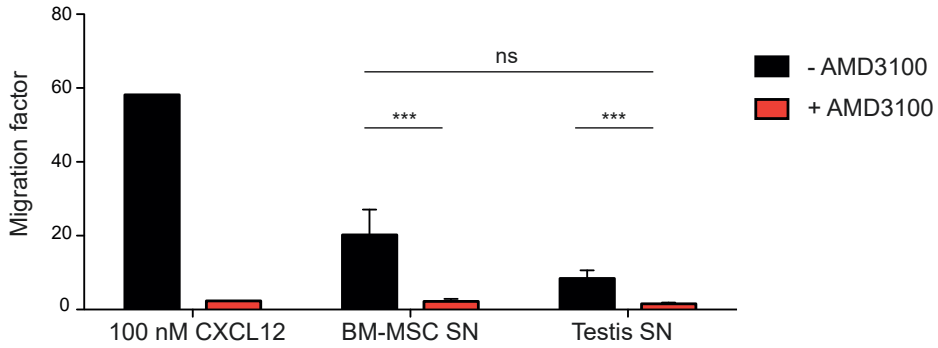

Figure 17: Nalm6 migration towards BM-MSC and testis stroma supernatant. The B-ALL cell line Nalm6 migrates towards medium supplemented with human recombinant CXCL12 (100nM), as well as towards supernatant (SN) of BM-MSC and testicular stroma cultures. Migration took place in tissue culture inserts at 37°C for 4 hours. Migration was inhibited by an AMD3100 treatment of Nalm6 cell prior transfer into the inserts. Values are displayed as mean ± SEM, p values (*p<0.05, ***p<0.001, ns=not significant) were calculated by Mann-Whitney U test, BM-MSC n=11; Testis stroma n=11.

However, when Nalm6 cells were treated with 1 µg/ml AMD3100 prior to the experiment, the number of migrating cells decreased to only 2-fold compared to the control. Both, supernatant of BM-MSC and testicular stroma cultures induced Nalm6 migration. The migratory effect of BM-MSC supernatant was stronger compared to the testis stroma supernatant, but the difference was not significant. Nevertheless, when Nalm6 cells were treated with the CXCR4 inhibitor AMD3100 migration towards supernatant was drastically reduced in both cases. These results show the specificity of the CXCR4-CXCL12 axis for Nalm6 migration towards BM-MSC and testicular stroma. By blocking only this pathway, migration was inhibited almost completely.

3.3 Establishing a CRISPR-Cas9 mediated *knock-out* (KO) of CXCR4 in Nalm6

3.3.1 Generation of a Nalm6 CXCR4 KO

CXCR4 blockage by AMD3100 inhibits Nalm6 migration towards BM-MSC and testicular stroma supernatant as shown in **Figure 17**. However, inhibition by a drug might have target-unspecific effects that would influence the cell migratory behaviour. Therefore, a Nalm6 CXCR4 *KO* cell line was generated using the CRISPR/Cas9 method. This method uses a part of the adaptive immune system of bacteria to introduce double-stranded DNA breaks at defined sites of the genome. This enables a distinct *KO* of genes in eukaryotic cells[167]. **Figure 18** illustrates the procedure of a CXCR4 KO in Nalm6 cell line. Cells were transiently transfected by nucleofection using an Amaxa device. Efficiency of the transfection was measured with a px458-GFP control plasmid (Cas9-GFP) 24 hours after electroporation. Untransfected cells (mock transfection) were more vital compared to Nalm6 cells transfected with the px458-GFP plasmid, however about 14% of the transfected cells expressed GFP (**Figure 18A**). To generate the CXCR4 KO, the px459-Puro (Cas9-Puromycin) plasmid was used in combination with two different sgRNAs targeting the exon 1 of human CXCR4. After 48 hours of culture transfected cells were treated for 48 hours with Puromycin (0.5µg/ml). As displayed in **Figure 18B** one week after Puromycin treatment both px459-Puro-sgRNA constructs led to a small population of Nalm6-CXCR4 KO cells (sgRNA 77 4.9%; sgRNA 90 12.6%). A magnetic activated cell sorting (MACS) targeting CXCR4 enriched this population, after seven days of culture the majority of the Nalm6 cells were CXCR4 negative (sgRNA 77 72.4%; sgRNA 90 77.6%). A second MACS CXCR4 sort resulted in a pure CXCR4 negative population in cells transfected with sgRNA 77 (>99%) and a mostly CXCR4 negative population in cells transfected with sgRNA 90 (92.6%). Within 26 days a stable Nalm6 CXCR4 KO cell line was generated that could be used for further functional studies.

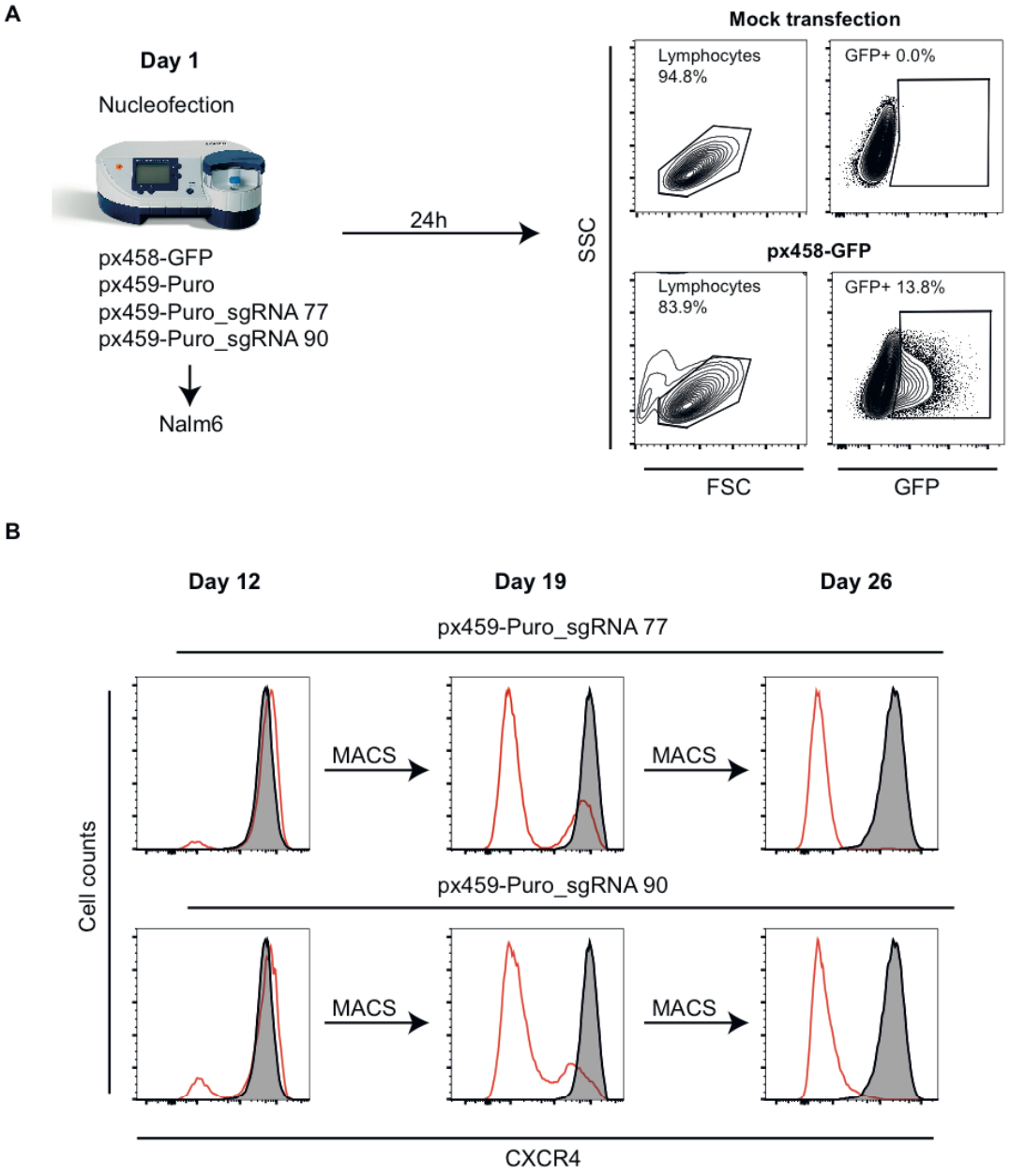

Figure 18: Generation of a Nalm6-CXCR4 KO cell line. (A) Nalm6 cells were transfected using the Amaxa nucleofection device. A px458-GFP plasmid was used as transfection control. 24 hours after nucleofection, 13.8% of the transfected cells were GFP positive. The px459-Puromycin plasmid (Puro) equipped with two different sgRNAs was used to generate the KO. To enrich for transfected cells, Nalm6 cells were treated with Puromycin for 48 hours. **(B)** A small population of Nalm6 cells was CXCR4 negative at day 12 (sgRNA77 4.9%, sgRNA 90 12.6%). At day 26 after two additional MACS CXCR4 sorting steps this percentage was enriched to 99% (sgRNA 77) and 92.6% (sgRNA 90). Histograms display fluorescence intensity, black filled lines represent the CXCR4 expression of control cells, and red solid lines show anti-CXCR4 staining of cells transfected with px459-Puro_sgRNA.

3.3.2 A CXCR4 KO does not influence *in vitro* survival of Nalm6 cells

Since the CXCR4-CXCL12 axis is relevant for ALL cell survival and proliferation[119] KO of CXCR4 might result in a retarded survival of Nalm6 cells in culture. Therefore a 48-hour culture of Nalm6 cells electroporated with px459-Puromycin plasmid without sgRNA (Nalm6

Puro control) and Nalm6 CXCR4 KO 77 was performed. Part of the cells was cultured in the presence of either BM-MSCs or testicular stroma cells. As shown in **Figure 19** both cell lines are highly vital, however they performed better when cultured without additional stroma support. While the Nalm6 cell lines have a living population of more than 90% in mono-culture, this value decreases to only 80% when co-cultured with stroma cells. No significant difference was observed between Nalm6 Puro control and Nalm6 CXCR4 KO 77 cells, neither when cultured with BM-MSCs nor testicular stroma. Despite the CXCR4 KO, the generated Nalm6 cell line is highly vital and not retarded in their *in vitro* growth.

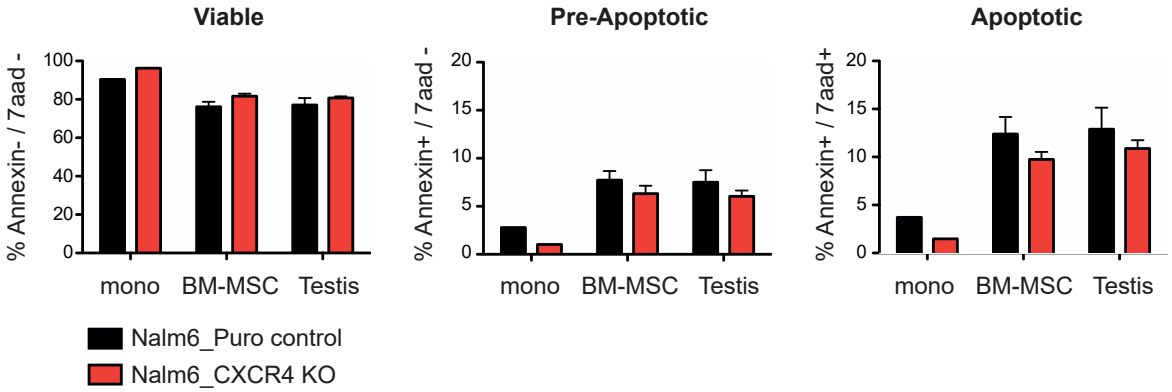

Figure 19: Co-culture of Nalm6 CXCR4 KO cells with primary patient stroma. Cells were cultured for 48 hours at 37°C in RPMI + 1% FCS + 1% P/S. Apoptosis was analysed by flow cytometry BM-MSC n=5; Testis stroma n=5

3.3.3 A CXCR4 KO on Nalm6 cells prevent cell migration towards human CXCL12

In order to perform a functional validation of the CXCR4 *KO* in Nalm6 cells the ability of the control cells (Nalm6 Puro control) and the Nalm6 cells transfected with the sgRNA 77 (Nalm6 CXCR4 KO 77) to migrate towards human CXCL12 was tested in a transwell migration assay. Cell lines were cultured at the same densities prior to the experiment and migration took place in 5 µm cell culture inserts for 4 hours at 37°C. As shown in **Figure 20** the control cells showed a stable migration towards CXCL12 in two independent experiments, while the Nalm6 CXCR4 KO 77 cells displayed a complete inhibition of migration towards CXCL12. The Nalm6 CXCR4 KO 77 cell line is therefore suitable to further study the relevance of the CXCR4-CXCL12 axis in testicular ALL relapse.

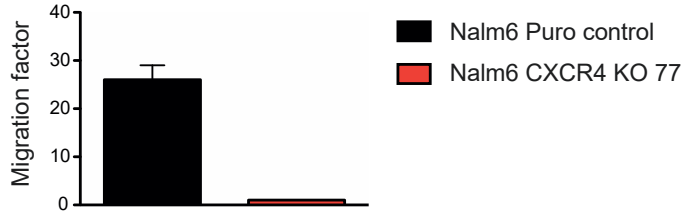

Figure 20: Migration of Nalm6 CXCR4 KO cells towards human CXCL12. The control Nalm6 cells migrate towards medium supplemented with human recombinant CXCL12 (100nM), while the cells having a CXCR4 KO show no migration. Migration took place in tissue culture inserts at 37°C for 4 hours. Values are displayed as mean ± SEM, Nalm6 Puro control n=2; Nalm6 CXCR4 KO 77 n=2.

3.3.4 A CXCR4 KO on Nalm6 cells significantly reduces cell migration towards cell culture supernatant

As already shown in chapter 3.2.5 inhibition of the CXCR4 receptor by a small inhibitor led to a complete inhibition of Nalm6 cells towards stroma cell supernatant of BM-MSC and testicular stroma cultures. As mentioned above, target-unspecific effects might influence this effect. By using the Nalm6 CXCR4 KO cell line these unwanted effects can be excluded. Nalm6 Puro control and Nalm6 CXCR4 KO 77 cells were used in a transwell migration assay. Migration was triggered by supernatants from BM-MSCs and testicular stroma cell cultures. As displayed in **Figure 21** Nalm6 Puro control cells show a strong migration towards the cell culture supernatants, despite a strong variation between the supernatant donors. In contrast the Nalm6 CXCR4 KO 77 cell line shows a significant reduction of migration towards the analysed supernatants. However, while CXCR4 inhibition by AMD3100 resulted into a complete inhibition of Nalm6 migration, a CXCR4 KO only reduces the migration. This observation supports the idea of unwanted target-unspecific effects by AMD3100. Nevertheless, the strong reduction of Nalm6 migration after a CXCR4 KO underlines the relevance of this chemokine receptor for testis directed ALL cell migration.

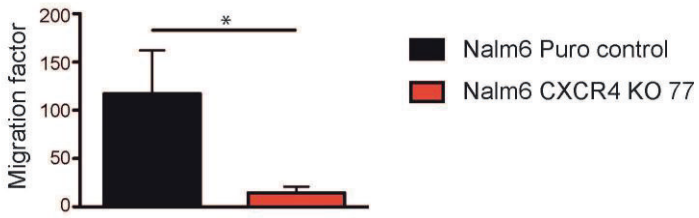

Figure 21: Migration of Nalm6 CXCR4 KO cells towards cell culture supernatant. The control Nalm6 cells (Nalm6 Puro control) migrate towards cell culture supernatant of BM-MSC and testicular stroma cultures, while Nalm6 CXCR4 KO 77 cells show a strong reduction of migration. Migration took place in tissue culture inserts at 37°C for 4 hours. Values are displayed as mean ± SEM, p values (*$p<0.05$) were calculated by Mann-Whitney U test, culture supernatants n=7.

3.4 Immune cells as part of the murine testicular TME

Patient derived BM-MSCs and testicular stroma provides a useful tool to study ALL tumour cell- stroma cell crosstalk *in vitro*. However, analysing the different stroma populations of the testis in humans is limited, because these cells are only present in very small numbers and difficult to isolate. Therefore, cellular and functional characterisation of the testicular TME was performed in mice. Macrophages, as the major immune cell population of the testis were the main focus of all testicular stroma cells in this work.

3.4.1 Age-dependent tMφ subsets are only detectable in C57BL/6N but not in NSG mice

Innate immune cells can be important players of the TME and have a supportive function in tumour growth and expansion[88,90,91]. In the testis, macrophages are the major type of innate immune cells and might be relevant for ALL cell engraftment within this organ. Two distinct subpopulations of tMφ were identified. Their ratio was found to be age dependent in C57BL/6N mice[52]. Immunosuppressed NSG mice still exhibit macrophages, however due to the lack of other immune cells, these macrophages are defective. The phenotype of tMφ in this mouse strain was compared to the phenotype in immunocompetent C57BL/6N mice using flow cytometry. Until now, this has not been covered in literature. **Figure 22 A** shows the gating strategy for the identification of tMφ within the living cell population. TMφ are defined by a $CD45^{+}CD11c\ Ly6C^{-}\ F4/80\ CD11b^{+}$ phenotype[52] and both tested mouse strains exhibited testicular macrophages that express these markers. TMφ are subdivided into interstitial ($CD64^{+}\ MHCII^{-}$) and peritubular ($CD64^{+}\ MHCII^{+}$) macrophages, according to their respective expression of CD64 and MHCII. While C57BL/6N mice of 2, 4 and 9 weeks display both subtypes, tMφ of NSG mice do not express either CD64 or MHCII (**Figure 22 B**). Therefore, an age dependent increase of peritubular macrophages was only visible in C57BL/6N mice but not in NSG mice. The majority of tMφ in both two week-old and in four week-old C57BL/6N mice are interstitial macrophages. However, about 80% of the detected tMφ in nine week-old C57BL/6N mice were peritubular macrophages (**Figure 22 C**). Observed differences between the marker expression of C57BL/6N and NSG mice depict the limitations of an immunodeficient mouse model. Macrophages of NSG mice lack some common markers of this innate immune cell type. However, while studies of the interaction of tumour cells and innate immune cells within the TME are restricted in NSG mice, other testicular cells types, such as peritubular cells or Sertoli cells, are still fully functional.

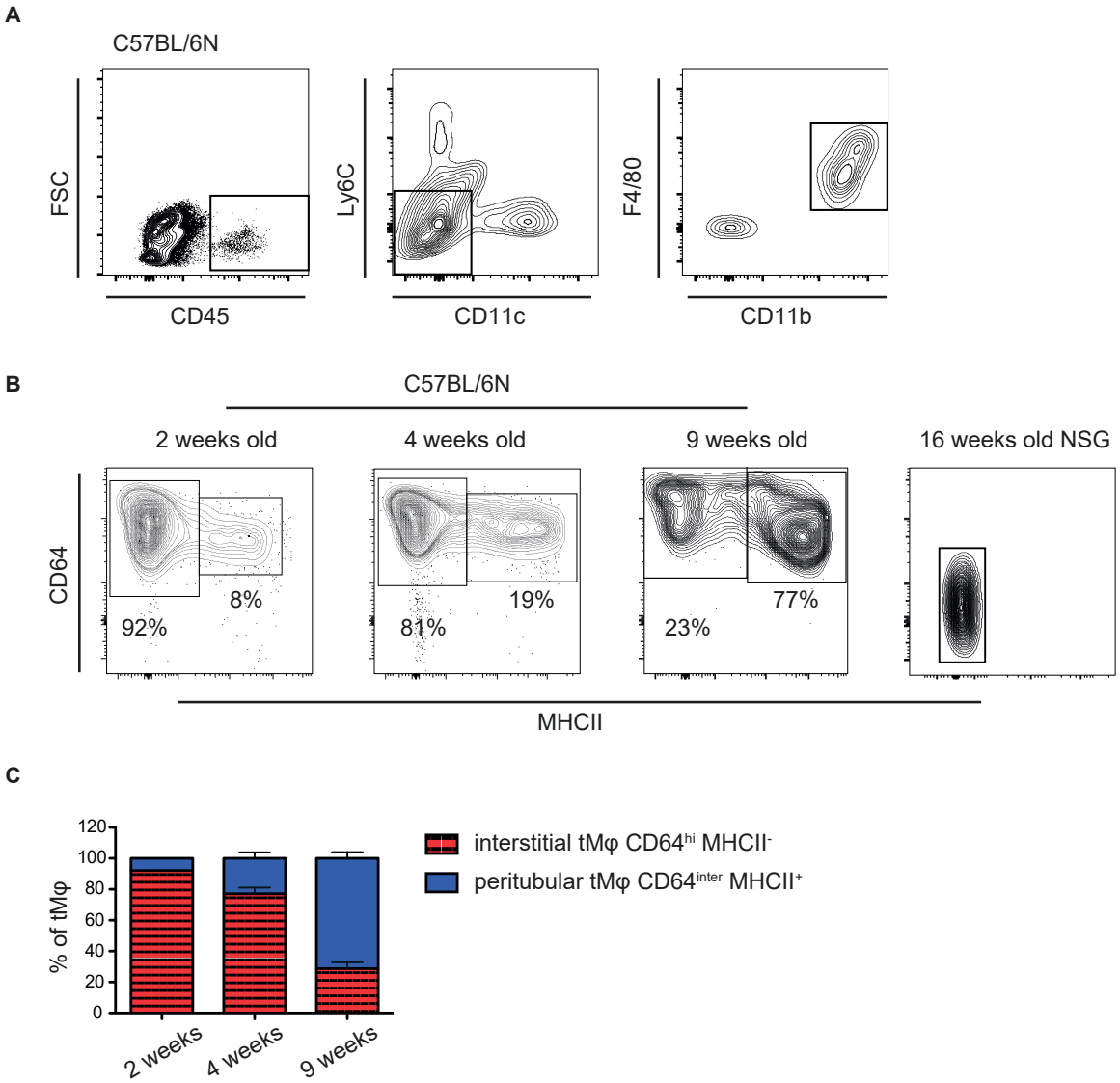

Figure 22: TMφ of NSG mice lack CD64 and MHCII. (A) Gating strategy of tMφ detected by flow cytometry. Living, single cells are gated for a $CD45^{+}CD11c^{-}$ $Ly6C^{-}$ $F4/80^{+}$ $CD11b^{+}$ phenotype. This strategy was applied in C57BL/6N and NSG mice. **(B)** Interstitial and peritubular macrophages are distinguished by their CD64 and MHCII expression. C57BL/6N mice of different ages express both markers on the surface of tMφ with changing ratios. TMφ of NSG mice do not express either of these markers. **(C)** The ratio of the two subtypes of tMφ changes with rising age in C57BL/6N. The majority of tMφ in a two week-old mouse are interstitial tMφ, while in nine week-old mice most tMφ belong to the peritubular subtype. 2 weeks n=1; 4 weeks n=2; 9 weeks n=3.

Since tMφ of NSG mice did neither express CD64 nor MHCII, the question arose whether they express other known macrophage markers to similar levels as tMφ in C57BL/6N mice. Three markers found to be expressed in both tMφ subtypes, CD54, CD115, and CX3CR1, were measured by flow cytometry on interstitial and peritubular macrophages of six to seven week-old C57BL/6N mice as well as on tMφ of NSG mice. CD54 is expressed in high levels by all analysed macrophages. As shown in **Figure 23**, both subtypes of tMφ in C57BL/6N mice express CD54 with a MFI of around 17,000, as compared to a CD54 expression of MFI 20,000 by tMφ in NSG mice. CD115 has the highest expression in interstitial macrophages

and by tMφ in NSG. Both express this marker significantly higher, when compared with peritubular macrophages. Finally, all analysed types of macrophages express CX3CR1, but with a MFI of about 40,000 its level is expressed to a significantly higher extent in tMφ of NSG mice as compared to both interstitial and peritubular tMφ in C57BL/6N mice with respective MFIs of about 25,000 to 30,000. However, none of the observed differences between the groups were significant. In summary, despite their lack of CD64 and MHCII, tMφ of NSG mice still express other relevant macrophage markers.

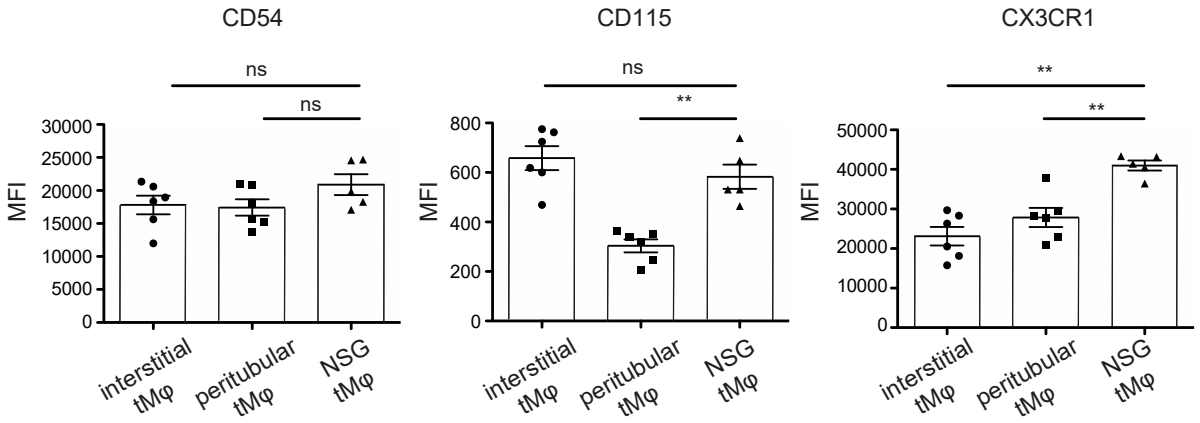

Figure 23: Expression of classical macrophage markers in C57BL/6N and NSG tMφ. Living, single cells were gated for a CD45+CD11c- Ly6C- F4/80+ CD11b+ phenotype. Expression levels of CD54, CD115 and CX3CR1 were detected by flow cytometry. Values are displayed as mean ± SEM, p values (**p<0.01, ns= not significant) were calculated by Mann-Whitney U test, all groups n=5-6. MFI= Mean fluorescence intensities.

3.4.2 Macrophages of NSG mice are able to express MHCII in the presence of an intact immune system

As shown above, the tMφ of NSG mice and C57BL/6N differ regarding their CD64 and MHCII marker expression. The function of macrophages is dependent on the presence of other cytokine secreting immune cells. A lack of these cells results in defect macrophages, as observed in immunodeficient NSG mice. However, the absence of certain markers on NSG macrophages might only be a temporary feature and reversible when macrophages are exposed to an intact immune system. Providing the organism with a naïve immune cell subset could result in a gain of function of the NSG macrophages. To proof this theory, NSG mice (eight week-old) were i.v. transplanted with BM-derived cells of a C57BL/6N mouse (four week-old) (**Figure 24A**). Recipient (NSG) and donor immune cells (C57BL/6N) can be differentiated by their expression of two CD45 variants. All cells of the hematopoietic system of NSG mice express CD45.1 while C57BL/6N cells express CD45.2. Thirty-three days after BM cell transplantation, NSG mice were sacrificed and macrophages in testis and spleen were analysed by flow cytometry. In both organs, donor as well as recipient immune cells were detected.

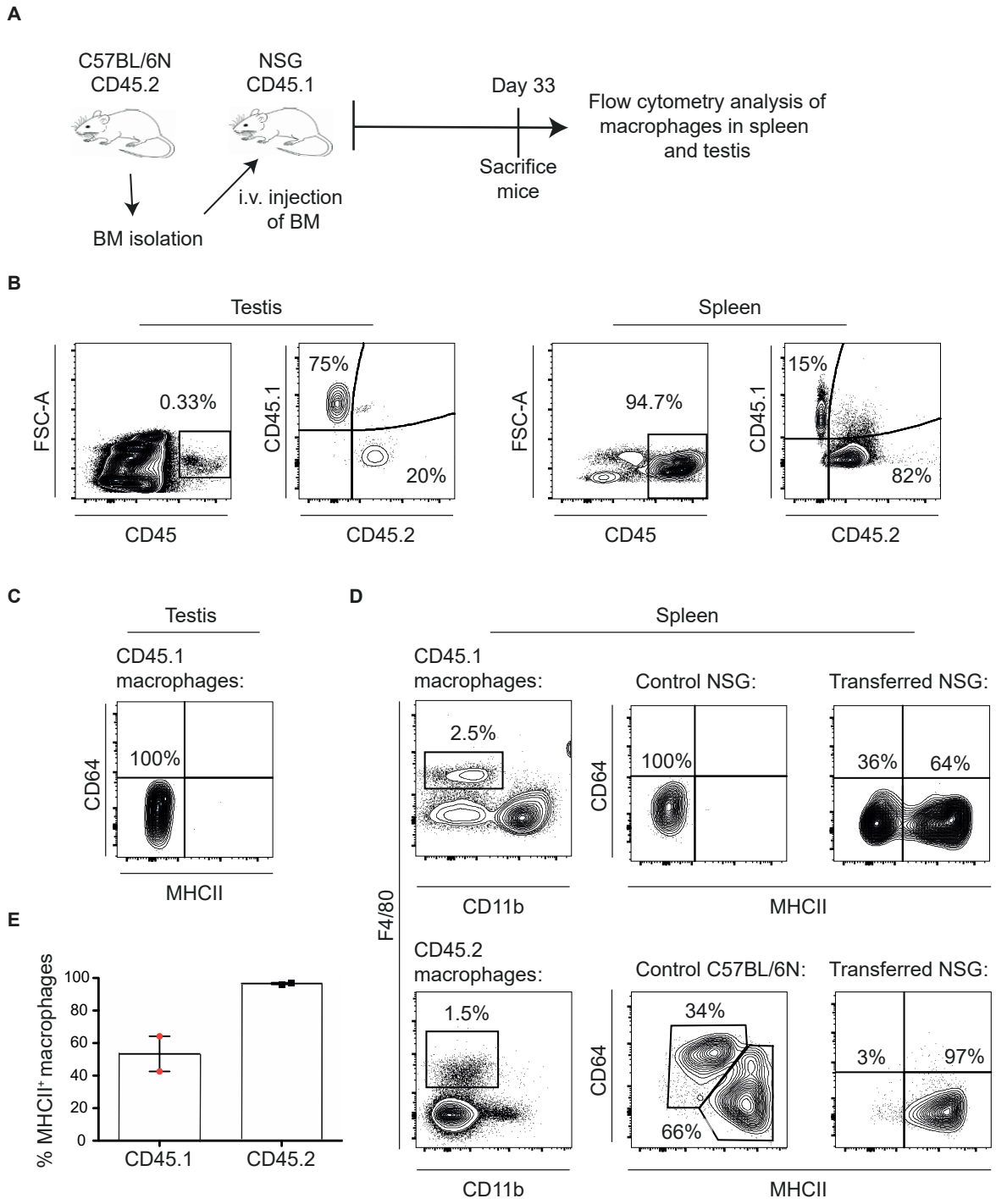

Figure 24: BM transfer from C57BL/6N into NSG mice. (A) Experimental setup of BM transplantation of C57BL/6N (four week-old) into NSG mice (eight week-old). After transplantation cells engraft for 33 days prior sacrifice of mice. **(B)** The ratio of CD45.1 and CD45.2 positive cells in testis and spleen was analysed by flow cytometry. **(C)** CD45.1 tMφ of transplanted NSG mice were analysed for CD64 and MHCII expression by flow cytometry. **(D)** Residential macrophages in spleen are F4/80 positive. Only C57BL/6N mice display CD64 and MHCII expression in their residential splenic macrophages, while NSG mice lack these markers. In C57BL/6N BM transplanted NSG mice, CD45.2 as well as CD45.1 residential splenic macrophages express MHCII. **(E)** About 50% of CD45.1 positive residential macrophages in BM transferred mice express MHCII, while nearly 100% of CD45.2 positive residential macrophages express this marker on their surface. Transplanted NSG mice analysed n=2.

However, in the testis a majority of all CD45 positive cells originated from NSG recipient mice, while in the spleen more than 80% of detected CD45 positive cells are donor cells (**Figure 24B**). In the testis only the recipient CD45 population expresses the phenotype qualifying them as tMφ ($CD45^+CD11c\ Ly6C^-\ F4/80\ CD11b^+$), while detected donor cells did not express this phenotype. As shown in **Figure 24C** the presence of immune cells of an immunocompetent donor mouse did not lead to an expression of CD64 and MHCII in the recipient's tMφ. NSG as well as C57BL/6N mice have small populations of $F4/80^+$ macrophages in their spleen (**Figure 24D**). Control C57BL/6N mice displayed two major populations of $F4/80^+$ macrophages in the spleen, expressing CD64 and MHCII in different levels. Macrophages of control NSG mice lack these markers in the spleen as in the testis. However, NSG mice transplanted with C57BL/6N BM cells expressed MHCII in part of the recipient $F4/80^+$ macrophages as well as in all donor $F4/80^+$ macrophages. CD64 was not neither detectable in donor nor in recipient macrophages. This effect was observed in the spleen of two NSG mice. The recipient macrophages were MHCII positive in 40% to 60%, while more than 95% of all donor macrophages expressed MHCII (**Figure 24E**). In summary, NSG macrophages are still ready to express MHCII, when the microenvironment provides them with the necessary factors. While this effect was only observed in splenic macrophages, tMφ might behave in the same way, when exposed to the new immune cell environment for a longer period. It remains unclear whether PDX-ALL cells might have a similar effect on macrophages in NSG mice. Single cell analysis of testis cells from the described PDX-ALL mouse model with testicular involvement might answer these questions.

3.4.3 Co-culture of PDX-ALL cells and testicular stroma

In order to study the interaction of tMφ and ALL cells in detail, an *in vitro* co-culture of C57BL/6N testicular macrophages and PDX-ALL cells was established. Here, the effect of ALL cells on surface marker expression and macrophage polarisation was of major interest. As shown in **Figure 25A**, four week-old mice were sacrificed and testes isolated and digested for 20 min in a digest solution (RPMI + 1 mg/ml collagenase II + 0.15 mg/ml DNaseI) before plated on a 24 well dish in Medium 199. After an incubation for 30 min at 34°C, wells were washed intensively with PBS and adherent cells were cultured for four hours at 34°C in *rich* macrophage medium (Medium 199 + 10% FCS + 1% P/S). The culture consists of different adherent cell types, including an enriched fraction of tMφ. Subsequently, either PDX-ALL cells or murine B cells were applied to the wells and co-cultured with the testicular cells for 20 hours in *reduced* macrophage medium (Medium 199 + 1% FCS + 1 % P/S). As a control condition testis cells were kept in mono-culture as well. After 20 hours culture PDX-ALL cells or B cells were washed off and testicular cells were detached using accutase. TMφ were characterised by flow cytometry before and after culture and the ratio of

interstitial and peritubular macrophages was compared. While about 60% of tMφ at day 0 had an interstitial macrophage phenotype, the majority of the macrophages after 24 hours of culture expressed markers of the peritubular tMφ (**Figure 25B-C**). Indeed, the number of interstitial cells was reduced by 50 % while the percentage of peritubular tMφ rose by 50%. This development was observed under all analysed conditions, regardless of whether PDX-ALL cells or murine B cells were applied to the culture or, macrophages were cultured on their own (**Figure 25D**). However, it is unclear whether cultured interstitial tMφ converted into the peritubular phenotype or just died faster in culture.

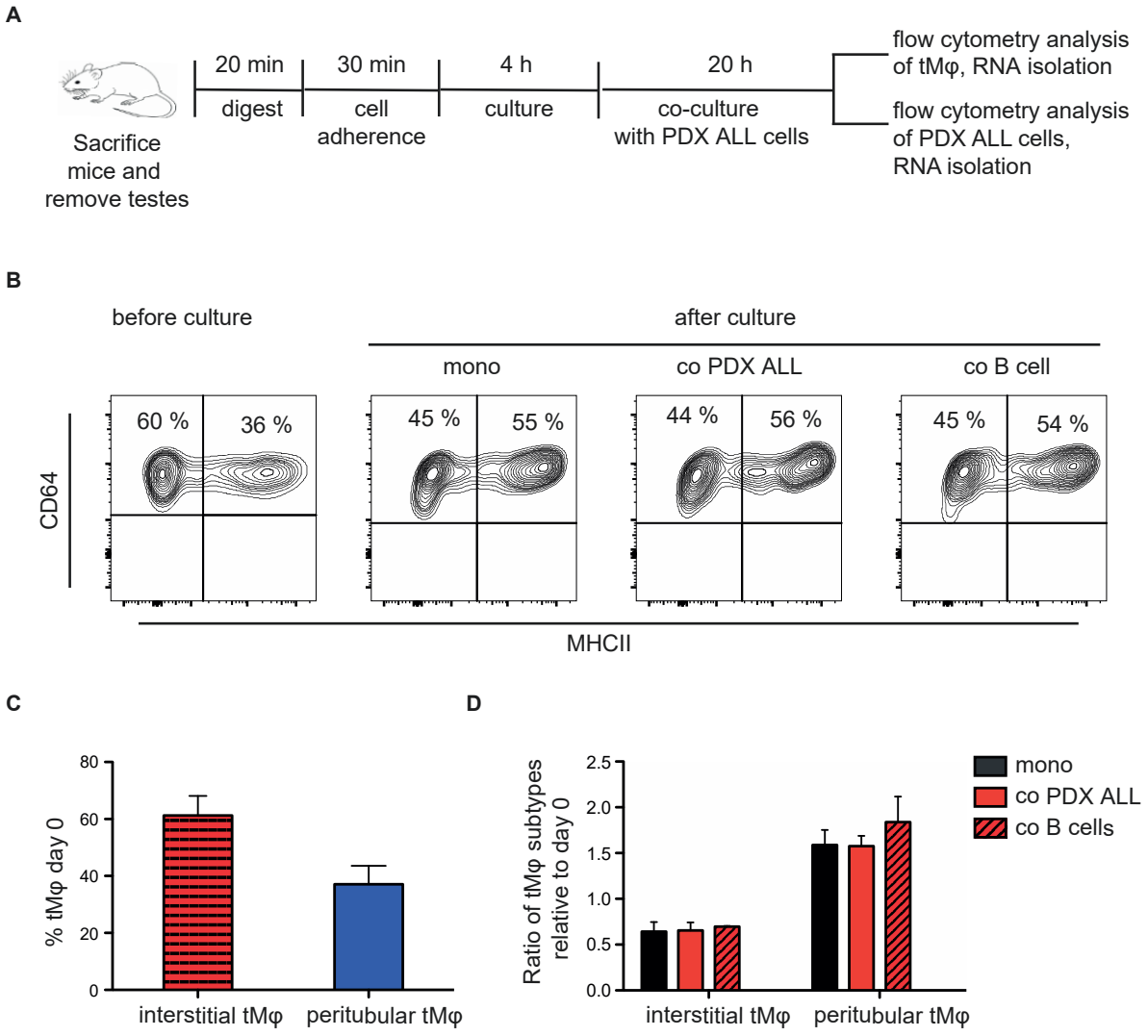

Figure 25: Co-culture of tMφ and PDX-ALL cells. (A) Experimental setup of tMφ isolation and culture. Macrophages were either cultured on their own or in the presence of PDX-ALL cells or B cells. Adherent macrophages and tumour/B cells were isolated 20 hours after starting the culture and analysed by flow cytometry and RT-PCR. **(B)** Representative plots of interstitial and peritubular tMφ before and after 20h of culture. Results are representative for 2-4 independent experiments. **(C)** Percentage of tMφ subtype at day 0 before culture. Bars represent mean ± SEM, n=4. **(D)** Change of percentage of tMφ subtypes after 24 hours of culture. mono n=4; co PDX-ALL n=4; co B cells n=2.

3.4.4 Co-culture with murine testicular stroma does not support PDX-ALL cell survival

Primary ALL cells PDX-ALL cells enter apoptosis within a few days when cultured *in vitro*. However, primary human testis stroma cells retard this process, when used as feeder cells for a 48 hour primary ALL culture. While a human culture system clearly had a positive effect on tumour cell survival it is unclear whether the murine testis cell culture might have a similar effect on the PDX-ALL cells. As shown in **Figure 26** no difference was observed in the survival of mono- and co-cultured PDX-ALL cells. Viability of tumour cells was around 70% after 20 hours of culture regardless of whether cells had additional stroma support. A longer culture period was not included because the ratio between the tMφ subpopulations changes over time. The ratio of pre-apoptotic and apoptotic cells was also comparable between the groups. In contrast to human testicular stroma the murine cells seem to have no effect on ALL cell survival in an *in vitro* culture. Apoptosis of PDX-ALL cells was only observed for a 20 hour culture period, a longer culture period might result in an advantage for tumour cells co-cultured with murine testis stroma.

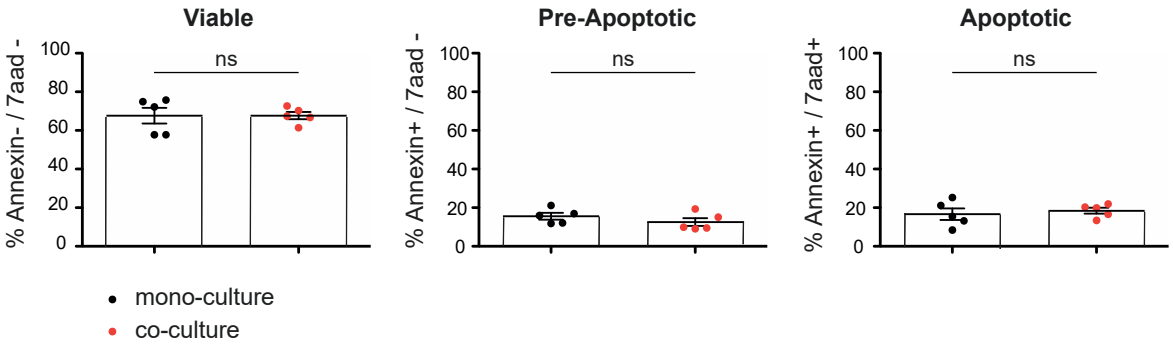

Figure 26: Apoptosis assay reveals no difference in survival of mono- or co-cultured PDX-ALL cells. Cells were cultured for 20 hours at 34°C in RPMI + 1% FCS + 1% P/S. Apoptosis was analysed by flow cytometry. Values are displayed as mean ± SEM, p values (*p<0.05, ns=not significant) were calculated by Mann-Whitney U test, Results are representative for 3 independent experiments; ALL samples n=2; murine testis stroma n=3.

A co-culture of tMφ with PDX-ALL cells showed neither an impact on the ratio of interstitial and peritubular tMφ, nor a survival advantage of the tumour cells. This observation could be related to the short time span of the experiment. Next, the isolated mRNA of the cultured macrophages and PDX-ALL cells was analysed.

3.4.5 Arg1 is up-regulated in interstitial tMφ co-cultured with PDX-ALL cells

Macrophages are a highly flexible type of immune cell and are able to polarize into different subgroups (M1/M2) depending on their environment[93]. These subgroups can be differentiated by the expression of certain markers. Cultured interstitial and peritubular tMφ were sorted using fluorescence associated cell sorting and RNA was isolated from both populations. Four markers were chosen to study the polarisation status of the isolated tMφ. Tested M1 makers were IL1b and Mmp9, while M2 macrophages were represented by IL10 and Arg1[52]. However only IL1b and Arg1 could be detected on gene expression level in analysed macrophage samples. As shown in **Figure 27** both subtypes of tMφ express IL1b and Arg1 mRNA regardless of whether they are cultured on their own or in the presence of either PDX-ALL or murine B cells. Interstitial tMφ show a significant increase of Arg1 expression when co-cultured with PDX-ALL but this effect was absent when interstitial tMφ were co-cultured with murine B cells. No significant changes in the Arg1 expression level were observed in peritubular tMφ or in IL1b expression in any of the two subtypes. Therefore, it can be concluded that only PDX-ALL cells were able to influence the polarisation of tMφ towards a tumour-favourable M2-status. This effect is limited to the interstitial tMφ that are found in higher abundance in younger mice.

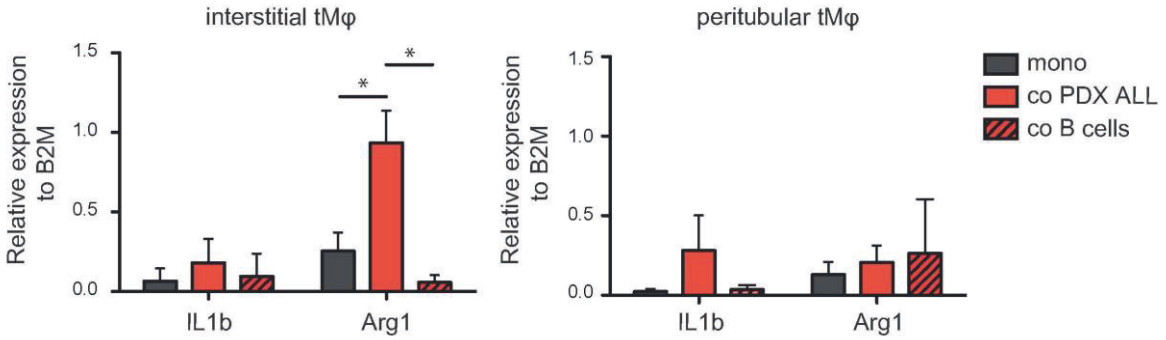

Figure 27: M1/M2 marker expression in cultured tMφ. After sorting and isolating the tMφ subtypes by flow cytometry RNA was isolated from the cells and used to perform a RT-PCR analysis. The M1 macrophage marker IL1b is only weakly expressed by both tMφ subtypes independent of the culture condition. The M2 marker Arg1 is significantly higher expressed by interstitial tMφ when co-cultured with PDX-ALL cells. Bars represent mean ± SEM; n=2-5, p values (*p<0.05) were calculated by unpaired two-tailed t test.

3.4.6 PDX-ALL cells express cytokines involved in M2 polarisation of macrophages

Macrophage polarisation towards the M1 or M2 subtype is regulated by signals, such as cytokine secretion, from their microenvironment[94]. PDX-ALL cells that were either mono- or co-cultured with tMφ were isolated and RNA was purified from these cells. The following, cytokine expression was measured by qRT-PCR analysis. In total five cytokines known to polarise macrophages towards the M2 stage were analysed (IL4, IL6, IL10, TGF-ß and M-

CSF) as well as one cytokine inducing M1 polarisation (INFy). As shown in **Figure 28**, qRT-PCR could detect only IL10, TGFß and M-CSF, while samples were negative for IL4, IL6 and also the M1 marker INFy. IL10 was expressed at very low levels, whereas the other two cytokines were detected in higher levels. No significant differences were observed between mono- or co-cultured PDX-ALL cells. Overall, cultured leukaemia cells constitutively expressed IL10, M-CSF and TGFß, cytokines responsible for M2 polarisation of macrophages.

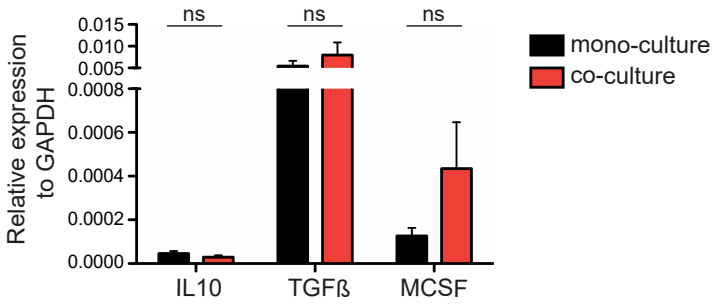

Figure 28: PDX-ALL cells express cytokines that trigger M2-polarisation of tMφ. After culturing PDX-ALL cells for 20 hours in mono- or co-culture with tMφ, RNA was isolated and analysed by qRT-PCR. IL10, TGFß and M-CSF were detected while no expression was observed for IL4, IL6 and INFy. Values are displayed as mean ± SEM, p values (*p<0.05, ns= not significant) were calculated by Mann-Whitney U test; n=4.

3.4.7 Testicular macrophages are detectable in human testis sections

The development of mouse tMφ was described in detail[52]. Human testicular macrophages were detected and studied in sections of adult donors[168], however, it is not clear if macrophages play a relevant role during early development in human testes. Sections of very young, healthy donors (prenatal and under one year old) were stained for CD68. As shown in **Figure 29**, the prenatal section does not yet show the structures of a more mature testis, while the second donor displays the segmentation in germ bands and the interstitial space. CD68 positive macrophages were found throughout the section in both donors. As described for adult men macrophages were mainly detected in the interstitium[169]. Considering the location and morphology, detected macrophages resemble the interstitial macrophages of the mouse testis. However, detailed studies on RNA and protein levels are necessary to further classify these macrophages. Sections of older donors (above one year up to 17 years) were also available but material was limited and sections very small. No CD68 positive cells could be detected in these sections, which is most likely related to pre-treatment of the material and the small size of the sections.

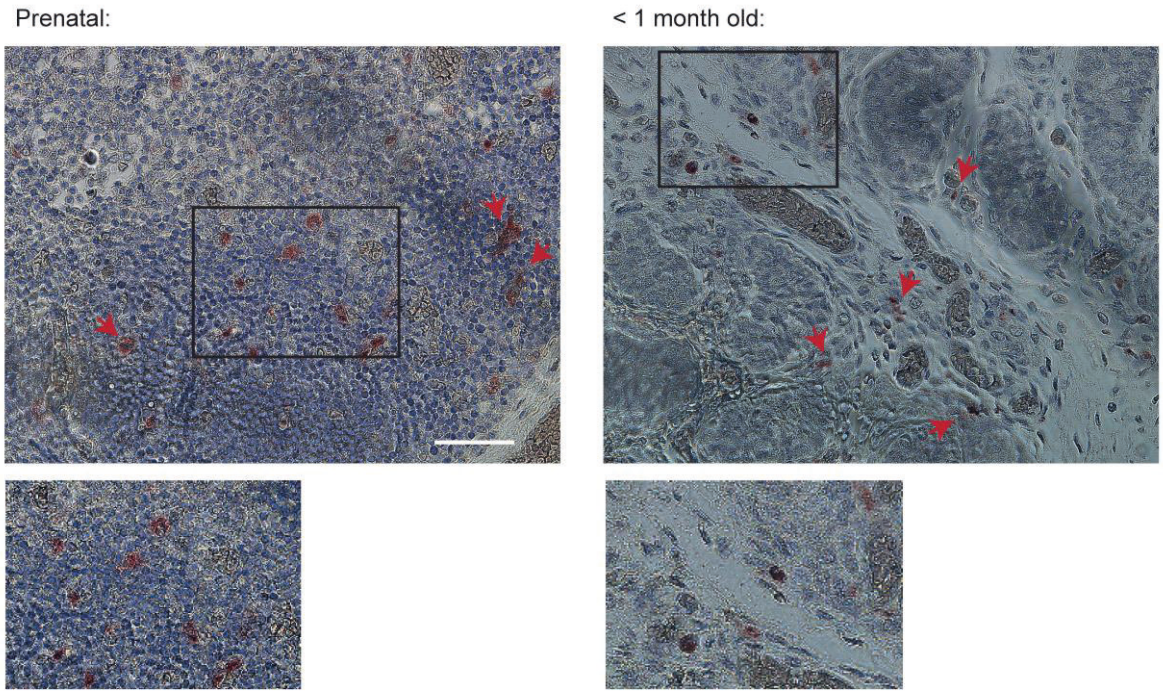

Figure 29: Macrophages can be detected by immunohistochemistry staining in human testis sections. Testis sections of a prenatal donor and a child below one month were stained for CD68 by immunohistochemistry. Both donors show CD68 positive cells, indicated by the red arrows, throughout the section. n=2, Bar 50 µm.

3.5 Sertoli cells and peritubular myoid cells (PTCs) as part of the testicular TME

3.5.1 Establishing the isolation of murine Sertoli cells and PTCs

While innate immune cells, as macrophages, are well known for their support function within the TME, also other cell types might provide a tumour favourable environment. The main somatic cell types within the testis are Sertoli cells, Leydig cells, macrophages and PTCs[44,50,51,55]. The previous chapter addressed in detail the possible interaction of tMφ and ALL cells. To study the interaction of leukaemia cells with other testicular cell types, the isolation of primary Sertoli cells and PTCs from mouse testis was established. **Figure 30A** displays the workflow necessary for the cell isolation. Testes of 8 mice were decapsulated and digested with collagenase and trypsin. PTCs were seeded after trypsin-inactivation and split when reaching confluency. By splitting the cells, remaining spermatids were removed, which succeeded in producing a higher purity of PTCs. Tubules left after trypsin digestion were further digested by hyaluronidase-DNase. Subsequently the cell suspension was filtered and Sertoli cells were seeded. After 48 hours Sertoli cells were treated with a hypotonic shock to remove remaining spermatids. In contrast to PTCs, Sertoli cells do not divide in culture. Therefore, intended analyses must be performed 2 hours after the

hypotonic shock. The purity of the adherent cells was determined by an immunofluorescent staining of α-SMA (PTCs) and Vimentin (Sertoli cells). **Figure 30B** depicts cultured cells four days post-isolation. All plated cells in the Sertoli cell dish were positive for Vimentin, which indicates that the purity of this population is very high. In the culture dish containing PTCs most cells were positive for α-SMA. Therefore, it can be concluded, that both cell types were successfully isolated. RNA of both cell types was isolated and used for the following RT-PCR analyses. The PTCs were also used for further co-culture experiments.

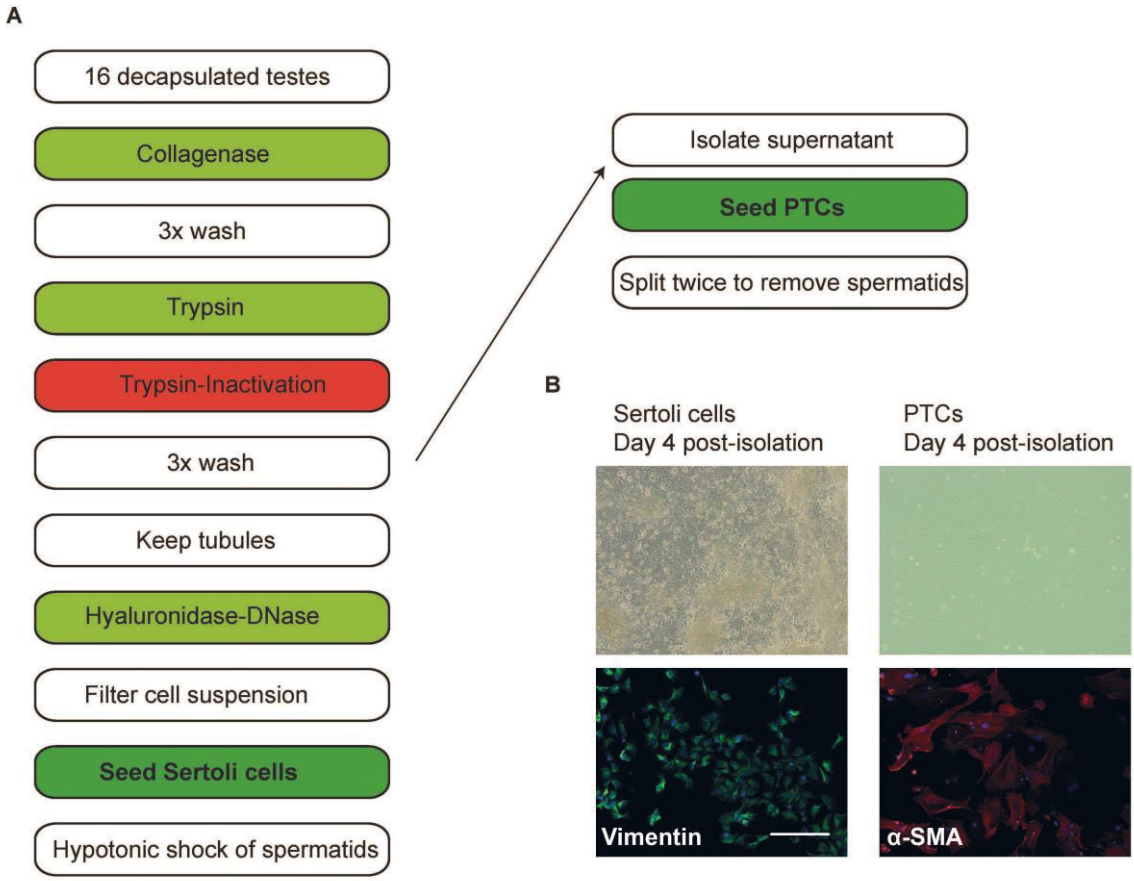

Figure 30: Isolation and characterisation of murine Sertoli cells and PTCs. (A) Workflow of Sertoli cells and PTC isolation from mouse. Testes of 7-8 animals were collected and digested consecutively with collagenase and trypsin. Following trypsin deactivation, PTCs were isolated by washing the tubules and collecting the emerging supernatant. Cells were split twice when the plate was confluent to remove all residual spermatids. Remaining tubules were digested with a Hyaluronidase-DNase I solution. The resulting cell suspension contained Sertoli cells and spermatids. After 48 hours cultured Sertoli cells were treated with 20 mM Tris buffer to remove residual spermatids by a hypotonic shock. **(B)** Purity of cultured cells was verified by an immunofluorescence staining of the isolated cells. Sertoli cells were stained with anti-Vimentin and PTCs with anti- α-SMA. Bar 50 µm.

3.5.2 Primary murine Sertoli cells and PTCs express CXCL12 and IL7

Since analysis of primary ALL patient samples revealed an up-regulation of IL7R in testicular relapses and a high expression of CXCR4 throughout all tested samples, isolated testicular cells were analysed for IL7 and CXCL12 expression by qRT-PCR. The murine BM stroma

cell line M2-10B4 was used as a positive control, the mouse lymphoma cell line EL4 acted as a negative control. Sertoli cells and PTCs isolated from C57BL/6N and NSG mice were analysed, as well as RNA isolated from complete NSG testes and the murine Sertoli cell line TM4. **Figure 31A** shows the relative expression to the reference gene B2M of all analysed samples. PTCs of both tested mouse strains displayed a higher CXCL12 expression level, compared to the isolated Sertoli cells. Especially C57BL/6N PTCs showed a very high CXCL12 expression, while PTCs of NSG mice had a comparable expression to TM4 cells. The CXCL12 expression of the entire testes of three NSG mice was higher than in Sertoli cells but lower than in tested PTCs. The relative expression of IL7 was very low, however most analysed samples showed a higher expression of IL7 compared to the M2-10B4 positive control.

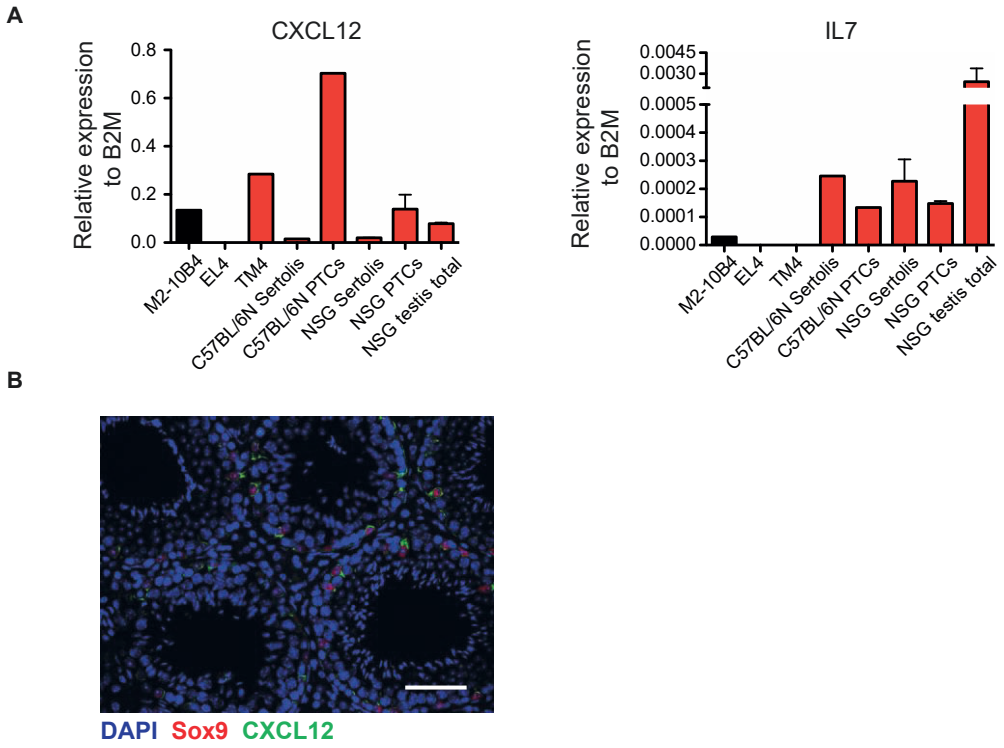

Figure 31: CXCL12 and IL7 expression in murine cell lines and primary testis cells. (A) After culturing Sertoli cells for four days and PTCs for one week, RNA was isolated from both cell populations. Generated cDNA was used to detect CXCL12 and IL7 expression. The murine BM stroma cell line M2-10B4 was used as a positive control and the murine lymphoma cell line EL4 as a negative control. Additionally, the murine Sertoli cell line TM4 was compared with the primary Sertoli cells. Isolated cells from NSG mice and C57BL/6N mice were used for analysis. The CXCL12 and IL7 expression of complete NSG testis tissue was compared to the isolated cell populations. C57BL/6N n=1; NSG n=2; NSG testis n=3 **(B)** Representative immunohistochemistry staining of a NSG testis section. CXCL12 is expressed on protein level by the Sertoli cells (Sox9 +) in the testis. Bar 50 µm.

While primary Sertoli cells of C57BL/6N had a higher IL7 expression compared to PTCs the Sertoli cell line was negative for this cytokine. The highest expression was detected in the total testis samples of NSG mice. This indicates another source of IL7 rather than Sertoli

cells or PTCs. The CXCL12 expression was additionally validated on the protein level by immunohistochemistry. However, as shown in **Figure 31B**, on the protein level only Sertoli cells (Sox9) express CXCL12.

Isolated PTCs of C57BL/6N and NSG mice and two murine cell lines were used to perform co-cultures with two PDX-ALL clones. Tumour cells were either cultured on their own or together with stroma cells for 48 hours in reduced medium (RPMI + 1% FCS + 1% P/S). Part of the wells were supplemented with 10 ng/ml human IL7. PDX-ALL donor #1064 showed the highest viability when co-cultured with isolated PTCs. TM4 cells provided no strong support for these cells. However, when supplemented with IL7, ALL-PDX #1064 survival increased in all analysed co-cultures, as well as in mono-culture. Also, PDX-ALL #1476 showed the highest viability when co-cultured with PTCs, but IL7 supplement gave no additional support. In summary, primary murine testis cells can support *in vitro* survival of PDX-ALL cells, while cell lines are less suitable. Human IL7 seems to additionally support tumour cells at least in one of the tested donors.

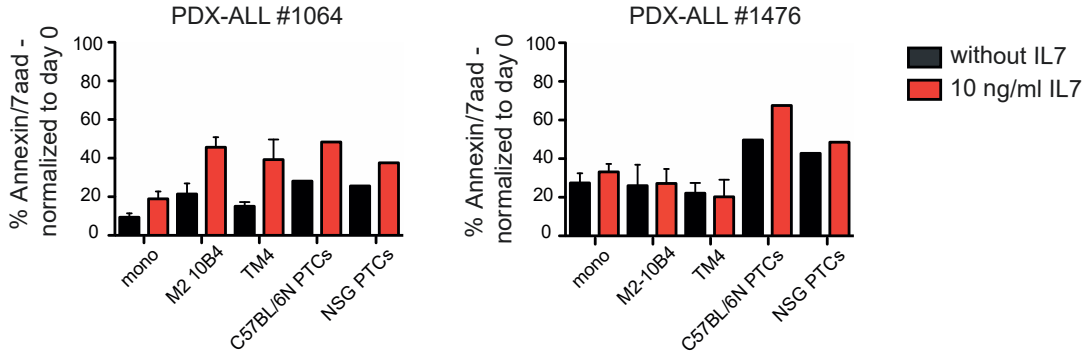

Figure 32: Effect of co-culture of PDX-ALL cells with murine stroma cells. Two PDX-ALL clones were either cultured on their own or kept in co-culture with primary PTCs from C57BL/6N and NSG mice or murine cell lines TM4 and M2-10B4. One part of the wells was treated with 10ng/ml human IL7. Both analysed clones showed a better survival when co-cultured with primary PTCs compared with mono-culture or cell lines. A positive effect of IL7 on cell survival was just observed with clone #1064, while #1476 had no additional advantage by this treatment. Mono n=5; M2-10B4 n=4; TM4 n=2; C57BL/6N n=1; NSG PTC n=1.

3.6 Establishing an *in vivo* ALL mouse model with testicular involvement

In vitro cultures are a useful tool to study isolated interactions of human cells in a controlled environment. However, these models are limited when it comes to studying complex processes that require multiple cellular players. Therefore, a novel murine ALL model with testicular infiltration was developed which allowed the study of the mechanism of leukaemia cell migration into the testis and their crosstalk with the TME. To unravel the mechanisms responsible for testis infiltration and survival of ALL cells within this extramedullary site an

adoptive transfer PDX-ALL model was used. Three PDX-B-ALL cell samples (PDX-ALL #1064, #1476, #3696) of paediatric relapse patients were provided by PD Dr. Cornelia Eckert (Charité-University Medicine, Berlin) that had been established in NSG mice (performed in the laboratory of Prof. Dr. Jean-Pierre Bourquin, medical faculty, University of Zürich).

3.6.1 Lentiviral transduction of PDX-ALL cells

In order to analyse tumour kinetics cells *in vivo* PDX-ALL cells were equipped with a luciferase-GFP construct by lentiviral transduction, which allows non-invasive bioluminescence imaging of tumour recipients. This technique requires a reporter construct that stably integrates luciferase into transduced cells. Luciferase converts D-luciferin to oxyluciferin, which results in a detectable light emission[170]. **Figure 33A** illustrates the experimental setup, required to generate a luciferase expressing PDX-ALL cell line. BM derived cells were transduced and cultured for four hours at 37°C. Afterwards cells were injected i.v. into NSG mice and tumour growth was monitored for 5-6 weeks. When mice developed profound leukaemia, they were scarified and BM and/or spleen derived PDX-ALL cells were sorted for GFP-positivity by flow cytometry. The GFP positive cell population was transplanted into NSG mice and cell growth was monitored for another 6-7 weeks. NSG mice were scarified; GFP positive cells were sorted by flow cytometry and frozen in aliquots for further experiments. As displayed in **Figure 33B** the three PDX-ALL patient cell samples were successfully transduced. Transduction efficiency was 3.6% to 4.2% in the three transduced cones. GFP positive cells were isolated by flow cytometry and expanded in NSG mice for another seven weeks. The percentage of luciferase-GFP expressing cells was increased to 30 to 80% and were enriched by another flow cytometry sort to more than 98%. Prior sacrifying mice, luciferase activity was controlled by IVIS imaging. All three clones displayed a profound luminescent signal, when mice were injected with luciferin substrate (**Figure 33C**).

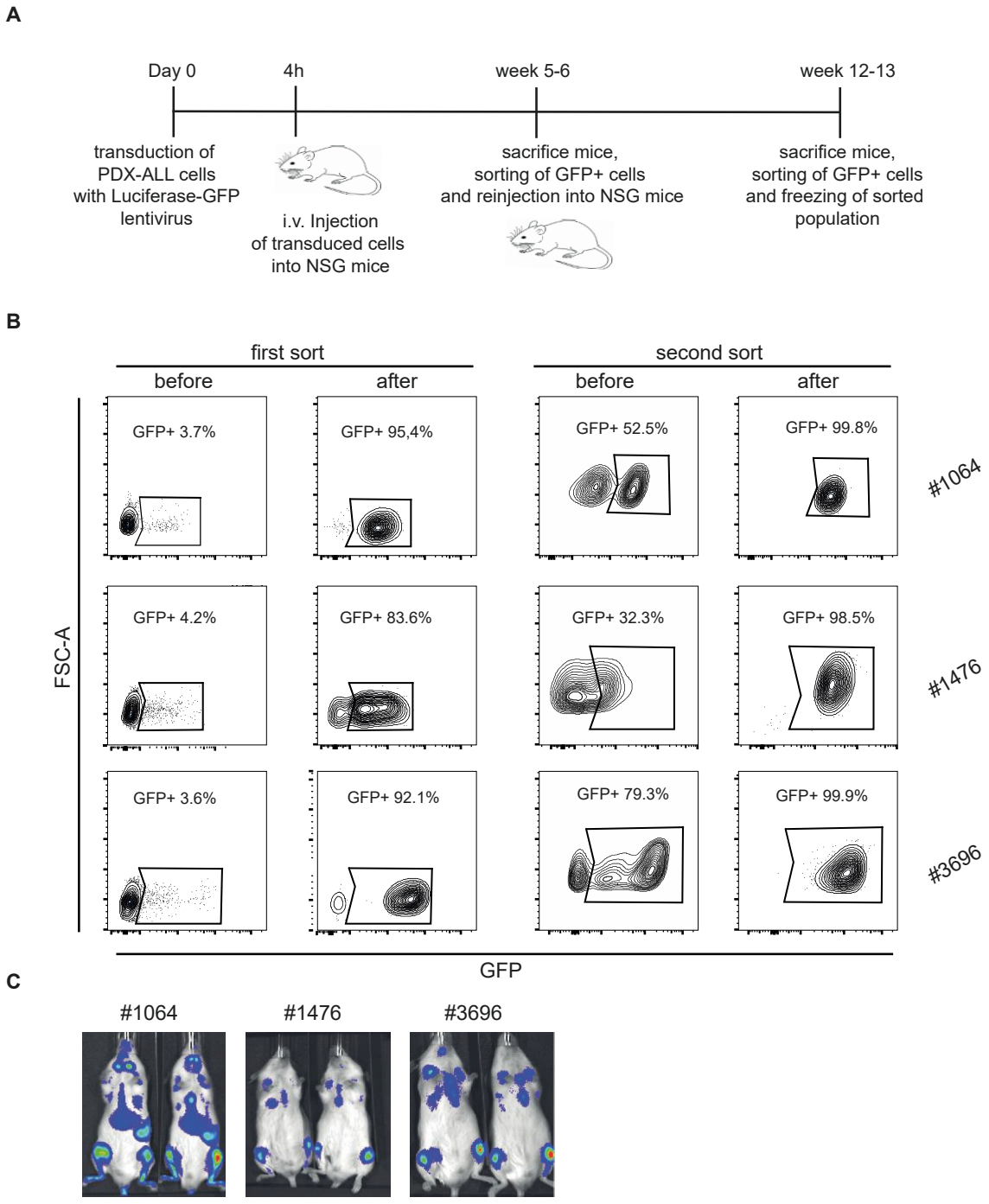

Figure 33: Lentiviral transduction of PDX-ALL cells with a luciferase-GFP construct. (A) Experimental setup of the generation of PDX-ALL Luciferase-GFP cells. A total of 12-13 weeks was required before a highly GFP positive population PDX-ALL cells were frozen for further experiments. **(B)** PDX-ALL cells of three patients were successfully transduced. The transduction efficiency was 3.6%-4.2% but a first flow cytometry sort enriched this population to 83% to 95%. After expanding these cells again in NSG mice 32%-79% GFP positive tumour cells could be recovered. A second sort led to a GFP expressing population of more than 98%. **(C)** IVIS imaging of mice, injected with transduced cells after the first sort. Exposure time: 60 s.

3.6.2 Characterisation of surface marker expression on luciferised PDX-ALL cells

An advantage of PDX models in cancer compared to cell lines is the assumption that these cells closely resemble the original tumour. They are biologically stable in regard to gene expression, mutations and therapeutic response[171]. To ensure that transduced cells still reflect the surface expression pattern of primary ALL samples they were characterised for the same chemokine receptors, adhesion molecules and the IL7R as were used for the primary ALL samples (2.1.1). Cells were first gated for single and live cells and then on distinct surface markers (CD19, CD45) before the protein of interest was analysed. **Figure 34** shows the histograms of nine chemokine receptors expression levels of transduced PDX-ALL lines. While CXCR4 is profoundly expressed in all three patient samples expression of all other chemokine receptors was negative. Donor #1064 (**Figure 34A** and **Table 13**) shows the highest CXCR4 expression but also donors #1476 and #3696 (**Figure 34B+C**) express the receptor at a substantial level.

Table 13: Chemokine receptor expression of transduced PDX-ALL cell samples.

	CCR5	CCR7	CCR9	CXCR1	CXCR2	CXCR3	CXCR4	CXCR5	CXCR7
#1064	-	-	-	-	-	-	+++	-	-
#1476	-	-	-	-	-	-	++	-	-
#3696	-	-	-	-	-	-	++	-	-

Chemokine receptor expression intensity was classified based on the measured MFI. MFI <200 -; MFI 200-500 +; MFI 500-2000 ++; MFI >2000 +++.

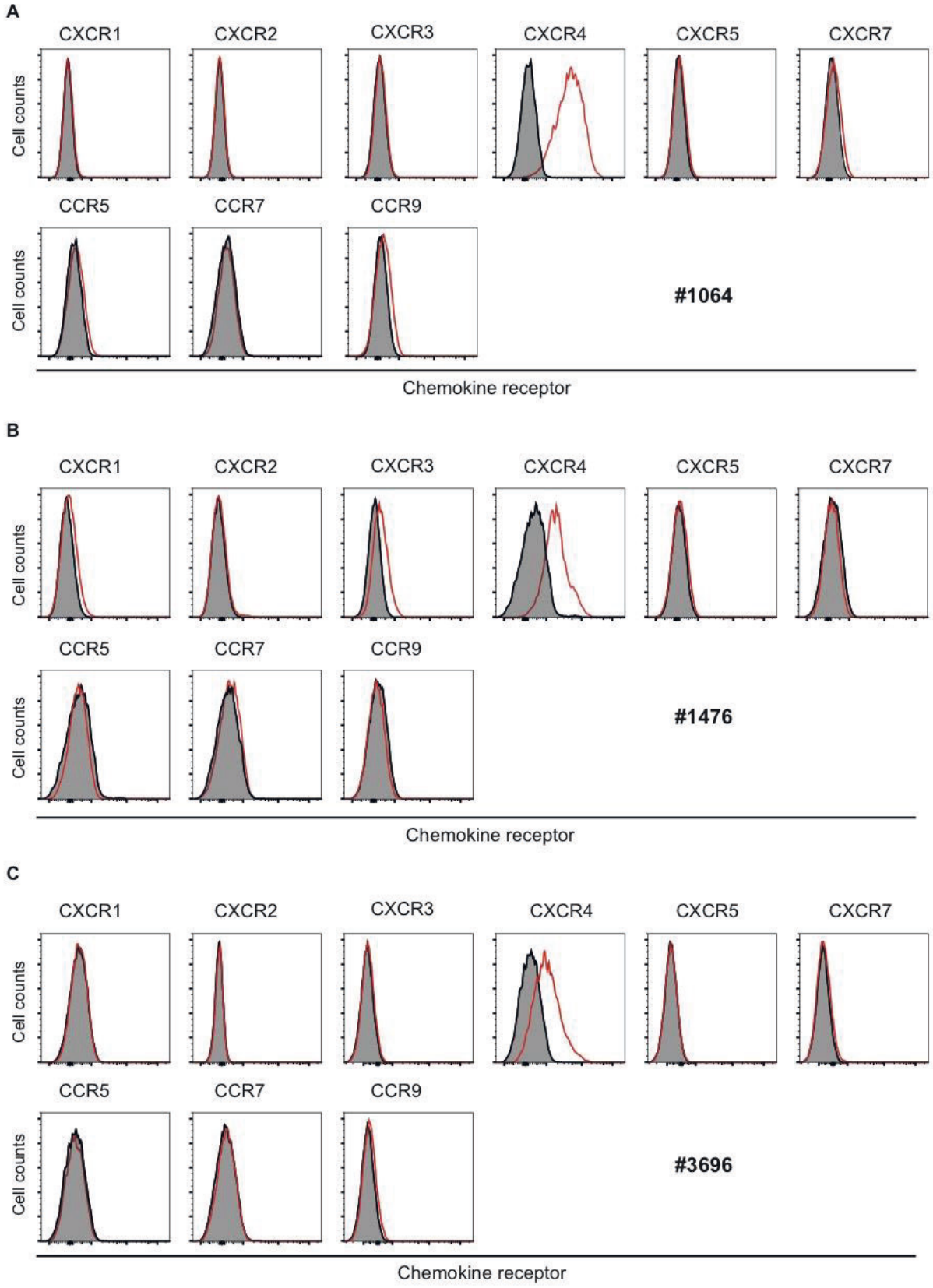

Figure 34: Chemokine receptor expression on transduced PDX-ALL cell lines. Transduced PDX-ALL cells of three donors **(A)** #1064 **(B)** #1476 **(C)** #3696, isolated from BM, were stained with an anti-chemokine receptor antibody or its matching isotype control. Doublets and dead cells were excluded. A histogram for each chemokine receptor is shown. Histograms display fluorescence intensity, black filled lines represent the isotype control, and red solid lines show anti-chemokine receptor staining.

Since the IL7R was shown to be an interesting factor for testicular ALL infiltration (see 2.1.2), the receptor was characterised for the three transduced PDX-ALL lines. As described above cells were first gated for single and live cells and then on distinct surface markers (CD19, CD45) before the IL7R was analysed. **Figure 35A** shows histograms of the IL7R expression of the three donors while **Figure 35B** summarises the MFI values of the donors. All samples express the receptor on their surface, however the sample #1064 has by far the highest expression level with a MFI of about 4500.

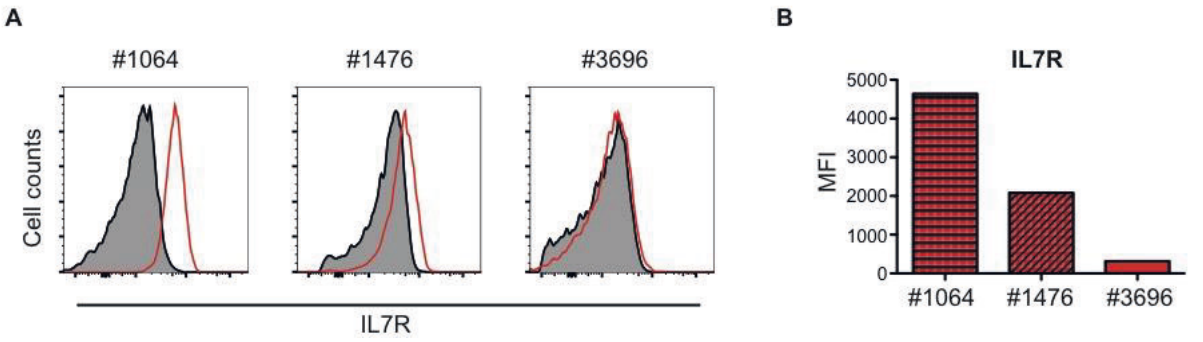

Figure 35: Surface expression of the IL7R on transduced PDX-ALL cell lines. Transduced PDX-ALL cells of three donors (#1064, #1476 and #3696), isolated from BM, were stained with an anti-IL7R antibody or its matching isotype control. Doublets and dead cells were excluded. **(A)** A histogram for each PDX-ALL cell line is shown. Histograms display fluorescence intensity, black filled lines represent the isotype control, and red solid lines show anti-chemokine receptor staining. **(B)** The bar diagram displays the IL7R MFI values for the PDX-ALL cell lines.

Furthermore, the surface expression of CD11a, CD44 and CD49d was analysed on the luciferised PDX-ALL samples. These adhesion molecules, which were highly expressed by primary ALL samples (Figure 10), are also detectable on the three PDX-ALL lines. CD11a reaches MFIs between 1,000 and 17,000 (**Figure 36A**), CD44 between 40,000 and 150,000 (**Figure 36B**) and CD49d between 30,000 and 50,000 (**Figure 36C**). All adhesion molecules show by far the strongest expression on the PDX-ALL line #1476, while the samples #1064 and #3696 display similar expression levels.

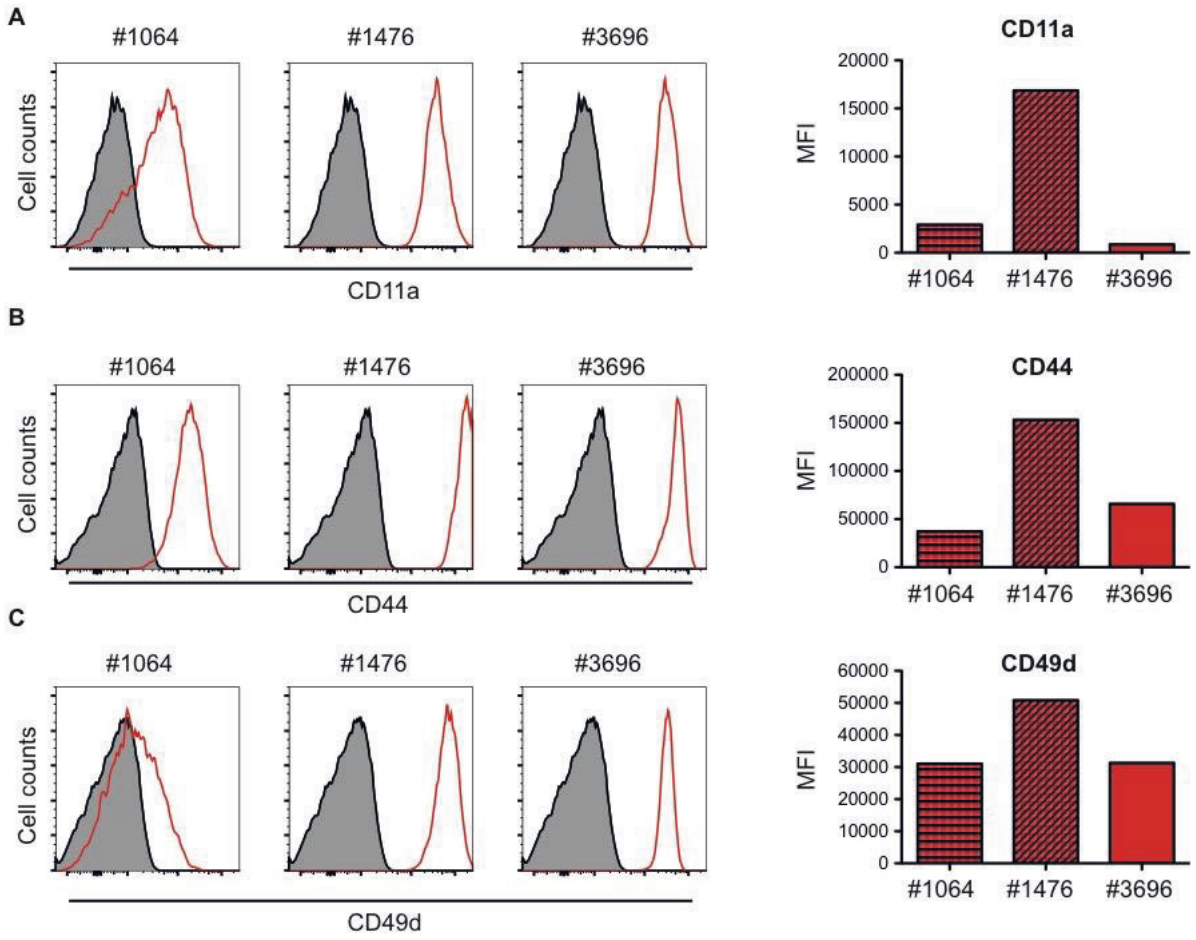

Figure 36: Surface expression of adhesion molecules on transduced PDX-ALL cell lines. Transduced PDX-ALL cells of three donors (#1064, #1476 and #3696), isolated from BM, were stained with an anti-adhesion molecule antibody or its matching isotype control. Doublets and dead cells were excluded. Cells were stained for **(A)** CD11a **(B)** CD44 and **(C)** CD49d. The histogram for each PDX-ALL cell line is shown. Histograms display fluorescence intensity, black filled lines represent the isotype control, and red solid lines show anti-adhesion molecule staining. The bar diagrams display the MFI values for the PDX-ALL cell lines.

The surface marker expression of the luciferised PDX-ALL cell lines is comparable to the analysed primary samples of paediatric patients, shown in 3.1. Luciferised cells allow *in vivo* tracking of ALL cell migration and survival and analysis of the tumour kinetics by IVIS imaging. All PDX-ALL lines express CXCR4; therefore they can be used to study the relevance of the CXCR4-CXCL121 axis for testis infiltration in a NSG mouse model.

3.6.3 PDX-ALL cells migrate towards murine CXCL12

To prove the ability of the human PDX-ALL samples to migrate towards murine CXCL12 an *in vitro* transwell migration assay was performed. PDX-ALL cells were thawed, and migration took place in 5 µm cell culture inserts for 4 hours at 37°C. All PDX-ALL samples showed a stable migration towards murine CXCL12 in two independent experiments (**Figure 37**). While sample #1476 displayed only a weak migration, samples #1056 and #3696 showed a very

strong migration with a migration factor of 60 and 140. These observations correlate with the CXCR4 expression levels on the PDX-ALL cells. Hence, all PDX-ALL samples reacted on murine CXCL12 and are therefore suitable for employing them in *in vivo* mouse experiments.

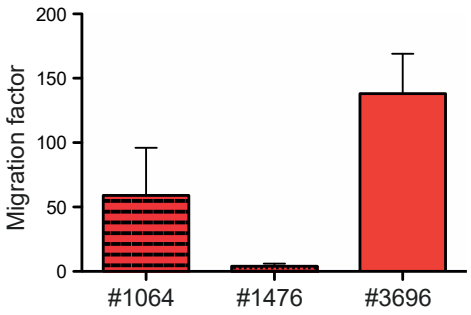

Figure 37: PDX-ALL cell migration towards murine CXCL12. The three transduced PDX-ALL cell lines migrate towards murine CXCL12 in a transwell migration assay. Sample #1476 shows the lowest migration ability while samples #1064 and #3696 both show a very strong migration towards murine CXCL12. Migration took place in tissue culture inserts at 37°C for 4 hours. Values are displayed as mean ± SEM, n=2.

3.6.4 Establishment of a testis-ALL PDX model in NOD/SCID gamma chain mice

The transduced and characterized PDX-ALL cells were used to establish a mouse model with testicular involvement. As illustrated in **Figure 38A** PDX-ALL cells were transplanted i.v. into NSG mice and leukaemia progression was monitored by weekly IVIS imaging from day 21 up to day 42 after PDX-ALL cell transfer (**Figure 38B**). At day 49-50 the experiment was terminated and the percentages of tumour blasts in the BM, spleen, blood and testis were determined by flow cytometry as shown exemplarily in a three week-old NSG mouse (**Figure 38C**). Cells were gated on lymphocytes, single and live cells before tumour cells were defined by human CD19, CD10 and CD45 expression. While BM and the spleen show a strong infiltration, the testes were only infiltrated by a small amount of ALL cells.

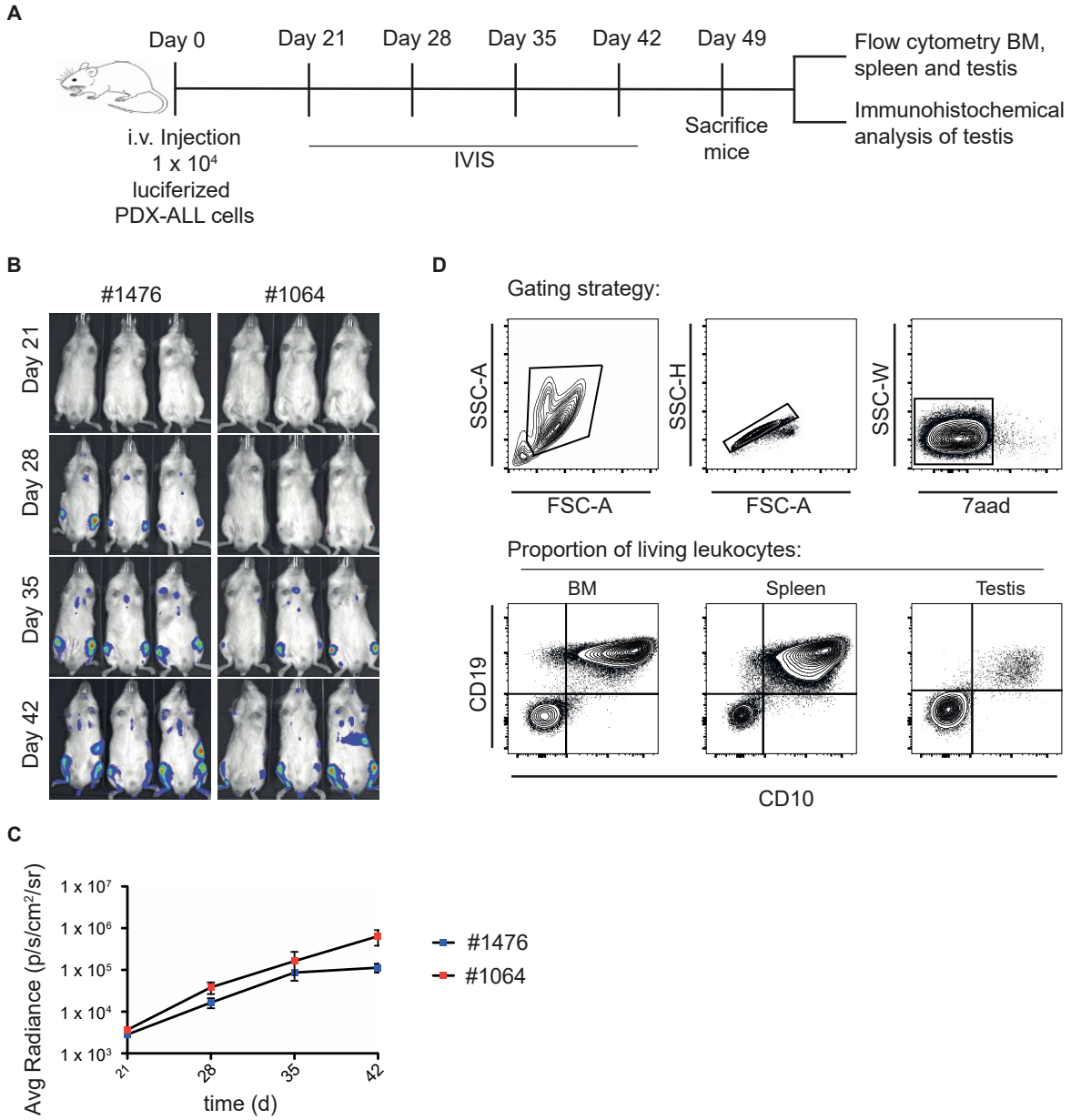

Figure 38: Establishment of an ALL-PDX model with testicular involvement in NOD/SCID gamma chain mice. (A) Experimental setup of PDX-ALL cell transplantation into NSG mice. PDX-ALL cells were i.v.injected into the tail vein. **(B)** The transplanted cells were monitored 3, 4, 5 and 6 weeks post transplantation using the IVIS technology to detect a luciferase signal emitted by the tumour cells. Exposure time: 60s. **(C)** Quantification of the luciferase signals measured by IVIS technology. **(D)** The tumour load in % of vital, single cells of all organs was determined by flow cytometry gated on CD45, CD19 and CD10 expression.

3.6.5 Pre-puberty mice show profound testicular involvement compared to post-puberty mice

Testicular infiltration is mainly observed in paediatric patients, therefore eight week-old (post-puberty) and three week-old (pre-puberty) NSG mice were compared for testicular involvement after adoptive transfer of PDX-ALL cells. In a first attempt 1 x 10^6 PDX-ALL cells were i.v. transplanted into each mouse. In pre- as well as post-puberty mice, the

development of profound leukaemia was observed within 35 days (**Figure 39A+B**). At this time point the experiment had to be terminated according to federal law regulating animal research. As shown in **Figure 39C**, only minor testicular infiltration of leukemic cells could be observed in post-puberty and pre-puberty NSG mice by the end of this experiment. The transplanted PDX-ALL cells grew very aggressively in the immunodeficient NSG mice; therefore, experiments performed with 1 x 10^6 PDX-ALL cells per animal had to be terminated after 5 weeks post-transplantation. Slowing down the tumour progression by transplanting a low number of tumour cells (1 x 10^4) resulted in a slower tumour progression and experiments had to be terminated only 49 days post-transplantation. As displayed in **Figure 39B+C**, the amount of leukaemia cells in the BM and spleen was comparable 49 days after PDX-ALL cell transfer in post-puberty and pre-puberty recipients, however the amount of testicular dissemination was significantly different.

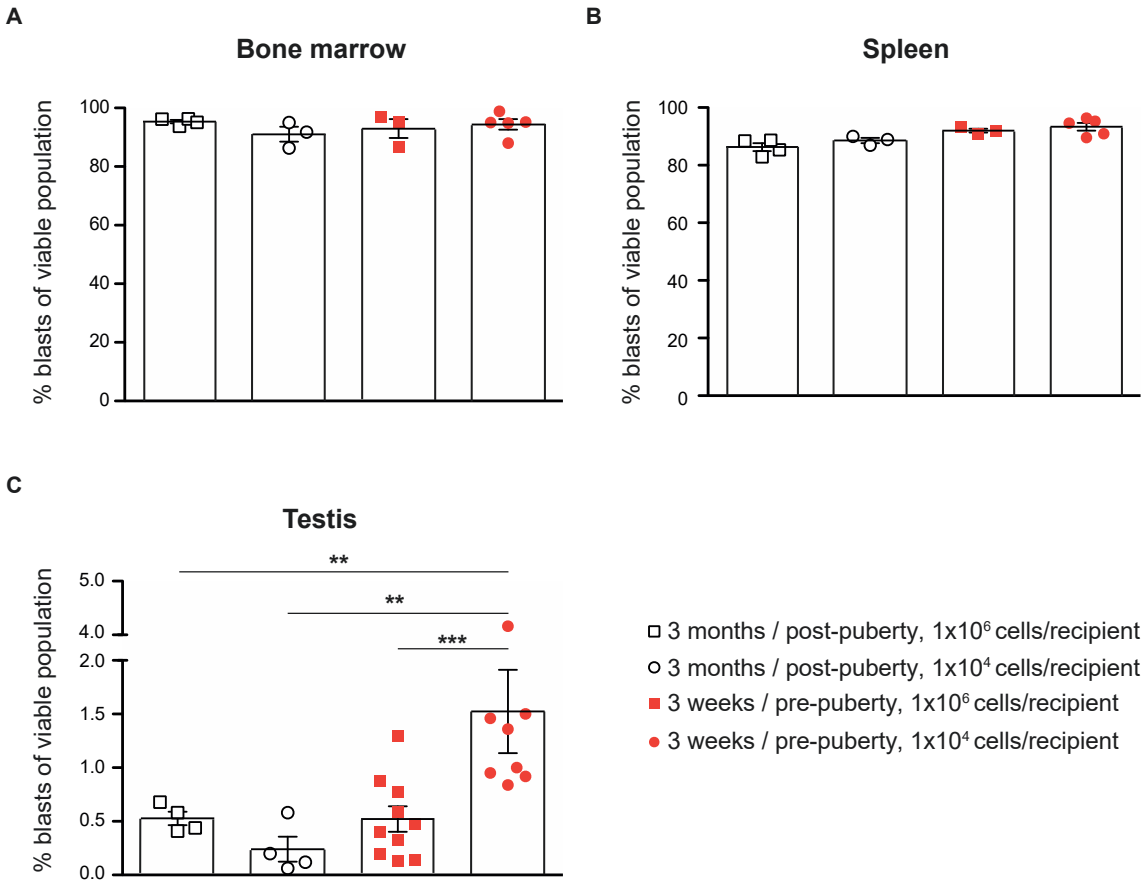

Figure 39: Tumour load in BM, spleen and testis determined by flow cytometry in pre- versus post-puberty mice. The recipients were either three week- or three month-old at the day of ALL transplantation. The percentage is based on all living, single leukocytes. Tumour burden of **(A)** BM and **(B)** spleen and **(C)** testes was compared in pre- and post-puberty mice, transplanted with either 1 x 10^6 or 1 x 10^4 PDX-ALL cells. Differences between the groups are displayed as mean ± SEM, p values (**p<0.01, *** p<0.001) were calculated by Mann-Whitney U test, 10^6, three month-old n=4; 10^4, three month-old n=4; 10^6, three week-old n=10; 10^4, three week-old n=8.

Pre-puberty mice, transplanted with 1 x 10^4 PDX-ALL cells showed an increase of tumour infiltration of the testis compared to post-puberty recipients, but also compared to pre-puberty mice, transplanted with 1 x 10^6 PDX-ALL cells. These results indicate that testicular dissemination and survival of leukemic cells is strongly supported by the testicular microenvironment before the onset of puberty. But also, a slow tumour progression is essential to allow infiltrating cells to start proliferation within this extramedullary organ.

Leukaemia cell localization within the testis was detected by immunohistochemistry. Histological staining of human testis sections described by Reid and Marsden showed that tumour cells invade the testis primarily in the interstitial space between the seminiferous tubules and are surrounded by Leydig cells and testicular macrophages (tMφ)[140].

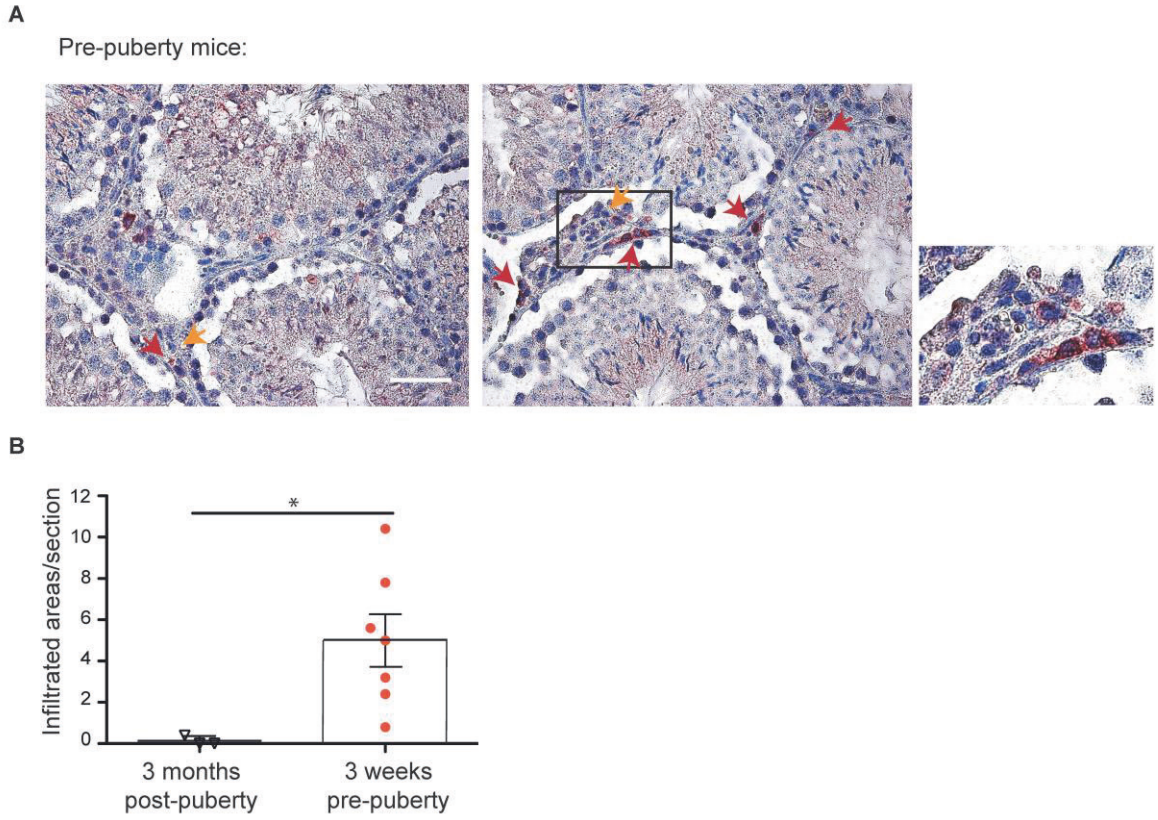

Figure 40: Immunohistochemical analysis of serial sections reveals tumour cell localisation. **(A)** Representative testicular sections stained with anti-human CD68 show that tumour cells, indicated by red arrows, within the testicular tissue are often located near blood vessels, indicated by orange arrows. PDX-ALL cells are located in the interstitial space. Bar 50 µm. **(B)** Infiltrated areas were quantified by immunohistochemistry, staining five sections per animal. Values are displayed as mean ± SEM, p values (*p<0.05) were calculated by Mann-Whitney U test, 10^4, three month-old n=3; 10^4, three week-old n=7.

Accordingly, the analysed sections of the PDX-ALL transplanted NSG mice revealed leukemic cell localization mainly in the interstitial space of the testes, often near blood vessels **(Figure 40A**). Five sections per animal were stained with an anti-human CD10

antibody to identify the tumour cells within the testicular organ and to quantify infiltrated areas. The significant infiltration of testis in pre-puberty mice was verified, while no CD10 positive leukaemia cells were detected in post-puberty mice (**Figure 40B**).

3.6.6 Treatment of mice with an anti-CXCR4 antibody inhibits testis infiltration

As described in 3.2.5 and 3.3.4, functional inhibition of CXCR4 on Nalm6 cells by AMD3100 treatment as well as a complete engineered CXCR4 KO reduces ALL cell migration to conditioned medium (CM) from BM-MSC and testicular stroma cultures drastically. Here, the developed ALL mouse model with testicular involvement using pre-puberty NSG mice enables further studies *in vivo*. An increased testicular infiltration with ALL cells was only observed when transplanting pre-puberty mice, therefore a treatment with an anti-CXCR4 antibody should be performed at an early stage during tumour development. However, the CXCR4-CXCL12 axis is important for tumour cell engraftment. Beginning the treatment early after tumour cell injection might inhibit the ALL engraftment and therefore the development of the tumour in the animal. Based on observations on human stem cell engraftment in NSG mice, antibody treatment was started four days post transplantation[172]. Injecting an anti-CXCR4 at this time point did not influence stem cell engraftment, but an earlier injection led to a reduced or inhibited engraftment. In order to block migration of PDX-ALL cells mice were treated twice weekly from day 4 to day 21 with either an anti-CXCR4 or anti-IgG (control) antibody. Tumour cell engraftment was monitored weekly by IVIS imaging from day 28 and mice were sacrificed on day 46 (**Figure 41A**) and in a repeated experiment on day 65. The inhibition of CXCR4 with the anti-CXCR4 antibody was validated by an *in vitro* transwell migration assay towards human CXCL12. Cells treated with anti-CXCR4 showed a strong reduction of migration towards CXCL12, whereas treatment with the control antibody did not alter migration of Nalm6 cells and the PDX-ALL donor #1064(**Figure 41B**). Both groups showed the same weight gain over the time of the experiment (**Figure 41C**). However, while mice treated with a control antibody showed increasing signals by IVIS imaging, the anti-CXCR4 treated group did not display a detectable signal (**Figure 41D+E**).

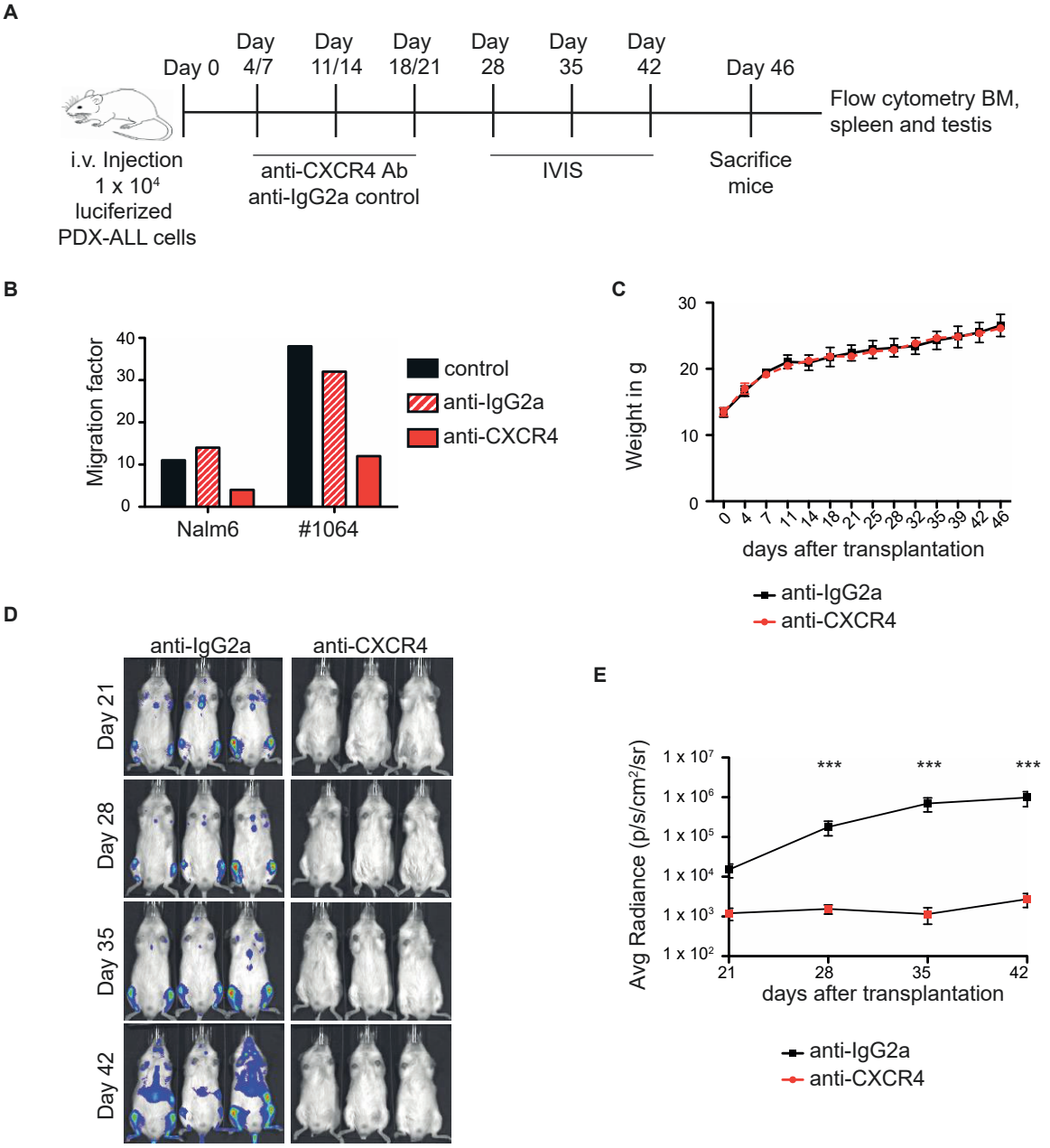

Figure 41: Retarding tumour cell engraftment with an anti-human CXCR4 antibody. (A) Experimental setup of PDX-ALL cell transplantation into NSG mice. PDX-ALL cells were i.v. injected into the tail vein. The antibodies were applied by i.p. injection. **(B)** Used antibodies were tested *in vitro* in a transwell migration assay. Nalm6 cells and the PDX-ALL clone #1064 were treated with the anti-IgG2a or anti-CXCR4 (1,25 µg/ml) for one hour prior to the experiment. **(C)** Body weight development of mice treated with either anti-IgG2a or anti-CXCR4. Anti-IgG2a n=3; anti-CXCR4 n=3. **(D)** The transplanted cells were monitored weekly starting from day 28 post-transplantation using the IVIS technology to detect a luciferase signal emitted by the tumour cells. Exposure time: 30s. **(E)** Quantification of detected IVIS signals. Anti-IgG2a n=3; anti-CXCR4 n=3. Values are displayed as mean ± SEM. p values (*** p<0.001) were calculated by Mann-Whitney U test.

Mice were sacrificed 46 to 65 days post-transplantation and the tumour burden of BM, spleen and testis was determined by flow cytometry. The tumour growth in the anti-CXCR4 treated group was clearly retarded (**Figure 42 A+B**). Only a few cells were detected in BM and the

percentage of blasts of the viable population in the spleen was about 2%. However, no tumour cells were detected in testes of animals treated with anti-CXCR4. The strong difference in tumour development between the anti-CXCR4 and the control group was also visible by comparing the spleen weight and total cell count of this organ. As displayed in **Figure 42C** spleens of control antibody treated mice reached around 320 mg, spleens of anti-CXCR4 treated mice had a weight of only 40 mg. Also, the total cell count showed significant differences between the groups. On average the spleens of the control animals had a 6-fold higher cell count compared to the anti-CXCR4 treated group. The CXCR4 expression of PDX-ALL cells in BM and the spleen was analysed by flow cytometry (**Figure 42D**). There was no difference in expression of this chemokine receptor in BM and spleen derived tumour cells between the groups.

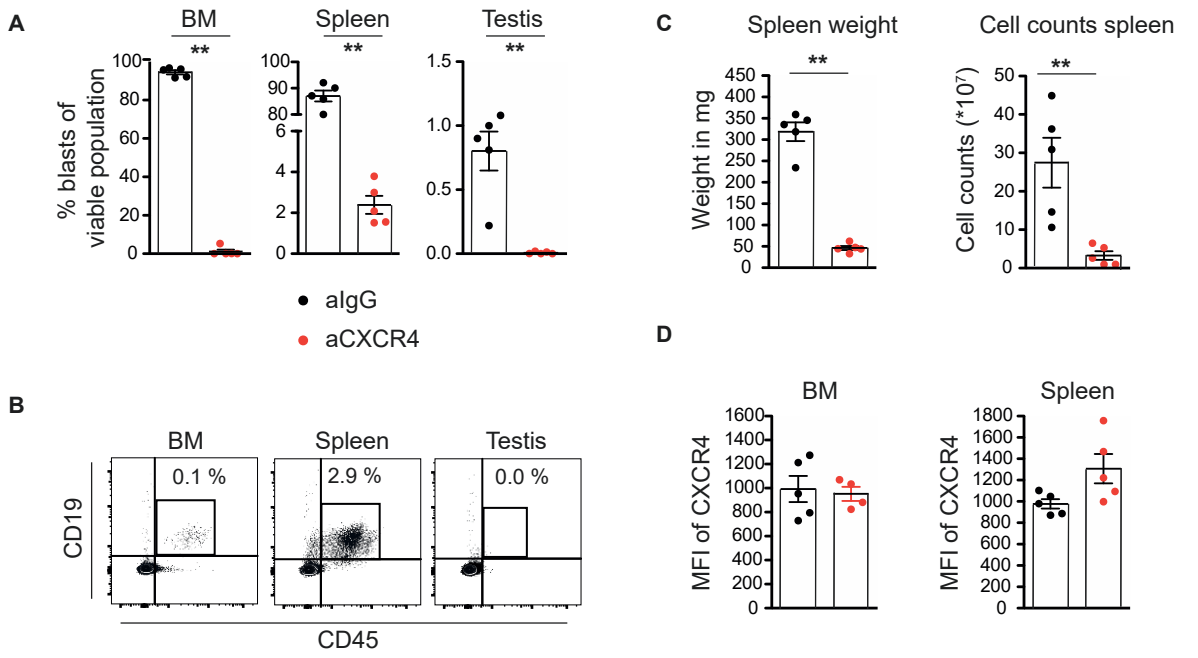

Figure 42: Anti-CXCR4 treatment inhibits testicular infiltration. (A) Treatment of mice with an anti-CXCR4 antibody lead to a drastically reduction of tumour burden in BM and spleen compared to the isotype treated control group. While little PDX-ALL populations were detected in BM and spleen in anti-CXCR4 treated mice, no tumour cells were measured in testes of these animals. **(B)** Representative plots of an anti-CXCR4 treated mice, showing tumour populations in BM and spleen. In testes no PDX-ALL cells were detected. The tumour load in % of all organs was determined by flow cytometry gated on CD45 and CD19 expression. **(C)** Spleen weight of all animals was measured and the total cell count was determined. **(D)** CXCR4 expression on PDX-ALL cells in BM and spleen was determined by flow cytometry. Anti-IgG2a n=5; anti-CXCR4 n=5. All values are displayed as mean ± SEM. p values (*** p<0.001) were calculated by Mann-Whitney U test.

In conclusion, an anti-CXCR4 treatment of mice transplanted with PDX-ALL cells led to a strong delay of tumour growth in all analysed organs. Nevertheless, BM and spleen showed minor populations of tumour cells, which prove the successful tumour cell engraftment. Only the testes of all analysed animals were free of tumour cells. Blockage of the CXCR4-CXCL12

axis to an early time point of the disease seems to effectively hinder tumour infiltration of the testes. Interfering with this pathway might be an option to prevent a testicular relapse in paediatric patients, when applied at an early stage of the disease, immediately after initial diagnosis.

4 Discussion

4.1 CXCR4 and IL7R are involved in testis directed ALL migration

Lymphocyte migration and recirculation is crucial for a functioning immune response. This so called “homing” guides lymphocytes into different microenvironments, where differentiation and survival of these cells is controlled. To ensure lymphocyte homing chemotaxis and cell adhesion steps are required, involving adhesion molecules and chemokines. Lymphocyte migration is part of a conserved physiological behaviour, which malignant cells and/or cells of numerous tumour entities use for rapid dissemination[173].

4.1.1 Chemokine receptor expression pattern on paediatric B-ALL samples

Within the last twenty years many efforts have been made to reveal the chemokine receptor expression of B cell malignancies. Studies using primary samples often resulted in contradictory results, probably because of the selection of patients or differences in processing of the material after extraction from the patients. In 2001, the lymphocyte-associated chemokine receptors CXCR4, CXCR5, CCR5 and CCR6 were analysed on different B cell tumour entities. The only receptor detectable in B-ALL samples was CXCR4[174]. Another study from 2004 extended the set of chemokine receptors and analysed CXCR3, CXCR4, CXCR5, CCR5, CCR6 and CCR7 expression on samples of different adult B cell malignancies. The expression patterns were highly variable between the different B cell malignancies. Chronic lymphoblastic leukaemia cells, small cell lymphocytic lymphoma and hairy cell leukaemia showed a broad range of receptor expression. However, the only chemokine receptor expressed by B-ALL cells was again CXCR4[175]. These observations complement with the results of the presented work. Nevertheless, here a modest CCR7 and CXCR3 expression was detected in some patients. Neither receptors were detected on B-ALL cells analysed in the 2004 study. This discrepancy might result from differences in processing the cells, e.g. the transport of the samples or freezing and thawing protocols. Another reason might be the use of different controls (isotype control or fluorescence minus one stainings) and the cut-off that was considered as a positive signal during flow cytometry analyses. Furthermore, analysed cells from the two mentioned studies were taken from adult patients, while the cohort in this work contained samples from paediatric patients exclusively. Considering the poor survival of adult compared to paediatric B-ALL patients (approximately 40 % versus 80%)[176] it seems obvious that the overall tumour biology and therefore also the chemokine receptor expression pattern might be different between these patient groups. A study from 2006 focussed on chemokine receptor expression in samples of a cohort of 38 B-ALL samples of paediatric patients with newly diagnosed B-ALL[177]. In contrast to the other two studies the authors included a wider range of receptors and analysed CXCR1, 2, 3, 4 -

CXCR5 as well as CCR1, 2, 3, 4, 5, 6 - CCR7. Analysed patients represented all different immunophenotypic subtypes of B-ALL (pro-, common-, pre- and mature B ALL), while the cohort in this thesis mainly included common B-ALL samples. The detected chemokine receptor pattern differs profoundly from observations in the presented thesis. CXCR2 and CXCR3 were detected in all analysed common B-ALL samples and CXCR1 and CXCR5 in most of them. Whereas the analysed samples in this thesis never showed CXCR1 and CXCR2 expression, there was only one case of a weak CXCR5 expression and occasionally a weak CXCR3 expression (9/30). CXCR4 was only observed in around 50% (8/17) of the common B-ALL samples included in the 2006 study. This observation is in contrast with the presented results, according to which CXCR4 was highly expressed by all paediatric patients after initial diagnosis as well as after relapse diagnosis. This might be due to the different background of the analysed samples. The 2006 study used samples taken from patients after initial diagnosis, most of whom did not have a relapse. The analysed samples of this thesis were exclusively taken from patients diagnosed with a relapse. A higher and consistent CXCR4 expression in this cohort could be connected to the fact that B-ALL cells with a high CXCR4 expression tend to be more aggressive. Therefore, it is more likely that the patients with a high CXCR4 expression will have a relapse. The authors further describe a CCR3, CCR4 and CCR7 expression in some of the common B-ALL samples, this concurs with the observation of CCR7 expression in a few of the tested patients of the cohort analysed in this work. However, while the authors claim expression of various CXCR and CCR on all B-ALL subtypes they only found the CXCR4-CXCL12 axis to be chemotactically active.

An advantage of the patient cohort in this work is the distinction of samples into different relapse groups and the availability of material from two different time points of the disease. Considering these conditions, the presented results are a valuable addition to the understanding of the chemokine receptor expression pattern of paediatric ALL cells. The high expression of CXCR4 in samples from paediatric ALL patients was already described by Crazzolara et al. in 2001[109]. The authors show a correlation between high CXCR4 expression and extramedullary organ infiltration and therefore designate CXCR4 to be a marker to predict extramedullary organ invasion. This correlation was absent in the presented study. Here, no specific up-regulation of CXCR4 expression in patients having a combined CNS or testis relapse compared to an isolated BM relapse was detected. This might be due to the relatively small number of CNS and testis relapse patient samples in combination with an overall high expression of CXCR4 in most of the samples. However, Crazzolara et al. only analysed spleen and liver, which are frequently infiltrated in ALL and do not mention other extramedullary sites or relapse situations. Therefore, their observations might not be

comparable with the presented results, but they underline the significance of CXCR4 for ALL cell migration towards extramedullary sites.

The prognostic value of CXCR4 was also observed for diffuse large B cell lymphomas (DLBCL), another B cell malignancy [178]. The authors found a high CXCR4 expression to be correlated with migration *in vitro* and dissemination *in vivo*. In a NOD/SCID mouse model, CXCR4 expression led to increased engraftment in the BM and decreased survival of mice. On the other hand, blockage of CXCR4 by the antagonist AMD3100 reduced the dissemination of DLBCL cells in the mouse model.

4.1.2 The IL7R is associated with testicular infiltration of paediatric patients

While chemokine receptors play a crucial role in tumour cell dissemination and survival, other surface markers have been identified to be involved in these processes too. The cytokine IL7 is produced by cells of the BM, thymus and other organs. The IL7R-IL7 axis is necessary for normal T- and B-cell development and peripheral homeostasis, but is also thought to take part in T-ALL and BCP-ALLprogression[151,179]. In 2018 Alsadeq et al. published an article suggesting that the IL7R is associated with CNS infiltration and relapse in paediatric ALL[180]. Applying current diagnostic methods, overt CNS involvement is rarely seen after initial diagnosis[181,182]. The CNS TME is suspected to play a crucial role in ALL cell migration, survival and chemoresistence[183]. Alsadeq et al. observed a high expression of IL7R in paediatric ALL patients who were already CNS^+ at initial diagnosis and considered an up-regulation of this receptor to predict CNS relapse[180]. The role of the IL7R in testicular infiltration of ALL relapse is unknown, therefore this receptor was included in the analysis.

In the analysed cohort, patients that were facing a testicular relapse already had a significant up-regulation of the IL7R at initial diagnosis compared to patients with an isolated BM relapse. This up-regulation was still present at relapse diagnosis. The analysed CNS relapse patients showed only a tendency towards IL7R up-regulation compared to isolated BM relapse patients. However, the tested CNS relapse cohort was rather small and increasing the number of analysed samples might have altered the outcome. This observation suggests that IL7R is not only an interesting diagnostic marker for CNS relapse but can also predict testicular infiltration after initial diagnosis. Alsadeq and colleagues demonstrated a correlation between IL7R expression on B-ALL cells and CNS infiltration of samples from children with newly diagnosed and relapsed ALL. They showed reduced ALL engraftment and CNS infiltration *in vivo* by using a monoclonal anti-IL7R antibody[180]. The IL7R ligand IL7 was already described to be present in cerebrospinal fluid and high levels of IL7 can be correlated with inflammatory CNS disease[184]. This suggests that IL7 might be produced by the CNS microenvironment upon different stimuli[185]. Up to now there is no study describing

IL7 expression in the testis. It is not clear whether the IL7R expression could only be a predictive marker for testicular relapse or - as it seems to be the case for CNS relapse- be a novel target for B-ALL treatment to prevent testis relapse.

Interestingly, CXCL12 and IL7 are known to collaborate in the activation of the proliferation of progenitor B-cells[186,187]. Thus, a link between the CXCR4 and IL7R in B-ALL development is possible. And indeed, an article published just recently suggests a synergism between IL7R and CXCR4 that is involved in the development of Philadelphia chromosome-positive (Ph^+) ALL[188]. The Ph^+ ALL develops upon a chromosomal translocation leading to a *BCR-ABL1* fusion gene. While only 3-5% of paediatric ALL patients are diagnosed with this fusion gene, their prognosis is unfortunately poor[189,190]. An interaction of IL7R and CXCR4 on the cell surface in *BCR-ABL1* positive B-cell progenitors favoured a malignant transformation and the manifestation of a Ph^+ ALL. Furthermore, the authors showed an elimination of ABL1 inhibitor-resistant Ph^+ patient ALL clones in a xenograft model upon an anti-IL7R treatment[188].

The role of IL7R expression in ALL development and relapse is not fully understood. More ALL relapse studies are needed to further investigate the promising insights of recent investigations. On the one hand, this includes IL7R inhibition in ALL xenograft models. On the other hand, it comprises the up-regulation of IL7R in testis relapse patients, which have been demonstrated in the present thesis.

4.2 Primary testicular stroma cultures are a promising tool to study ALL-testis stroma interaction

4.2.1 Testis stroma cultures support *in vitro* ALL cell survival

Studying primary ALL cells in vitro is difficult since tumour cells get apoptotic within a few hours when kept in culture dishes. However, survival of primary ALL cells in culture can be improved by using a feeder layer. In 1992 Manabe et al. described an improved survival of leukemic cells when co-culturing them with BM stroma cells in a serum-free environment[165]. BM-MSC are still the most frequently used tool to culture ALL cells *in vitro* and even an expansion of primary leukemic cells was described in long-term co-culture approaches[159]. Even if a 2D culture of a single cell type does not reflect the complex TME, BM-MSCs are a useful instrument to study interaction of ALL cells with the BM microenvironment. A similar approach to study the testicular microenvironment is still lacking. In this thesis, primary patient stroma from both sources, BM and testis was used to study the survival of relapsed leukemic cells in *in vitro* co-culture experiments. In this work, BM-MSCs and testicular stroma

both provided support for the primary ALL cells to a similar extent. Interestingly, the effect on *in vitro* survival was rather dependent on the leukemic patient sample than on the source of stromal feeder cells. As described in the study from 1992[165], ALL cells behave extremely heterogeneous in culture. While some patient samples were very vital in mono-culture for 48 hours others were highly apoptotic under the same conditions. Most patients' ALL samples profited when cultured together with either BM-MSCs or testicular stroma, indicating that the testis derived stroma cells have a similar effect on the survival of primary leukemic cells as the one described for BM-MSCs. In 1999, Nishii et al. observed that not only the direct ALL cell to stroma contact can support survival of primary B-ALL cells but also the supernatant of stromal cultures has this potential[191]. Therefore, they searched for cytokines that might be responsible for the improved survival. They found that IL3 and IL7 under certain conditions and CXCL12 in all cases reduced apoptosis of primary B-ALL cells. CXCL12 is a crucial chemokine within the stem cell niche of the BM and is produced by BM-MSC at high levels[172,192]. Within the testis, CXCL12 is considered to be responsible for the stem cell organisation within the seminiferous tubules. Interfering with the CXCR4-CXCL12 axis in an undifferentiated spermatogonia cell culture led to a reduction of spermatogonial stem cells, partly due to a decrease of proliferation.[47]. The role of CXCL12 within the BM and the testis shows some similarities. It seems feasible, that not only BM-MSCs but also testis stroma can secrete CXCL12 in culture and could support leukemic cell survival via the CXCR4-CXCL12 signalling axis. Analysing supernatants of BM-MSC and testis stroma cultures for their CXCL12 levels revealed similar concentrations of the chemokine in both cultures. The CXCL12 level was even higher, when BM-MSCs or testis stroma cells were co-cultured with the B-ALL cell line Nalm6. The observed effect was not significant though since the patient derived stroma cultures were very heterogeneous in their reaction towards ALL cell contact. The increased CXCL12 level upon tumour cell contact does not support the observations of van den Berk et al., from 2014[192]. In the study from 2014 lower CXCL12 levels were measured in BM samples of B-ALL patients compared to healthy controls. However, samples taken after induction therapy showed the same level of CXCL12 as observed in healthy control samples. The BM-MSCs and testis stroma cells used in this work are both derived from relapse patients who already experienced a broad spectrum of therapeutic approaches during frontline therapy. This might be a reason for the observed differences in CXCL12 expression pattern compared to the study from 2014.

Based on the presented results it can be concluded that the testis, as the bone marrow, provides a favourable microenvironment for leukemic cells. This is partially related to tumour-stroma contact but also to soluble factors, such as CXCL12 that support ALL survival. The testicular stroma cultures are therefore a valuable tool to study the ALL interaction with its microenvironment in this extramedullary organ *in vitro*. However, a 2D *in vitro* culture lacks

the complexity of a three-dimensional microenvironment. Sieber et al. published a 3D BM culture, a so-called bone marrow-on-a-ship[193]. This culture system, using BM-MSCs on a three-dimensional scaffold, allows the long-term culture of hematopoietic stem cells. A similar approach, a testis-on-a-ship, might be an option to improve testis-ALL *in vitro* studies in future.

4.2.2 *In vitro* CXCR4 is involved in testis directed migration

While the CXCL12-CXCR4 axis is an important signalling pathway involved in survival, proliferation and development within the BM[120] another key function of this axis is to trigger migration of stem cells[172]. In 2000 Bradstock et al. demonstrated that also B-ALL migration towards BM is regulated by CXCL12 [194]. By using the CXCR4 antagonist AMD3100 migration of Nalm6 cells and primary ALL samples towards murine BM stroma was completely inhibited[121]. In 2015, Arnaud et al. demonstrated that murine testis-conditioned medium (testis-CM) has the ability to trigger migration of the pre-B-ALL cell lines REH and Nalm6 and AMD3100 reduced this migration[145]. In this thesis, human testis-CM was used to study migration of Nalm6 cells. Additionally, human BM-MSC-conditioned medium (BM-CM) was used and compared with the testis-CM. Both, testis-CM and BM-CM, had a similar concentration of CXCL12 and were able to trigger Nalm6 migration in a transwell migration assay. When treating Nalm6 cells with AMD3100 prior to the assay, migration was completely inhibited. This reduction was much stronger compared to the effect observed by Arnaud et al in a murine system[145]. However, quantification methods of the migrated cells differed between this study and the one presented by Arnaud et al., which could explain observed differences. Considering the described results, *in vitro* migration of B-ALL cells towards human testis stroma cells seems to be primarily controlled via the CXCR4-CXCL12 signalling axis and can be blocked by a CXCR4 antagonist.

The specificity of AMD3100 towards CXCR4 was already studied by Hatse et al. in 2002[166]. In this study the authors analysed the interaction of AMD3100 with CXCR1, CXCr2, CXCR3 and CXCR4 and CCR1 - CCR9, by measuring the intracellular calcium mobilisation and by performing migration assays. They observed an exclusive receptor interaction of AMD3100 with CXCR4 while all other tested chemokine receptors were unaffected by an AMD3100 treatment. However, the complete inhibition of Nalm6 migration towards BM-CM and testis-CM raises the question if treatment of Nalm6 cells with AMD3100 might have target-unspecific effects that would influence the cell migratory behaviour. A study by Randhawa et al., from 2016 already addressed this problem and compared the inhibition potential of AMD3100 and a CRISPR-Cas9 mediated CXCR4 KO on different B-ALL cell lines[124]. Migration potential of both genetic and pharmacological modified cell lines were analysed by transwell migration assays. While treatment of Nalm6 cells with AMD3100 inhibited migration

towards recombinant CXCL12 by 50%, a CXCR4 KO in Nalm6 cells reduced migration by 80%. A similar approach was used in this thesis. The complete reduction of migration towards BM-CM and testis-CM after AMD3100 might be related to the lower amount of CXCL12 in the conditioned media compared to the recombinant CXCL12 used by Randhawa et al. The generated Nalm6-CXCR4 KO cell line used in transwell migration assays showed a complete inhibition of migration towards recombinant CXCL12. However, when testis-CM was used in transwell migration assays Nalm6 CXCR4 KO cells still showed some migration towards the supernatants. This observation supports the idea of unwanted target-unspecific effects by AMD3100. Nevertheless, the strong reduction of Nalm6 migration after a CXCR4 KO underlines the relevance of this chemokine receptor for testis directed ALL cell migration.

The CXCR4-CXCL12 signalling axis is also an important pathway for spermatogonial stem cells within the testis, as already discussed above[47]. Sertoli cells express CXCL12 throughout the entire testicular development and thereby regulate SSC fate decisions[49]. While the relevance of CXCL12 in B-ALL migration towards the testis is still discussed, a contrary mechanism was already described for testicular germ cell tumours (TGCT), the most common solid malignancy in young adult men[195,196]. Derived from testicular germ cells, TGCT cells express CXCR4 and develop metastasis in organs known for high CXCL12 expression, such as bone marrow and lymph nodes[195]. The impact of CXCL12 on TGCT cell migration was confirmed by McIver et al., in 2013[197]. These observations underline the importance of the CXCR4-CXCL12 axis in migration of naturally CXCR4 positive cells into other organs with high CXCL12 expression. High expression of CXCR4 in TGCT cells is related to the circumstance, that CXCL12 is an important chemokine in testicular development and organisation. CXCR4 expressing ALL cells, circulating in the peripheral blood, could follow the CXCL12 gradient of the testis. This thesis supports this notion by showing migration towards testis-CM and inhibition of this migration by either AMD3100 treatment or a CXCR4 KO on the B-ALL cell line Nalm6.

4.3 The testicular tumour microenvironment

An important topic in the field of tumour immunology is the identification of microenvironmental cellular and molecular suppressors of the immune response against tumour cells. Interfering with these pathways is a possibility to enhance the endogenous anti-tumour response and block immune escape during cancer progression. One intensively studied cellular component participating in this tumour promoting processes are macrophages[95]. Macrophages are typically classifies into classically activated M1 macrophages and alternatively activated M2 macrophages[198]. Tumour infiltrating

macrophages, so called TAMs, show characteristics of both types, but are considered to have a stronger manifestation of the M2 type[199].

4.3.1 PDX-ALL cells have an impact on tMφ polarisation

Macrophages are an important component of a functioning innate immune system. However, a malignant microenvironment can influence macrophage polarisation towards a tumour favourable phenotype[101]. Until now, only few studies analysed the effect of these TAMs on ALL progression but there is evidence that macrophages also play a role in this tumour entity. Komohara et al. analysed samples of 58 T-ALL patients and found, that a high amount of M2 polarised TAMs is associated with poor clinical outcomes[200]. *In vitro* co-cultures of T-ALL cell lines with M2 polarised monocyte-derived macrophages led to an increased proliferation of the leukemic cells. In 2015, Chen et al. found evidence that ALL cells have a different impact on macrophages depending on the analysed organ. TAMs from BM and spleen showed considerable differences on expression of genes and spleen TAMs stimulated ALL cell proliferation to a greater extent compared to the BM TAMs[201]. Within the testis macrophages are the major type of innate immune cells and a potential source of TAMs. Leukaemia cells can shape their microenvironment by secreting growth factors and cytokines. It was shown that chronic myeloid leukaemia cells express factors affecting the cytokine secretion of BM macrophages and thereby alter their TME[202].

In this thesis *in vitro* co-cultures were used to analyse the impact of PDX-ALL cells on mouse testicular macrophages (tMφ). A mouse testicular stroma culture containing tMφ was either mono-cultured or co-cultured with PDX-ALL cells or murine B-cells isolated from C57B6/N mouse spleen. Analysing the tMφ after a 20-hour co-culture with PDX-ALL revealed an up-regulation of the M2 marker *Arg1* in interstitial but not in peritubular tMφ on RNA level. To exclude an effect, that is caused by cells from the B-cell linage in general, mouse testicular stroma was also co-cultured with isolated B-cells from the mouse spleen. The up-regulation of *Arg1* in interstitial tMφ was absent when macrophages were co-cultured with murine B-cells. Interstitial and peritubular tMφ were not altered in their M1 marker expression in any of the tested conditions. The enzyme Arg1 is associated with M2 polarisation of macrophages and a TAM phenotype[203]. By metabolizing L-arginine into urea and L-ornithine Arg1 provides molecules for the downstream generation of proline and polyamines, both involved in macrophage proliferation. Additionally, Arg1 reduces T-cell activation by locally reducing the L-arginine concentration[204]. In 2018 Arlauckas et al. described $Arg1^+$ macrophages to be more abundant in tumour tissues compared to healthy organs[205]. The same year Yang et al. published an article claiming that TAMs in a murine T-ALL model expressed high levels of Arg1[206].

Polarisation of macrophages into the M1 or M2 state but also into M2-like TAMs is to a great extent controlled by cytokines. Several cytokines involved in TAM development were already identified[95,207,208]. In this thesis, the cytokine secretion of PDX-ALL cells that were either mono- or co-cultured with the murine testicular stroma containing tMφ were analysed on the RNA level for their expression of TAM inducing cytokines IL4, IL6, IL10, TGFß and M-CSF. Additionally, the expression of the M1-phenotype inducing cytokine INFy was analysed. While no expression of either INFy or the TAM inducing cytokines IL4 and IL6 was detected, lower levels of IL10 and higher levels of TGFß and M-CSF were detected in co-culture compared to mono-culture. High levels of M-CSF were detected in several tumour entities, such as breast cancer, ovarian cancer and cervical cancer compared to non-malignant tissue[209,210]. In 1991, Janowska-Wieczorek et al. analysed the M-CSF-1 levels of peripheral blood of 316 patients with malignant and premalignant hematologic disorders. They found elevated levels of M-CSF-1 in patients compared to healthy controls and assumed a production of the cytokine either by the malignant cells themselves or an altered cytokine production of the microenvironment upon leukaemia progression[211]. A study from 2015 using a lymphoma xenograft mouse model found a correlation between M-CSF levels within the TME and infiltrating TAMs. The authors analysed the influence of different M-CSF isoforms and found different influences of the isoforms on TAMs. The secreted M-CSF isoform is involved in recruitment and polarisation of TAMs, while the membrane bound form enhances TAM proliferation within the TME[212]. While the M-CSF analysed in this thesis was not distinguished into the different isoforms, it is likely, that PDX-ALL cells express one or even both isoforms and thereby influence the polarisation of interstitial tMφ towards a TAM phenotype. High levels of secreted M-CSF were considered to be associated with poor prognosis in colorectal and breast cancer[213,214]. In 2018, Komohara et al. published an article discussing M-CSFR as a potential target in T-ALL therapy. The authors detected elevated levels of M-CSF as well as of the receptor on a T-ALL cell line. Inhibiting the receptor led to an induction of apoptosis of these cells and the authors claim that a M-CSFR inhibition might be a possible additional therapy against T-ALL, based on direct and indirect mechanisms[215].

The other TAM inducing cytokine that was detected in high levels in mono- and co-cultured PDX-ALL cells is TGF-ß. In 2016, Zhang et al. showed that macrophages treated with TGF-ß expressed higher levels of M2 markers, such as IL-10 and Arg1[216]. This supports the observations in this thesis, according to which interstitial tMφ showed an up-regulation of Arg1 in presence of PDX-ALL cells. Interestingly, this effect was not observed in peritubular tMφ which might be related to their stronger M1 phenotype manifestation. Interstitial tMφ, which occur in higher abundance in younger mice are characterised by a M2-like phenotype. Exposure towards M2 inducing cytokines might be therefore more effective on this subpopulation. This might be one reason, why testicular involvement is more frequently seen

in boys compared to adult men. Assuming a similar age-related distribution of the macrophage subpopulations in humans as in mice, would provide the juvenile testis with a higher potential to develop TAMs derived from interstitial tMφ upon ALL infiltration. By shaping their testicular microenvironment towards a tumour favourable status, leukemic cells would have an advantage in survival within the juvenile testis. In contrast, the adult testis is mainly populated by peritubular tMφ. This macrophage subpopulation seems to be less capable to polarise towards the M2 status. Therefore, the adult testis would be a less-favourable site for extramedullary ALL cell growth.

The therapeutic potential of targeting the TAMs is already shown in solid cancers. One example are patients with non-small cell lung cancer who have a significantly better prognosis when increased counts of M1-like TAMs are detected in the tumour stroma[217]. But also, haematological malignancies might benefit from a TAM directed therapy approach. In 2018, Yang et al. showed that a repolarisation of TAMs in AML and T-ALL mouse models towards a M1 phenotype eliminated the pro-leukemic effect of the macrophages[218]. The authors showed that not the total amount of TAMs but the M2-like TAMs are correlated with a worse prognosis. They also found a tissue-specific polarisation of TAMs in both models. While BM TAMs showed more M1 characteristics, spleen TAMs had a stronger M2 manifestation. By targeting the IRF1-SAPK/JNK pathway to induce M1 polarisation of TAMs, Yang et al. were able to were able to prolong survival in the leukemic mouse models[218]. Interfering with the macrophage polarisation within the testis might be an option to reduce the pro-leukemic effect of the juvenile testis in ALL patients. However, the testicular development and function relies on its immunopriviledged status. Manipulation of the immune cell subsets of the testis might interfere with this special status and disrupt a physiological development of this organ.

4.3.2 Peritubular cells support PDX-ALL survival

While macrophages are already well acknowledged for their role in tumour progression, other stromal elements are yet to be studied in more detail. One testicular cell type potentially involved in tumour progression are PTCs. The main function of these myoid cells is the transport of immobile spermatozoa towards the rete testis by propulsion[219]. However, new studies suggest that their role is more complex and involves secretion of several growth factors and cytokines that contribute to testicular development and function. Most studies were performed in rodent models, due to the easier access to healthy tissue. It is important to point out that PTCs of rodents occur as a monolayer around the seminiferous tubules. In contrast humans have several layers of PTCs surrounding the tubules, and these cells are therefore more abundant compared to rodents[220]. In this thesis PTCs from C57BL/6N and NSG mice were isolated and characterised for their IL7 and CXCL12 expression on mRNA

level. While CXCL12 was detected in very high levels, IL7 was only expressed in low levels. On the protein level, CXCL12 was only expressed by Sertoli cells but not PTCs. However, when PDX-ALL cells were co-cultured with the isolated PTCs they showed an increased viability compared to mono-cultured PDX-ALL cells. A potential reason for the advantage in tumour cell survival might be related to the secretome of the PTCs. In 2000, Verhoeven et al. published an article claiming that the androgen-dependent interaction between PTCs and Sertoli cells is mediated by the *Peritubular factor that modulates Sertoli cell function* (PModS) molecule[221]. The PModS molecule modulates the secretion of transferrin and inhibin by Sertoli cells[221], both thought to be involved in increased invasiveness and poor prognosis in several tumour entities[222–224]. Other interesting cytokines secreted by PTCs are TGFß[225] and IL6[226]. As already mentioned both cytokines are involved in the polarisation of macrophages to a M2 status. Another PTC secreted product is the chemokine CCL2, that is a mediator of inflammation and macrophage recruitment and activation[227]. However it is also described to be involved in the regulation of the TME[228] and therefore another factor provided by PTCs that might be relevant for tumour cell survival within the testis. In 2011, Diéz-Torre et al. suggested that PTCs might be the precursors of cancer-associated fibroblasts within the testis and therefore a factor that benefits TGCT progression.

Taking all these findings about the PTC biology into account it seems reasonable that they play a role in shaping the TME especially upon ALL infiltration of the testis. While little is known about their role in tumour progression this highly specialised cell type is an interesting candidate for future studies about the testicular TME.

4.4 The established PDX-ALL mouse model with testicular involvement is suitable to study relevant pathways *in vivo*

So far only few ALL rodent models with testicular involvement were published. However, such models are indispensable to study the cellular and molecular mechanisms responsible for this infiltration. The establishment of such a model is rather challenging. Most ALL cell lines grow very aggressively and mice must be sacrificed before the testis is populated by tumour cells. In this thesis an adoptive xenotransplantation model with testicular involvement using NSG mice was established and used to study the relevance of the CXCR4-CXCL12 axis for testicular infiltration.

4.4.1 Testicular involvement in PDX-ALL model was only observed in pre-puberty NSG mice

During the establishment of the PDX-ALL model with testicular involvement, different conditions were tested and compared for their ability to produce profound levels of testicular ALL infiltrations. Post-puberty mice showed only very low levels of infiltrating ALL cells in flow cytometry and no infiltration by immunohistochemistry analysis. In contrast, pre-puberty mice had a significantly higher infiltration, especially when transplanted with only 1 x 10^4 PDX-ALL cells instead of 1 x 10^6 cells. The elongated tumour progression seems to be favourable for ALL cell proliferation within the testis. This observation underlines experiences from the clinics, which indicate that mainly paediatric patients, but rarely adults, show testicular relapses. However, comparing these results with the literature reveals some discrepancies that will be discussed in this chapter.

In 1984, Jackson et al. published an article describing the transplantation of the murine B-ALL cell line L1210 into BDF_1 mice, a strain suitable for transplantation research[141]. While the cell line rapidly developed leukaemia with a fatal outcome after 7-8 days, no testicular involvement was described. This agrees with the observations made during this work, according to which a fast tumour progression leads to lower counts of ALL cells in the testis. Jackson et al. do not mention the age of the recipient mice; hence no comparison is possible with regard to age-dependent infiltration of the testis.

In the same year, Jackson et al., published a second study, presenting a rat T-cell leukaemia model with testicular involvement[142]. Adoptively transferred leukaemia cells led to a fatal outcome in transplanted rats within three weeks. T-ALL cells were either injected intramuscular or intratesticular inoculated. Both methods resulted in massive gonadal invasion, that was limited to the interstitial space, shown by immunohistochemistry staining's. In 1993, Jahnukainen et al. presented another T-ALL rat model with testicular involvement[143]. In contrast to Jackson et al., this study considered the age-related differences in testicular infiltration that were mentioned above. Injecting sexually immature rats i.p. with a rat T-ALL cell line resulted in testicular infiltration in all animals. In contrast only 42% of the transplanted sexually mature rats showed testicular infiltration. As in the Jackson study, infiltrates were limited to the interstitial space, shown by immunohistochemistry staining's, however, only small areas were affected. Comparing these results with observations made in this thesis, it seems that rat testes provide an easier access for leukemic cells compared to the NSG mouse model. In contrast to the presented NSG mouse model, even the post-puberty rats showed frequent testicular involvement. Nevertheless, the differences in infiltration of mature and immature rat testis caused the authors to declare a correlation between sexual maturity and frequency of testicular infiltration. The authors assume that

physiological changes during puberty are responsible for the smaller number of testicular relapses in men compared to boys[143]. This assumption was confirmed by using this model in a further study, inhibiting the testicular steroidogenesis of early-puberty by estradiol treatment[144]. Suppressing the testicular activity resulted in lower counts of ALL cells in the testes of rats, supporting the idea of the tumour favourable microenvironment of the juvenile testis. However, despite these promising results, the rat T-ALL model was not used in further publications.

Newer studies that mention testicular relapses used NSG mice and adoptively transferred them with either the B-ALL cell lines Nalm6 and REH or PDX-ALL cells. These studies are therefore better to compare to the model used in this thesis. In 2015, Arnaud et al. published an article, claiming a CD9 associated testicular infiltration with Nalm6 cells in NSG mice[145]. A higher CD9 expression was related to a stronger testicular infiltration in the presented mouse model, as analysed by flow cytometry. After treating four week-old mice with busulfan they were inoculated with 10 x 10^6 cells and sacrificed four weeks post-transplantation. Busulfan is a sterilisation drug, that is also used for germ cell depletion in preparation of spermatogonial stem cell transplantation[229]. However, despite this manipulation of the testicular environment only few mice in the $CD9^{high}$ group showed more than ten Nalm6 cells/10^5 testis cells. Since the authors did not perform immunohistochemistry staining of the testis samples it remains unclear, weather the observed infiltrates might be blood-born contaminations. In this thesis, all testes were not only analysed by flow cytometry but additionally testicular infiltration was confirmed by immunohistochemistry. Performing the anti-CD10 staining on the testis sections allowed visualising the location of the tumour cells within the tissue and exclusion of the effect of blood-born contaminations.

The most recent study presenting an ALL mouse model with testicular involvement was published in 2019 by Velázquez-Avila et al[146]. Here, REH or PDX-ALL cells were injected into the tail vein and tumour growth was monitored by analysis of peripheral blood. Mice were killed five to six weeks post-transplantation and several organs, including the testis, were analysed by flow cytometry. All analysed organs were reported to have been highly infiltrated by human $CD45^+$ REH cells. However, it remains unclear how ALL cells were detected since the authors only show the ratio of murine $CD45^+$ to human $CD45^+$ cells. A high cell number injected into post-puberty mice also resulted in testicular infiltration, which is not reflected by the data of this thesis. However, the 2019 study needs to be interpreted with caution because it lacks technically sufficient staining procedures. For instance, the authors did not include additional B-ALL marker, such as CD19 or CD10. They also did not show any histological staining, that would proof the tissue infiltration of the testis.

In summary, during the last four decades numerous approaches were performed to establish a rodent model to study ALL testis interaction but up to now, none of the published models were satisfying. Recent mouse model studies focussed on other extramedullary organs and analysed the testis only additionally. It is not always clear, if detected cells were only blood-born contaminations or real tissue infiltrations.

The PDX-ALL model with testicular involvement developed in this thesis has the advantage, that testis infiltration was confirmed by immunohistochemistry staining. Besides, it reflects the preferred infiltration of the juvenile testis and does not rely on any manipulation of the testicular behaviour by drug treatment. Therefore, it is a promising model to study mechanisms for migration to and survival within the testis at an early stage of ALL cell dissemination.

4.4.2 Limitations of the NSG mouse model

In vitro studies contributed to an increasing understanding of molecular mechanisms responsible for malignancies, however the complex and dynamic *in vivo* situation cannot be reflected by cell culture systems and only single aspects can be studied. Findings from *in vitro* studies still need confirmation by *in vivo* models or/and patient data. The lack of a complete microenvironment, vascularisation and the three-dimensional structure are a limitation in cell culture-based studies. While some tissues, as the BM are already used in more complex 3D cultures[193], this option is not yet available for the testis. To overcome these problems, the engraftment of PDX cancer cells in immunodeficient mice was established. This attempt enables the observation of human tumour cells that maintain their functional characteristics and the study of their interaction with a complex microenvironment[230]. NSG mice are a very potent mouse model, that allows engraftment of a wide range of primary solid and haematological tumours. This is possible due to a lack of B-, T- and NK-cells and the missing signalling through various interleukin receptors. Disabling this signalling leads to a dysfunction of both, the adaptive and innate immunity[231]. This dysfunction is an advantage for the engraftment of primary tumour cells; however, it also causes limitations in TME studies. Therefore, this thesis revealed the differences in the presence of tMφ subpopulations of NSG and C57B6/N mice. While the tMφ of C57B6/N mice can be distinguished in interstitial and peripheral macrophages by their CD64 and MHCII expression, tMφ of NSG mice lack both markers. As already discussed, macrophages are an important compound of the TME and can create a tumour favourable environment. Macrophages are still expressed in NSG mice but due to the lack of certain cytokine signalling pathways they are disabled in their function. However, tMφ, support Leydig cells during testosterone production[51]. This function needs to be preserved in NSG mice otherwise crucial mechanisms during development and reproduction would be impaired. Furthermore, a

BM transfer experiment presented in this thesis showed the ability of NSG macrophages to alter their expression pattern upon immune system reformation. The engraftment of BM cells of immune competent mice in immune deficient NSG mice led to an MHCII expression in splenic macrophages. This shows the flexibility of NSG macrophages and their ability to react towards environmental influences. It is possible that an interaction of PDX-ALL cells and macrophages within the testis activate the expression of proteins, which are usually absent in NSG mice. Therefore, the drawback of a disabled innate immune system in NSG mice might not be obstructive when studying the interaction of ALL cells with their testicular TME.

4.4.3 The CXCR4-CXCL12 axis is relevant for testicular ALL cell infiltration

Based on the high CXCR4 expression in all analysed paediatric ALL samples and the successful ALL migration blockage by AMD3100 in transwell migration assays, the relevance of the CXCR4-CXCL12 axis for testicular ALL cell infiltration was also examined *in vivo*. Already in 1999 it was shown, that the CXCR4-CXCL12 axis is an important pathway for homing of hematopoietic stem cells into the BM[172]. Only two years later, Shen et al. demonstrated the dependence of pre-B-ALL cells and Nalm6 cells on CXCR4 to engraft in the BM of NOD/SCID mice[232]. Soon it was discovered that the CXCR4 inhibitor AMD3100 mobilised hematopoietic stem cells from the BM into the peripheral blood in healthy volunteeres[233]. The same observation was described in 2007 by Juarez et al. for paediatric ALL cells in an *in vivo* mouse model[123]. The authors described a significant decrease of leukemic cells in peripheral blood, spleen, and BM of mice after treatment with AMD3100. They conclude that CXCR4 inhibition leads to a reduced engraftment of leukemic cells in mice. Juarez et al. started AMD3100 treatment when ALL cells were detectable in peripheral blood by flow cytometry. However, this is only the case in a PDX-ALL mouse model, when tumour progression is already advanced, and mice have reached a post-puberty stage. Since testis infiltration is age-dependent it seemed more reasonable to block the potential pathway responsible for testis directed migration at an early stage of leukemic development. A CXCR4 blocking protocol, published by Peled et al. in 1999 was used[172]. The authors proofed the CXCR4 dependence of hematopoietic stem cell engraftment by using anti-CXCR4 antibodies at different time points after human stem cell transplantation into NOD/SCID mice. Antibodies were applied i.p. 30 min, 24 hours and 4 days post-transplantation. While a treatment after 30 min and 24 hours resulted in no or low engraftment, injecting an antibody 4 days post-transplantation did not influence the engraftment efficiency. Accordingly, in this thesis NSG mice were treated from day 4 post-transfer of PDX-ALL cells twice weekly with an anti-CXCR4 or control antibody. The antibodies were applied over three weeks before mice were monitored by IVIS imaging. As

soon as control mice showed profound engraftment by IVIS imaging they were sacrificed and analysed by flow cytometry. All control animals showed a strong ALL infiltration of BM and spleen by IVIS imaging and flow cytometry. In contrast, the CXCR4 antibody treated animals showed a strong retardment of engraftment in all organs. The anti-CXCR4 treatment led to a reduction of tumour cells in all analysed organs but did not completely inhibit the engraftment in NSG mice. The testis, in contrast, was free of tumour cells. These results indicate a correlation of CXCR4 expression and testis infiltration. While an anti-CXCR4 treatment did not inhibit an initial ALL infiltration of BM and spleen, it inhibited the penetration of the testes completely.

Considering *in vitro* and *in vivo* results from this work, it can be inferred that the CXCR4-CXCL12 axis plays a crucial role in testis infiltration during paediatric ALL. This finding contributes to the understanding of the mechanism of the migratory behaviour of ALL cells and might be considered in the development of novel therapy strategies. The CXCR4-CXCL12 axis is a signalling pathway already widely noted as a potential treatment target in other tumour entities. In 2005 Sipkin et al. described highly specialized anatomic regions within the murine bone marrow that express the adhesion molecule E-selectin as well as CXCL12[234]. By expressing these proteins, homing of ALL and multiple myeloma (MM) cells to these unique regions was facilitated. Interfering with the interaction of CXCL12 and CXCR4 *in vivo* resulted in an inhibition of Nalm6 homing towards these niches. A similar approach was performed by Azab et al. in 2009[118]. Here, disrupting *in vivo* the CXCL12-CXCR4 axis with AMD3100 enhances the sensitivity of MM cells to Bortezomid treatment[118]. Interfering with the adhesion of tumour cells within their BM TME resulted in an increase of circulating MM cells. Lacking their stromal support makes the tumour cells leave their protective tissue niche and subsequently makes them more vulnerable towards drug treatment.

Sipkin et al., 2005 and Azab et al., 2009 also proved the relevance of the CXCR4-CXCL12 axis for ALL and MM cell homing. They showed that inhibiting this axis leads to a release of tumour cells from their niches, which makes them easier targets for drug treatment. Including a CXCR4-directed treatment during the initial therapy in paediatric ALL might reduce the cases of testicular relapses. Using anti-CXCR4 antibodies in paediatric cancer treatment has been already discussed for hematopoietic and solid tumour entities. In 2017 an anti-CXCR4 IgG antibody treatment in mice effectively mobilized AML PDX cells into peripheral blood[235]. The authors suggest that this effect could be beneficial for AML patients who are resistant to chemotherapy. In 2014, an anti-CXCR4 (Ulocuplimab) antibody was applied in a phase 1 clinical trial in adults. In total 73 AML relapse patients were treated with Ulocuplimab in combination with chemotherapeutical drugs. Another 30 patients were already injected with

Ulocuplimab, one week prior to starting the chemotherapy treatment. Both strategies increased the response rate achieved with chemotherapy alone[236].

These published preclinical and first clinical data suggests that the application of an anti-CXCR4 antibody is safe and may foster the release of leukemic cells into peripheral blood. While this was already shown for leukaemia cells from the bone marrow, the presented PDX-ALL model with testicular involvement suggests a similar effect on testicular ALL cells. However, it is still unclear if the antibody hinders the testicular infiltration or inhibits the survival of the cells within the testis.

4.5 Conclusion and future perspectives

4.5.1 Conclusion

The overall aim of this study was to dissect the molecular and cellular mechanism involved in testicular infiltration in paediatric ALL relapse. Therefore, a defined cohort of primary patient samples was analysed to identify potential surface markers involved in testicular infiltration. Furthermore, comprehensive *in vitro and in vivo* analyses were performed to study interaction of leukemic cells with their testicular microenvironment. The presented results confirm the crucial role of the CXCR4-CXCL12 axis in ALL cell migration and demonstrate its relevance for testis directed migration in *in vitro* migration assays. A second surface marker, IL7R, was identified to be significantly up-regulated in patients facing a testicular relapse. Its role in ALL cell migration and survival to and within the testis still needs to be investigated further.

While homing receptor pattern expression on ALL cells was extensively studied using human cells, the cellular stromal elements within the testicle potentially contributing to leukemic cell migration and to a leukemic-permissive survival niche were studied in a mouse model. The focus was on tMφ and their behavior upon ALL cell exposure. *In vitro* assays demonstrated a polarization of interstital tMφ towards the M2 state, detectable by an Arg1 up-regulation. This observation indicates an ability of the testicular tissue to react towards leukemic cell infiltration in a tumour favourable manner. Other testicular subpopulations that were studied are Sertoli cells and PTCs. Both cells expressed CXCL12 and IL7 on the mRNA level, but only Sertoli cells expressed CXCL12 also on the protein level.

Most importantly, this study presents the successful establishment of an *in vivo* PDX-ALL model with testicular involvement. Other studies analysed relatively low numbers of ALL cells isolated from the mouse testis by flow cytometry. However, it remained unclear if detected cells were only blood-born contaminations or real infiltrations and if so, where within the

testes the cells were located. The presented results show the presence and localisation of ALL cells within the testicular tissue by immunohistochemistry. Furthermore, a correlation between the age of the recipient animal and testicular infiltration could be shown. By treating the PDX-ALL cell transplanted mice with an anti-CXCR4 antibody a strong reduction of tumour cell engraftment in all analysed organs was achieved. The blockage of the CXCR4-CXCL12 axis might be an effective treatment option during first phases of frontline treatment in order to hinder tumour infiltration of the testes. Overall, the presented animal model is highly suitable to validate functional signalling axes, relevant for testis directed leukemic cell migration. **Figure 43** shows the cellular interactions of ALL cells with their testicular TME, as concluded from the presented study.

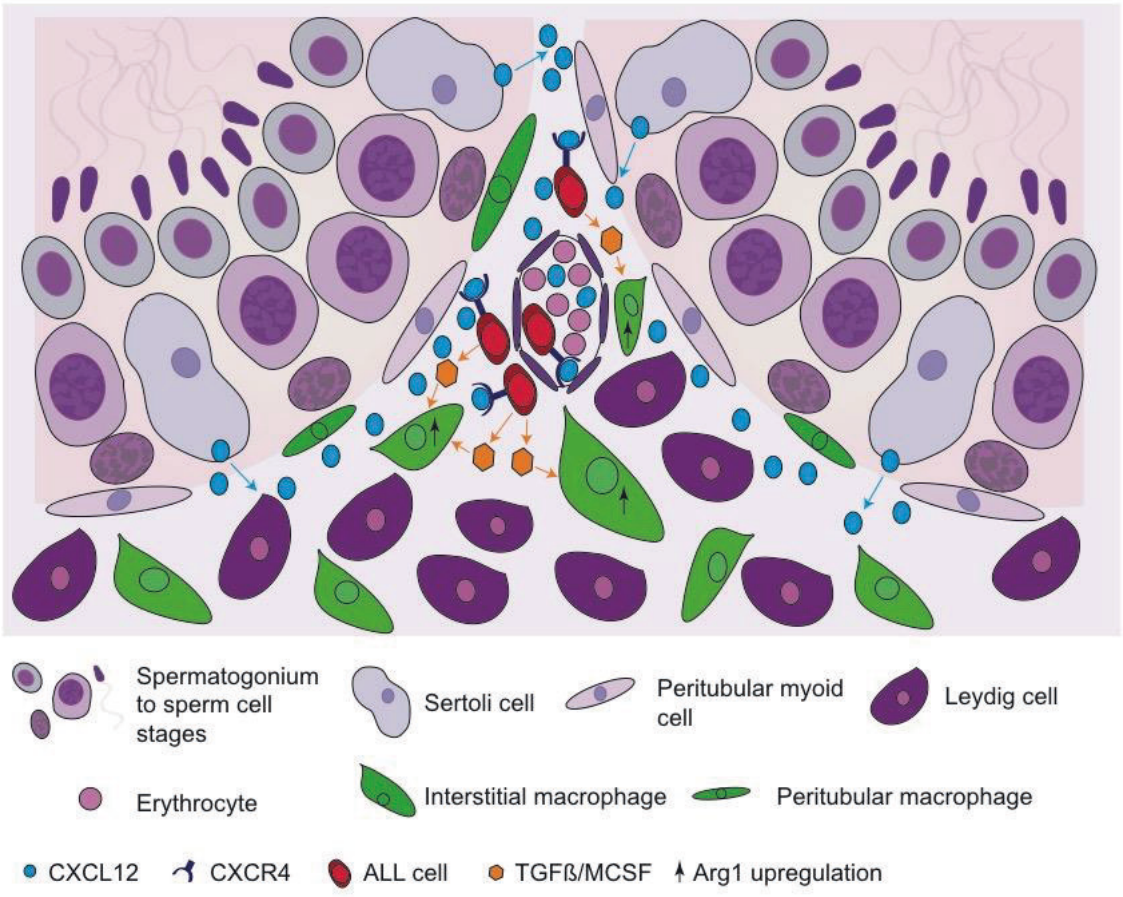

Figure 43: Molecular interaction of ALL cells with their testicular TME. Transplanted PDX-ALL cells follow a CXC12 gradient, produced by Sertoli cells in the seminiferous tubules. Within the testis they settle in the interstitial space, starting an interaction with the interstital tMφ. This interaction results in a M2 polarisation of the macrophages and the creation of a tumour favourable microenvironment.

Sertoli cells secrete CXCL12 into the interstitial space and thereby create a CXCL12 gradient. The chemokine binds to the CXCR4 receptor on the ALL cell surface and thus triggers the tumour cell migration into the testis. Here, ALL cells assemble in the interstitial

space near the blood vessels. The ALL cells secrete cytokines, such as TGF-ß and MCSF that cause macrophage polarisation toward the immune suppressive and tumour favourable M2 state. While the peritubular tMφ are unaffected by this cytokine exposure, the interstitial tMφ start to upregulate Arg1. Arg1 again has a positive effect on cell proliferation and can thereby enhance tumour growth.

While paediatric patients with an ALL have a very good prognosis currently, patients that have an ALL relapse have a strongly reduced EFS. Although the prognosis of testicular relapses is relatively good compared to isolated BM or CNS relapses; the required treatment includes an orchiectomy, a process that drastically reduces the life quality of the young patients. Interfering with or blocking of the CXCR4-CXCL12 axis, by an antibody treatment in an early stage of the therapy might be an option to prevent a testicular relapse in paediatric patients.

4.5.2 Future perspectives

Single-cell RNA-seq. technology is a powerful tool to study gene expression with high resolution[237]. It allows the identification of small cell populations within a complex mixture of different cell types, as in the testis, and the modelling of the cell-cell interaction from molecular data[238]. The newly developed PDX-ALL mouse model is currently utilized to identify additional pathways relevant for ALL cell survival within the testis by single-cell RNA-seq. of testicular somatic cells. Green et al. recently published a roadmap of murine spermatogenesis defined by single-cell RNA-seq and described seven somatic cell types, 12 germ cell clusters and many subtypes of all these populations[239]. A similar approach could improve our understanding of transcriptomic changes of specific testicular cell types upon leukaemia cell-stroma cell crosstalk and their role for leukaemia cell survival within the testis. The PDX-ALL mouse model as well as the established isolation of the testicular stroma populations, such as tMφ and PTCs, will be useful tools to validate pathways relevant for ALL cell survival within the testis, identified by single-cell RNA-seq.

5 Literature

1. Kuhlen, M., Klusmann, J. H. & Hoell, J. I. Molecular Approaches to Treating Pediatric Leukemias. *Front. Pediatr.* **7**, 1–12 (2019).
2. Puumala, S. E., Ross, J. A., Aplenc, R. & Spector, L. G. Epidemiology of childhood acute myeloid leukemia. *Pediatr. Blood Cancer* **60**, 728–733 (2013).
3. Linabery, A. M. & Ross, J. A. Trends in childhood cancer incidence in the U.S. (1992-2004). *Cancer* **112**, 416–432 (2008).
4. Löwenberg, B., Downing, J. R. & Burnett, A. Acute Myeloid Leukemia. *New Engl. J. Med.* **341**, 1051–1062 (1999).
5. Stanulla, M. & Schrappe, M. Treatment of Childhood Acute Lymphoblastic Leukemia. *Semin. Hematol.* **46**, 52–63 (2009).
6. Teachey, D. T. & Pui, C. H. Comparative features and outcomes between paediatric T-cell and B-cell acute lymphoblastic leukaemia. *Lancet Oncol.* **20**, e142–e154 (2019).
7. Inaba, H., Greaves, M. & Mullighan, C. G. Acute lymphoblastic leukaemia. *The Lancet* **381**, 1943–1955 (2013).
8. Yiallouros, M. Acute lymphoblastic leukaemia (ALL) - Brief Information. *Competence Netw. Paediatr. Oncol. Haematol.* 3–11 (2017).
9. Redaelli, A., Laskin, B. L., Stephens, J. M., Botteman, M. F. & Pashos, C. L. A systematic literature review of the clinical and epidemiological burden of acute lymphoblastic leukaemia (ALL). *Eur. J. Cancer Care (Engl).* **14**, 53–62 (2005).
10. Clarke, R. T. *et al.* Clinical presentation of childhood leukaemia: A systematic review and meta-analysis. *Arch. Dis. Child.* **101**, 894–901 (2016).
11. Stephen P. Hunger, M.D., and Charles G. Mullighan, M. . Acute Lymphoblastic Leukemia in Children. *N. Engl. J. Med.* **373**, 1541–1552 (2015).
12. Harrison, C. J. Cytogenetics of paediatric and adolescent acute lymphoblastic leukaemia. *Br. J. Haematol.* **144**, 147–156 (2009).
13. Ma, X. *et al.* Rise and fall of subclones from diagnosis to relapse in pediatric B-acute lymphoblastic leukaemia. *Nat. Commun.* **6**, 1–12 (2015).
14. Wiemels, J. L. *et al.* Prenatal origin of acute lymphoblastic leukaemia in children. *Lancet* **354**, 1499–1503 (1999).
15. Gandemer, V. *et al.* Excellent prognosis of late relapses of ETV6/RUNX1-positive childhood acute lymphoblastic leukemia: Lessons from the FRALLE 93 protocol. *Haematologica* **97**, 1743–1750 (2012).
16. Nachman, J. B. *et al.* Outcome of treatment in children with hypodiploid acute lymphoblastic leukemia. *Blood* **110**, 1112–1115 (2007).
17. Holmfeldt, L. *et al.* The genomic landscape of hypodiploid acute lymphoblastic leukemia. *Nat. Genet.* **45**, 242–252 (2013).
18. Moorman, A. V *et al.* Prognostic eff ect of chromosomal abnormalities in childhood B-cell precursor acute lymphoblastic leukaemia : results from the UK Medical Research Council ALL97 / 99 randomised trial. *Lancet Oncol.* **11**, 429–438 (2010).
19. Arico, M. *et al.* Clinical Outcome of Children With Newly Diagnosed Philadelphia Chromosome – Positive Acute Lymphoblastic Leukemia Treated Between 1995 and 2005. *J. Clin. Oncol.* **28**, 4755–4761 (2010).
20. Farber, S., Diamond, L. K., Mercer, R. D., Sylvester, R. F. & Wolff, J. A. Temporary Remissions in Acute Leukemia in Children Produced by Folic Acid Antagonist, 4-

Aminopteroyl-Glutamic Acid (Aminopterin). *N. Engl. J. Med.* **238**, 787–793 (1948).

21. Pinkel, D. P., Simone, J. V, Hustu, H. O. & J, R. “Total therapy” of childhood acute lymphocytic leukemia. *Pediatr. Res.* **5**, 408–408 (1971).

22. Riehm, H., Langermann, H. J., Gadner, H., Odenwald, E. & Henze, G. The berlin childhood acute lymphoblastic leukemia therapy study, 1970–1976. *American Journal of Pediatric Hematology/Oncology* **2**, 299–306 (1980).

23. Mitchell, C. D. *et al.* Benefit of dexamethasone compared with prednisolone for childhood acute lymphoblastic leukaemia: Results of the UK Medical Research Council ALL97 randomized trial. *Br. J. Haematol.* **129**, 734–745 (2005).

24. Schrappe, M. *et al.* Long-term results of four consecutive trials in childhood ALL performed by the ALL-BFM study group from 1981 to 1995. *Leukemia* **14**, 2205–2222 (2000).

25. Pui, C. H. & Evans, W. E. Treatment of acute lymphoblastic leukemia. *N. Engl. J. Med.* **354**, 166–178 (2006).

26. Landier, W. *et al.* Development of risk-based guidelines for pediatric cancer survivors: The Children’s Oncology Group Long-Term Follow-Up Guidelines from the Children’s Oncology Group Late Effects Committee and Nursing Discipline. *J. Clin. Oncol.* **22**, 4979–4990 (2004).

27. Mody, R. *et al.* Twenty-five-year follow-up among survivors of childhood acute lymphoblastic leukemia: A report from the Childhood Cancer Survivor Study. *Blood* **111**, 5515–5523 (2008).

28. Pui, C. H., Carroll, W. L., Meshinchi, S. & Arceci, R. J. Biology, risk stratification, and therapy of pediatric acute leukemias: An update. *J. Clin. Oncol.* **29**, 551–565 (2011).

29. Ko, R. H. *et al.* Outcome of patients treated for relapsed or refractory acute lymphoblastic leukemia: A therapeutic advances in childhood leukemia consortium study. *J. Clin. Oncol.* **28**, 648–654 (2010).

30. Nguyen, K. *et al.* Factors Influencing Survival After Relapse From Acute Lymphoblastic Leukemia: A Children’s Oncology Group Study. *Leukemia* **22**, 2142–50 (2008).

31. Hucks, G. & Rheingold, S. R. The journey to CAR T cell therapy: the pediatric and young adult experience with relapsed or refractory B-ALL. *Blood Cancer J.* **9**, 1–9 (2019).

32. Jacobs, J. E. & Hastings, C. Isolated extramedullary relapse in childhood acute lymphocytic leukemia. *Curr. Hematol. Malig. Rep.* **5**, 185–191 (2010).

33. Barnett M.J., Greaves M.F., Amess J.A.L., Gregory W.M., Rohatiner A.Z.S., Dhaliwal H.S., Slevin M.L., Biruls R., Malpas J.S., L. T. A. Treatment of acute lymphoblastic leukaemia in adults. *Br. J. Haematol.* **64**, 455–468 (1986).

34. Garcia, A. V *et al.* Isolated primary testicular B lymphoblastic lymphoma: an unusual presentation. *J. Pediatr. Hematol. Oncol.* **35**, e88-90 (2013).

35. Barredo, J. C. *et al.* Isolated late testicular relapse of B-cell acute lymphoblastic leukemia treated with intensive systemic chemotherapy and response-based testicular radiation: A Children’s Oncology Group study. *Pediatr. Blood Cancer* **65**, (2018).

36. Bhojwani, D. & Pui, C.-H. Relapsed childhood acute lymphoblastic leukaemia. *Lancet Oncol.* **14**, e205-17 (2013).

37. Gaudichon, J. *et al.* Mechanisms of extramedullary relapse in acute lymphoblastic leukemia: Reconciling biological concepts and clinical issues. *Blood Reviews* **36**, 40–56 (2019).

38. Pérez, C. *et al.* Dual role of immune cells in the testis: Protective or pathogenic for germ cells? *Spermatogenesis* **3**, 1–12 (2013).

39. Li, N., Wang, T. & Han, D. Structural, cellular and molecular aspects of immune privilege in the testis. *Front. Immunol.* **3**, 1–12 (2012).

40. Middendorff, R. *et al.* The tunica albuginea of the human testis is characterized by complex contraction and relaxation activities regulated by cyclic GMP. *J. Clin. Endocrinol. Metab.* **87**, 3486–3499 (2002).

41. Holstein, A. F., Schulze, W. & Davidoff, M. Understanding spermatogenesis is a prerequisite for treatment. *Reprod. Biol. Endocrinol.* **1**, 1–16 (2003).

42. Roosen-Runge, E. C. & Holstein, A. F. The human rete testis. *Cell Tissue Res.* **189**, 409–433 (1978).

43. Davidoff, M. S., Breucker, H., Holstein, A. F. & Seidl, K. Cellular architecture of the lamina propria of human seminiferous tubules. *Cell Tissue Res.* **262**, 253–61 (1990).

44. Griswold, M. D. The central role of Sertoli cells in spermatogenesis. *Semin. Cell Dev. Biol.* **9**, 411–416 (1998).

45. Franca LR, Hess ER, Dufour JM, Hofmann MC, G. M. The Sertoli cell: one hundred fifty years of beauty and plasticity. *Physiol. Behav.* **176**, 189–212 (2016).

46. Sylvester, S. R. & Griswold, M. D. The Testicular Iron Shuttle: A “Nurse” Function of the Sertoli Cells. *J. Androl.* **15**, 381–385 (1994).

47. Yang, Q. E., Kim, D., Kaucher, A., Oatley, M. J. & Oatley, J. M. CXCL12-CXCR4 signaling is required for the maintenance of mouse spermatogonial stem cells. *J. Cell Sci.* **126**, 1009–1020 (2013).

48. Westernströer, B. *et al.* Profiling of Cxcl12 receptors, Cxcr4 and Cxcr7 in murine testis development and a spermatogenic depletion model indicates a role for Cxcr7 in controlling Cxcl12 activity. *PLoS One* **9**, 1–18 (2014).

49. Westernströer, B. *et al.* Developmental expression patterns of chemokines CXCL11 , CXCL12 and their receptor CXCR7 in testes of common marmoset and human. *Cell Tissue Res* **361**, 885–898 (2015).

50. Zirkin, B. R. & Papadopoulos, V. Leydig cells: Formation, function, and regulation. *Biol. Reprod.* **99**, 101–111 (2018).

51. Hutson, C. Interactions Macrophages Between Testicular and Leydig Minireview Is the Production of the Testicular-Derived. 394–398 (1998).

52. Mossadegh-Keller, N. *et al.* Developmental origin and maintenance of distinct testicular macrophage populations. *J. Exp. Med.* **214**, 2829–41 (2017).

53. Fijak, M. & Meinhardt, A. The testis in immune privilege. *Immunol. Rev.* **213**, 66–81 (2006).

54. Shechter, R., London, A. & Schwartz, M. Orchestrated leukocyte recruitment to immune-privileged sites: Absolute barriers versus educational gates. *Nat. Rev. Immunol.* **13**, 206–218 (2013).

55. Maekawa, M., Kyoko, K. & Nagamo, T. Peritubular Myoid Cells in the Testis : Their Structure and Function. *Arch. histol. Cytol.* **59**, 1–13 (1996).

56. Clermont, Y. Contractile Elements in the Limiting Membrane of the Seminiferous Tubules of the Rat. *Exp. Cell Res.* **15**, 438–440 (1958).

57. Yan Cheng, C. & Mruk, D. D. The blood-testis barrier and its implications for male contraception. *Pharmacol. Rev.* **64**, 16–64 (2012).

58. Fawcett, D. W., Leak, L. V. & Heidger, P. M. Electron microscopic observations on the

structural components of the blood-testis barrier. *J. Reprod. Fertil. Suppl.* **10**, 105–22 (1970).

59. Setchell, B. P. & Waites, G. M. Changes in the permeability of the testicular capillaries and of the 'blood-testis barrier' after injection of cadmium chloride in the rat. *J. Endocrinol.* **47**, 81–86 (1970).

60. Setchell, B. P. Blood-testis barrier, junctional and transport proteins and spermatogenesis. *Adv. Exp. Med. Biol.* **636**, 212–33 (2008).

61. Chiquoine, A. D. Observations on the early events of cadmium necrosis of the testis. *Anat. Rec.* **149**, 23–35 (1964).

62. Hawkins, B. T. & Davis, T. P. The Blood-Brain Barrier / Neurovascular Unit in Health and Disease. **57**, 173–185 (2005).

63. Paolinelli, R., Corada, M., Orsenigo, F. & Dejana, E. The molecular basis of the blood brain barrier differentiation and maintenance. Is it still a mystery? *Pharmacol. Res.* **63**, 165–71 (2011).

64. Tung, K., Teuscher, C. & Meng, A. Autoimmunity to Spermatozoa and the Testis. *Immunol. Rev.* **55**, 217–255 (1981).

65. Suescun, M. O., Calandra, R. S. & Lustig, L. Alterations of Testicular Function after Induced Autoimmune Orchitis in Rats. *J. Androl.* **15**, 442–448 (1994).

66. Tung, K. S. K., Unanue, E. . & Dixon, F. J. Immunological Events Associated with Immunization by Sperm in Incomplete Freund ' s Adjuvant1. *Int. Arch. Allergy* **41**, 565–574 (1971).

67. Itoh, M., Terayama, H., Naito, M., Ogawa, Y. & Tainosho, S. Tissue microcircumstances for leukocytic infiltration into the testis and epididymis in mice. *J. Reprod. Immunol.* **67**, 57–67 (2005).

68. De Michele, F. *et al.* In vitro formation of the blood-testis barrier during long-term organotypic culture of human prepubertal tissue: Comparison with a large cohort of pre/peripubertal boys. *Mol. Hum. Reprod.* **24**, 271–282 (2018).

69. Mellor, A. L. & Munn, D. H. Immune privilege: A recurrent theme in immunoregulation? *Immunological Reviews* (2006). doi:10.1111/j.1600-065X.2006.00443.x

70. Filippini, A. *et al.* Immunology and immunopathology of the male genital tract Control and impairment of immune privilege in the testis and in semen. *Hum. Reprod. Update* **7**, 444–449 (2001).

71. Maddocks, S. & Setchell, B. P. Recent evidence for immune privilege in the testis. *J. Reprod. Immunol.* **18**, 9–18 (1990).

72. Setchell, B. P., Uksila, J., Maddocks, S. & Pöllänen, P. Testis physiology relevant to immunoregulation. *J. Reprod. Immunol.* **18**, 19–32 (1990).

73. Kaur, G., Long, C. R. & Dufour, J. M. Genetically engineered immune privileged Sertoli cells. *Spermatogenesis* **2**, 1–9 (2012).

74. Selawry, H. P. & Whittington, K. Extended Al log raft Survival of Islets Grafted into Intra-abdominally Placed Testis. *Diabete* **33**, 405–406 (1984).

75. Head, J. R. & Billingham, R. E. Immune prividege in the testis, evaluation of potential local factors. *Transplantation* **40**, 269–275 (1985).

76. Selawry, H. P. & Whittington, K. B. Prolonged Intratesticular Islet Allograft Survival is Not Dependent on Local Steroidogenesis. *Horm. metabol. Res.* **20**, 562–565 (1988).

77. Cameron, D. F., Whittington, K., Schultz, R. E. & Selawry, H. P. Succsessful islet/abdominal testis transplantation does nor require Leydig cells. *Transplantation*

50, 649–653 (1990).

78. Whitmore, W. F., Karsh, L. & Gittes, R. F. The role of germinal epithelium and spermatogenesis in the priviledged survival of intratesticular grafts. *J. Urol.* **134**, 782–786 (1985).

79. Cesaris, D. *et al.* Immunosuppressive Molecules Produced By Sertoli Cells Cultured in Vitro : Biological Effects On Lymphocytes. *Biochem. Biophys. Res. Commun.* **186**, 1639–1646 (1992).

80. Hedger, M. P. & Meinhardt, A. Cytokines and the immune-testicular axis. *J. Reprod. Immunol.* **58**, 1–26 (2003).

81. Bhushan, S. *et al.* Molecular and Cellular Endocrinology Testicular innate immune defense against bacteria. *Mol. Cell. Endocrinol.* **306**, 37–44 (2009).

82. Theas, A. S., Lustig, L., Guazzone, V. A. & Jacobo, P. Cytokines and Chemokines in Testicular Inflammation : A Brief Review. *Microsc. Res. Tech.* **72**, 620–628 (2009).

83. Mital, P., Kaur, G. & Dufour, J. M. Immunoprotective Sertoli cells: making allogeneic and xenogeneic transplantation feasible. *Reproduction* **139**, 495–504 (2010).

84. Chen, J.-J., Sun, Y. & Nabel, G. J. Regulation of the Proinflammatory Effects of Fas Ligand (CD95L). *Science (80-.).* **282**, 1714–1717 (1998).

85. Chen, F. *et al.* New horizons in tumor microenvironment biology: Challenges and opportunities. *BMC Med.* **13**, 1–13 (2015).

86. Höpken, U. E. & Rehm, A. Targeting the Tumor Microenvironment of Leukemia and Lymphoma. *Trends in Cancer* **5**, 351–364 (2019).

87. Wang, M. *et al.* Role of tumor microenvironment in tumorigenesis. *J. Cancer* **8**, 761–773 (2017).

88. Butt, A. Q. & Mills, K. H. G. Immunosuppressive networks and checkpoints controlling antitumor immunity and their blockade in the development of cancer immunotherapeutics and vaccines. *Oncogene* **33**, 4623–4631 (2014).

89. Baruch, K. *et al.* Breaking immune tolerance by targeting Foxp3+ regulatory T cells mitigates Alzheimer's disease pathology. *Nat. Commun.* **6**, 1–12 (2015).

90. Parker, K. H. *et al.* HMGB1 enhances immune suppression by facilitating the differentiation and suppressive activity of myeloid-derived suppressor cells. *Cancer Res.* **74**, 5723–5733 (2014).

91. Biswas, S. K. & Mantovani, A. Macrophage plasticity and interaction with lymphocyte subsets: Cancer as a paradigm. *Nat. Immunol.* **11**, 889–896 (2010).

92. Wynn, T. A., Chawla, A. & Pollard, J. W. Macrophage biology in development , homeostasis and disease. *Nature* **496**, 445–455 (2013).

93. Murray, P. J. Macrophage Polarization. *Annu. Rev. Physiol.* **79**, 541–566 (2017).

94. Lin, Y., Xu, J. & Lan, H. Tumor-associated macrophages in tumor metastasis: Biological roles and clinical therapeutic applications. *J. Hematol. Oncol.* **12**, 1–16 (2019).

95. Liu, Y. & Cao, X. The origin and function of tumor-associated macrophages. *Cell. Mol. Immunol.* **12**, 1–4 (2015).

96. Shand, F. H. W. *et al.* Tracking of intertissue migration reveals the origins of tumor-infiltrating monocytes. *PNAS* **111**, 7771–7776 (2014).

97. Franklin, R. A. *et al.* The cellular and molecular origin of tumor-associated macrophages. *Cancer Immunol.* **344**, 921–926 (2014).

98. Laoui, D. *et al.* Tumor-associated macrophages in breast cancer : distinct subsets , distinct functions. *Int. J. Dev. Biol.* **55**, 861–867 (2011).

99. Pollard, J. W. Macrophages define the invasive microenvironment in breast cancer. *J. Leukoc. Biol.* **84**, 623–630 (2008).

100. Ohtaki, Y. *et al.* Stromal Macrophage Expressing CD204 is Associated with Tumor Aggressiveness in Lung Adenocarcinoma. *J. Thoractic Oncol.* **5**, 1507–1515 (2010).

101. Li, Y., James, M., Yang, Y. & Tian, C. The Role of Tumor-Associated Macrophages in Leukemia. *Acta Haematol.* **143**, 112–117 (2019).

102. Chen, S.-Y. *et al.* Organ-Specific Microenvironment Modifies Diverse Functional and Phenotypic Characteristics of Leukemia-Associated Macrophages in Mouse T Cell Acute Lymphoblastic Leukemia. *J. Immunol.* (2015). doi:10.4049/jimmunol.1400451

103. Zabel, B. A. *et al.* Chemoattractants, extracellular proteases, and the integrated host defense response. *Exp. Hematol.* **34**, 1021–1032 (2006).

104. Fernandez, E. J. & Lolis, E. Structure, Function, and Inhibition of Chemokines. *Annu. Rev. Pharmacol. Toxicol.* **42**, 469–499 (2002).

105. Rostene, W., Patrick, K. & Parsadaniantz, S. M. Chemokines : a new class of neuromodulator? *Nat. Rev. Neurosci.* **8**, 859–904 (2007).

106. Salamonsen, L. A., Hannan, N. J. & Dimitriadis, E. Cytokines and chemokines during human embryo implantation: Roles in implantation and early placentation. *Semin. Reprod. Med.* **25**, 437–444 (2007).

107. Li, M. & Ransohoff, R. M. The roles of chemokine CXCL12 in embryonic and brain tumor angiogenesis. *Semin. Cancer Biol.* **19**, 111–115 (2009).

108. Mantovani, A. *et al.* The chemokine system in cancer biology and therapy. *Cytokine Growth Factor Rev.* **21**, 27–39 (2010).

109. Crazzolara, R. *et al.* High expression of the chemokine receptor CXCR4 predicts extramedullary organ infiltration in childhood acute lymphoblastic leukaemia. *Br. J. Haematol.* **115**, 545–53 (2001).

110. Tarnowski, M. *et al.* CXCR7: A new SDF-1-binding receptor in contrast to normal CD34+ progenitors is functional and is expressed at higher level in human malignant hematopoietic cells. *Eur. J. Haematol.* **85**, 472–483 (2010).

111. Buonamici, S. *et al.* CCR7 signalling as an essential regulator of CNS infiltration in T-cell leukaemia. *Nature* **459**, 1000–4 (2009).

112. Arnold, J. M., Huggard, P. R., Cummings, M., Ramm, G. A. & Chenevix-Trench, G. Reduced expression of chemokine (C-C motif) ligand-2 (CCL2) in ovarian adenocarcinoma. *Br. J. Cancer* **92**, 2024–2031 (2005).

113. Valković, T., Lučin, K., Krstulja, M., Dobi-Babić, R. & Jonjić, N. Expression of monocyte chemotactic protein-1 in human invasive ductal breast cancer. *Pathol. Res. Pract.* **194**, 335–40 (1998).

114. Kleine-Lowinski, K., Gillitzer, R., Kühne-Heid, R. & Rösl, F. Monocyte-chemo-attractant-protein-1 (MCP-1)-gene expression in cervical intra-epithelial neoplasias and cervical carcinomas. *Int. J. Cancer* **82**, 6–11 (1999).

115. Nagarsheth, N., Wicha, M. S. & Zou, W. Chemokines in the cancer microenvironment and their relevance in cancer immunotherapy. *Nat. Rev. Immunol.* **17**, 559–572 (2017).

116. Höpken, U. E. & Rehm, A. Homeostatic chemokines guide lymphoma cells to tumor growth-promoting niches within secondary lymphoid organs. *J. Mol. Med.* **90**, 1237–1245 (2012).

117. Lippitz, B. E. Cytokine patterns in patients with cancer : a systematic review. *Lancet Oncol.* **14**, e218–e228 (2013).

118. Azab, A. K. *et al.* CXCR4 inhibitor AMD3100 disrupts the interaction of multiple myeloma cells with the bone marrow microenvironment and enhances their sensitivity to therapy. *Blood* **113**, 4341–4351 (2009).

119. Zhao, H. *et al.* CXCR4 over-expression and survival in cancer : A system review and meta-analysis. *Oncotarget* **6**, 5022–5040 (2014).

120. Kortesidis, A. *et al.* Stromal-derived factor-1 promotes the growth , survival , and development of human bone marrow stromal stem cells. *Blood* **105**, 3793–3801 (2005).

121. Juarez, J., Bradstock, K. F., Gottlieb, D. J. & Bendall, L. J. Effects of inhibitors of the chemokine receptor CXCR4 on acute lymphoblastic leukemia cells in vitro. *Leukemia* **17**, 1294–1300 (2003).

122. Burger, M. *et al.* Small peptide inhibitors of the CXCR4 chemokine receptor (CD184) antagonize the activation, migration, and antiapoptotic responses of CXCL12 in chronic lymphocytic leukemia B cells. *Blood* **106**, 1824–1830 (2005).

123. Juarez, J. *et al.* CXCR4 antagonists mobilize childhood acute lymphoblastic leukemia cells into the peripheral blood and inhibit engraftment. *Leukemia* **21**, 1249–1257 (2007).

124. Randhawa, S. *et al.* Effects of Pharmacological and Genetic Disruption of CXCR4 Chemokine Receptor Function in B-Cell Acute Lymphoblastic Leukaemia. *Physiol. Behav.* **174**, 425–436 (2016).

125. Grotendorst, G. R., Rahmanie, H. & Duncan, M. R. Combinatorial signaling pathways determine fibroblast proliferation and myofibroblast differentiation. *FASEB J.* **18**, 469–479 (2004).

126. Kalluri, R. & Zeisberg, M. Fibroblasts in cancer. *Nat. Rev. Cancer* **6**, 392–401 (2006).

127. Wiseman, B. S. & Werb, Z. Stromal Effects on Mammary Gland Development and Breast Cancer. *Science (80-.).* **296**, 1046–1050 (2002).

128. He, X. *et al.* Expression of galectin-1 in carcinoma-associated fibroblasts promotes gastric cancer cell invasion through upregulation of integrin ß1. *Cancer Sci.* **105**, 1402–1410 (2014).

129. Jung, E. *et al.* Galectin-1 expression in cancer-associated stromal cells correlates tumor invasiveness and tumor progression in breast cancer. *Int. J. Cancer* **120**, 2331–2338 (2007).

130. Saussez, S. *et al.* Adhesion / Growth-regulatory Tissue Lectin Galectin-1 in Relation to Angiogenesis / Lymphocyte Infiltration and Prognostic Relevance of Stromal Up-regulation in Laryngeal Carcinomas. *Anticancer Res.* **29**, 59–66 (2009).

131. Van den Brule, F. A., Waltregny, D. & Castronovo, V. Increased expression of galectin-1 in carcinoma- associated stroma predicts poor outcome in prostate carcinoma patients. *J. Pathol. J Pathol* **193**, 80–87 (2001).

132. Musumeci, M. *et al.* Control of tumor and microenvironment cross-talk by miR-15a and miR-16 in prostate cancer. *Oncogene* **30**, 4231–4242 (2011).

133. Bronisz, A. *et al.* Reprogramming of the tumour microenvironment by stromal PTEN-regulated miR-320. *Nat. Cell Biol.* **14**, 159–167 (2012).

134. Haubeiss, S. *et al.* Dasatinib reverses Cancer-associated Fibroblasts (CAFs) from primary Lung Carcinomas to a Phenotype comparable to that of normal Fibroblasts. *Mol. Cancer* **9**, 1–8 (2010).

135. Burt, R. *et al.* Activated stromal cells transfer mitochondria to rescue acute lymphoblastic leukemia cells from oxidative stress. *Blood* **134**, 1415–1429 (2019).

136. Jacoby, E., Chien, C. D. & Fry, T. J. Murine models of acute leukemia: Important tools in current pediatric leukemia research. *Front. Oncol.* **4**, 1–14 (2014).

137. Tiedemann, K., Chessells, J. M. & Sandland, R. M. Isolated testicular relapse in boys with acute lymphoblastic leukaemia: Treatment and outcome. *Br. Med. J.* **285**, 1614–1616 (1982).

138. Ortega, J. J., Javier, G. & Torán, N. Testicular infiltrates in children with acute lymphoblastic leukemia: A prospective study. *Med. Pediatr. Oncol.* **12**, 386–393 (1984).

139. Pui, C. H. *et al.* Elective testicular biopsy during chemotherapy for childhood leukaemia is of no clinical value. *Lancet* **326**, 410–412 (1985).

140. Reid, H. & Marsden, H. B. Gonadal infiltration in children with leukemia and lymphoma. *J. Clin. Pathol.* **33**, 722–729 (1980).

141. Jackson, H., Jackson, N. C., Bock, M. & Lendon, M. Testicular relapse in acute lymphoblastic leukaemia: studies with an experimental mouse model. *Br J Cancer* **49**, 73–78 (1984).

142. Jackson, H., Jackson, N. C., Bock, M. & Lendon, M. Testicular invasion and relapse and meningeal involvement in a rat t-cell leukaemia. *Br. J. Cancer* **50**, 617–624 (1984).

143. K. Jahnukainen, I. Morris, S. Roe, T.T. Salmi, A. M. & P. P. A rodent model for testicular involvement in acute lymphoblastic leukaemia. *Br. J. Cancer* **67**, 885–892 (1993).

144. Jahnukainen, K., Saari, T., Morris, I. D., Salmi, T. T. & Pöllänen, P. Regulation of testicular infiltration in acute lymphoblastic leukaemia of the rat. *Leukemia* **8**, 458–464 (1994).

145. Arnaud, M. P. *et al.* CD9, a key actor in the dissemination of lymphoblastic leukemia, modulating CXCR4-mediated migration via RAC1 signaling. *Blood* **126**, 1802–1812 (2015).

146. Velázquez-Avila, M. *et al.* High cortactin expression in B-cell acute lymphoblastic leukemia is associated with increased transendothelial migration and bone marrow relapse. *Leukemia* **33**, 1337–1348 (2019).

147. Kauerhof, A. C. *et al.* Investigation of activin A in inflammatory responses of the testis and its role in the development of testicular fibrosis. *Hum. Reprod.* **34**, 1536–1550 (2019).

148. Kamenov, B. & Longenecker, B. M. Further Evidence for the existence of homing receptors on murine leukemia cells which mediate adherence to normal bone marrow stromal cells. *Leuk. Res.* **9**, 1529–1537 (1985).

149. Ninomiya, M. *et al.* Homing, proliferation and survival sites of human leukemia cells in vivo in immunodeficient mice. *Leukemia* **21**, 136–142 (2007).

150. Corcione, A. *et al.* Chemokine receptor expression and function in childhood acute lymphoblastic leukemia of B-lineage. *Leuk. Res.* **30**, 365–372 (2006).

151. Ribeiro, D., Melão, A. & Barata, J. T. IL-7R-mediated signaling in T-cell acute lymphoblastic leukemia. *Adv. Biol. Regul.* **53**, 211–222 (2013).

152. Alsadeq, A. *et al.* IL7R is associated with CNS infiltration and relapse in pediatric B-cell precursor acute lymphoblastic leukemia. *Blood* (2018). doi:10.1182/blood-2018-04-844209

153. Simmons, P. J., Zannettino, A., Gronthos, S. & Leavesley, D. Potential Adhesion Mechanisms for Localisation of Potential Adhesion Mechanisms for Localisation of Haemopoietic Progenitors to Bone Marrow Stroma. *Leuk. Lymphoma* **12**, 353–363 (1994).

154. Mengarelli, A. *et al.* Adhesion Molecule Expression , Clinical Features and Therapy Outcome in Childhood Acute Lymphoblastic Leukemia. *Leuk. Lymphoma* **40**, 625–630 (2001).

155. Zittermann, S. I. *et al.* Modulation of CD44 in acute lymphoblastic leukemia identifies functional and phenotypic differences of human B cell precursors. *Eur. J. Haematol.* **66**, 377–382 (2001).

156. Meerschaert, J. & Furie, M. B. The adhesion molecules used by monocytes for migration across endothelium include CD11a/CD18, CD11b/CD18, and VLA-4 on monocytes and ICAM-1, VCAM-1, and other ligands on endothelium. *J. im* **154**, 4099–4112 (1995).

157. Shishido, S., Bönig, H. & Kim, Y. Role of integrin alpha4 in drug resistance of leukemia. *Front. Oncol.* **4**, 1–10 (2014).

158. Ede, B. C., Asmaro, R. R., Moppett, J. P., Diamanti, P. & Blair, A. Investigating chemoresistance to improve sensitivity of childhood T-cell acute lymphoblastic leukemia to parthenolide. *Haematologica* **103**, 1493–1501 (2018).

159. Pal, D. *et al.* Long-term in vitro maintenance of clonal abundance and leukaemia-initiating potential in acute lymphoblastic leukaemia. *Leukemia* **30**, 1691–1700 (2016).

160. De Rooij, B. *et al.* Acute lymphoblastic leukemia cells create a leukemic niche without affecting the CXCR4/CXCL12 axis. *Haematologica* **102**, 389–393 (2017).

161. Pham, H., Tonai, R., Wu, M., Birtolo, C. & Chen, M. CD73, CD90, CD105 and cadherin-11 RT-PCR screening for mesenchymal stem cells from cryopreserved human cord tissue. *Int. J. Stem Cells* **11**, 26–38 (2018).

162. Ramos, T. L. *et al.* MSC surface markers (CD44, CD73, and CD90) can identify human MSC-derived extracellular vesicles by conventional flow cytometry. *Cell Commun. Signal.* **14**, 1–14 (2016).

163. Harkness, L., Zaher, W., Ditzel, N., Isa, A. & Kassem, M. CD146/MCAM defines functionality of human bone marrow stromal stem cell populations. *Stem Cell Res. Ther.* **7**, 1–13 (2016).

164. Boutter, J., Huang, Y., Marovca, B. & Vonderheit, A. Image-based RNA interference screening reveals an individual dependence of acute lymphoblastic leukemia on stromal cysteine support. *Oncotarget* **5**, 11501 (2014).

165. Manabe, B. A., Coustan-smith, E., Behm, F. G., Raimondi, S. C. & Campana, D. Bone Marrow-Derived Stromal Cells Prevent Apoptotic Cell Death in B-Lineage Acute Lymphoblastic Leukemia. *Blood* **79**, 2370–2377 (1992).

166. Hatse, S., Princen, K., Bridger, G., Clercq, E. De & Schols, D. Chemokine receptor inhibition by AMD3100 is strictly confined to CXCR4. *FEBS Lett.* **527**, 255–262 (2002).

167. Jinek, M. *et al.* A programmable dual-RNA-guided DNA endonuclease in adaptive bacterial immunity. *Science* **337**, 816–21 (2012).

168. Frungieri, M. B. *et al.* Number, distribution pattern, and identification of macrophages in the testes of infertile men. *Fertil. Steril.* **78**, 298–306 (2002).

169. Pollanen, P. & Niemi, M. Immunohistochemical identification of macrophages, lymphoid cells and HLA-antigens in the human testis. *Int. J. Androl.* **10**, 37–42 (1987).

170. Zinn, K. R. *et al.* Noninvasive bioluminescence imaging in small animals. *ILAR J.* **49**,

103–115 (2008).

171. Lai, Y. *et al.* Current status and perspectives of patient-derived xenograft models in cancer research. *J. Hematol. Oncol.* **10**, 1–14 (2017).

172. Peled, A. *et al.* Dependence of Human Stem Cell Engraftment and Repopulation of NOD:SCID Mice on CXCR4. *Science (80-.).* **283**, 845–848 (1999).

173. Pals, S. T., De Gorter, D. J. J. & Spaargaren, M. Lymphoma dissemination: The other face of lymphocyte homing. *Blood* **110**, 3102–3111 (2007).

174. Dürig, J., Schmücker, U. & Dührsen, U. Differential expression of chemokine receptors in B cell malignancies. *Leukemia* **15**, 752–6 (2001).

175. Wong, S. W. J. & Fulcher, D. A. Chemokine receptor expression in B-cell lymphoproliferative disorders. *Leuk. Lymphoma* **45**, 2491–2496 (2004).

176. Pulte, D. *et al.* Survival of adults with acute lymphoblastic leukemia in Germany and the United States. *PLoS One* **9**, e85554 (2014).

177. Corcione, A. *et al.* Chemokine receptor expression and function in childhood acute lymphoblastic leukemia of B-lineage. *Leuk. Res.* **30**, 365–372 (2006).

178. Moreno, M. J. *et al.* CXCR4 expression enhances diffuse large B cell lymphoma dissemination and decreases patient survival. *J. Pathol.* **235**, 445–455 (2015).

179. Barata, J. T., Durum, S. K. & Seddon, B. Flip the coin: IL-7 and IL-7R in health and disease. *Nat. Immunol.* **20**, 1584–1593 (2019).

180. Alsadeq, A. *et al.* IL7R is associated with CNS infiltration and relapse in pediatric B-cell precursor acute lymphoblastic leukemia. *Blood* **132**, 1614–1617 (2018).

181. Cario, G. *et al.* High interleukin-15 expression characterizes childhood acute lymphoblastic leukemia with involvement of the CNS. *J. Clin. Oncol.* **25**, 4813–4820 (2007).

182. Williams, M. T. S. *et al.* The ability to cross the blood-cerebrospinal fluid barrier is a generic property of acute lymphoblastic leukemia blasts. *Blood* **127**, 1998–2006 (2016).

183. Alsadeq, A. & Schewe, D. M. Acute lymphoblastic leukemia of the central nervous system: On the role of PBX1. *Haematologica* **102**, 611–613 (2017).

184. Lundmark, F. *et al.* Variation in interleukin 7 receptor α chain (IL7R) influences risk of multiple sclerosis. *Nat. Genet.* **39**, 1108–1113 (2007).

185. Mazzucchelli, R. I. *et al.* Visualization and identification of IL-7 producing cells in reporter mice. *PLoS One* **4**, (2009).

186. Hayashi, S. I. *et al.* Stepwise progression of B lineage differentiation supported by interleukin 7 and other stromal cell molecules. *J. Exp. Med.* **171**, 1683–1695 (1990).

187. Nagasawa, T. CXCL12/SDF-1 and CXCR4. *Front. Immunol.* **6**, 10–12 (2015).

188. Abdelrasoul, H. *et al.* Synergism between IL7R and CXCR4 drives BCR-ABL induced transformation in Philadelphia chromosome-positive acute lymphoblastic leukemia. *Nat. Commun.* **11**, 395–410 (2020).

189. Arico, M. Outcome of treatment in children with Philadelphia chromosome-positive acute lymphoblastic leukemia. *N. Engl. J. Med.* **342**, 998–1006 (2000).

190. Schultz, K. R. *et al.* Long-term follow-up of imatinib in pediatric Philadelphia chromosome-positive acute lymphoblastic leukemia: Children's oncology group study AALL0031. *Leukemia* **28**, 1467–1471 (2014).

191. Nishii, K. *et al.* Survival of human leukaemic B-cell precursors is supported by stromal

cells and cytokines: Association with the expression of bcl-2 protein. *Br. J. Haematol.* **105**, 701–710 (1999).

192. van den Berk, L. C. J. *et al.* Disturbed CXCR4/CXCL12 axis in paediatric precursor B-cell acute lymphoblastic leukaemia. *Br. J. Haematol.* **166**, 240–249 (2014).

193. Sieber, S. *et al.* Bone marrow-on-a-chip: Long-term culture of human haematopoietic stem cells in a three-dimensional microfluidic environment. *J. Tissue Eng. Regen. Med.* **12**, 479–489 (2018).

194. Bradstock, K. F. *et al.* Effects of the chemokine stromal cell-derived factor-1 on the migration and localization of precursor-B acute lymphoblastic leukemia cells within bone marrow stromal layers. *Leukemia* **14**, 882–888 (2000).

195. Gilbert, D. *et al.* Clinical and biological significance of CXCL12 and CXCR4 expression in adult testes and germ cell tumours of adults and adolescents. *J. Pathol. J Pathol* **217**, 94–102 (2009).

196. Horwich, A., Shipley, J. & Huddart, R. Testicular germ-cell cancer. *Lancet* **367**, 754–765 (2006).

197. McIver, S. C. *et al.* The chemokine CXCL12 and its receptor CXCR4 are implicated in human seminoma metastasis. *Andrology* **1**, 517–529 (2013).

198. Lawrence, T. & Natoli, G. Transcriptional regulation of macrophage polarization: Enabling diversity with identity. *Nat. Rev. Immunol.* **11**, 750–761 (2011).

199. Mantovani, A., Sozzani, S., Locati, M., Allavena, P. & Sica, A. Macrophage polarization: Tumor-associated macrophages as a paradigm for polarized M2 mononuclear phagocytes. *Trends Immunol.* **23**, 549–555 (2002).

200. Komohara, Y. *et al.* Clinical significance of CD163+ tumor-associated macrophages in patients with adult T-cell leukemia/lymphoma. *Cancer Sci.* **104**, 945–951 (2013).

201. Chen, S.-Y. *et al.* Organ-Specific Microenvironment Modifies Diverse Functional and Phenotypic Characteristics of Leukemia-Associated Macrophages in Mouse T Cell Acute Lymphoblastic Leukemia. *J. Immunol.* **194**, 2919–29 (2015).

202. Jafarzadeh, N. *et al.* Alteration of cellular and immune-related properties of bone marrow mesenchymal stem cells and macrophages by K562 chronic myeloid leukemia cell derived exosomes. *J. Cell. Physiol.* **234**, 3697–3710 (2019).

203. Mantovani, A. & Allavena, P. The interaction of anticancer therapies with tumor-associated macrophages. *J. Exp. Med.* **212**, 435–445 (2015).

204. Bronte, V. & Murray, P. J. Understanding local macrophage phenotypes in disease: Modulating macrophage function to treat cancer. *Nat. Med.* **21**, 117–119 (2015).

205. Arlauckas, S. P. *et al.* Arg1 expression defines immunosuppressive subsets of tumor-associated macrophages. *Theranostics* **8**, 5842–5854 (2018).

206. Yang, X. *et al.* Hepatic leukemia-associated macrophages exhibit a pro-inflammatory phenotype in Notch1-induced acute T cell leukemia. *Immunobiology* **223**, 73–80 (2018).

207. Van Dyken, S. J. & Locksley, R. M. Interleukin-4- and interleukin-13-mediated alternatively activated macrophages: roles in homeostasis and disease. *Annu Rev Immunol.* **31**, 317–343 (2013).

208. Mauer, J. *et al.* Interleukin-6 signaling promotes alternative macrophage activation to limit obesity-associated insulin resistance and endotoxemia. *Nat. Immunol.* **29**, 997–1003 (2012).

209. Kacinski, B. M. CSF-1 and its receptor in ovarian, endometrial and breast cancer. *Ann. Med.* **27**, 79–85 (1995).

210. Kirma, N. *et al.* Elevated expression of the oncogene c-fms and its ligand, the macrophage colony-stimulating factor-1, in cervical cancer and the role of transforming growth factor-β1 in inducing c-fms expression. *Cancer Res.* **67**, 1918–1926 (2007).

211. Janowska-Wieczorek, A. *et al.* Increased circulating colony-stimulating factor-1 in patients with preleukemia, leukemia, and lymphoid malignancies. *Blood* **77**, 1796–1803 (1991).

212. Liao, J. *et al.* Diverse in vivo effects of soluble and membrane-bound M-CSF on tumor-associated macrophages in lymphoma xenograft model. *Oncotarget* **7**, 1354–1366 (2015).

213. Aharinejad, S. *et al.* Elevated CSF1 serum concentration predicts poor overall survival in women with early breast cancer. *Endocr. Relat. Cancer* **20**, 777–783 (2013).

214. Mroczko, B. *et al.* Serum macrophage-colony stimulating factor levels in colorectal cancer patients correlate with lymph node metastasis and poor prognosis. *Clin. Chim. Acta* **380**, 208–212 (2007).

215. Komohara, Y. *et al.* Potential anti-lymphoma effect of M-CSFR inhibitor in adult T-cell leukemia/lymphoma. *J. Clin. Exp. Hematop.* **58**, 152–160 (2018).

216. Zhang, F. *et al.* TGF-β induces M2-like macrophage polarization via SNAILmediated suppression of a pro-inflammatory phenotype. *Oncotarget* **7**, 52294–52306 (2016).

217. Ohri, C. M., Shikotra, A., Green, R. H., Waller, D. A. & Bradding, P. Macrophages within NSCLC tumour islets are predominantly of a cytotoxic M1 phenotype associated with extended survival. *Eur. Respir. J.* **33**, 118–126 (2009).

218. Yang, X. *et al.* Repolarizing heterogeneous leukemia-associated macrophages with more M1 characteristics eliminates their pro-leukemic effects. *Oncoimmunology* **7**, e1412910 (2018).

219. Romano, F. *et al.* The contractile phenotype of peritubular smooth muscle cells is locally controlled: Possible implications in male fertility. *Contraception* **72**, 294–297 (2005).

220. Díez-Torre, A., Silván, U., Moreno, P., Gumucio, J. & Aréchaga, J. Peritubular myoid cell-derived factors and its potential role in the progression of testicular germ cell tumours. *Int. J. Androl.* **34**, 252–265 (2011).

221. Verhoeven, G., Hoeben, E. & De Gendt, K. Peritubular cell-Sertoli cell interactions: factors involved in PmodS activity. *Andrologia* **32**, 42–45 (2000).

222. Mylonas, I. *et al.* Inhibin/activin subunits (inhibin-α, -βA and -βB) are differentially expressed in human breast cancer and their metastasis. *Oncol. Rep.* **13**, 81–88 (2005).

223. Balanathan, P. *et al.* Elevated level of inhibin-α subunit is pro-tumourigenic and pro-metastatic and associated with extracapsular spread in advanced prostate cancer. *Br. J. Cancer* **100**, 1784–1793 (2009).

224. Habashy, H. O. *et al.* Transferrin receptor (CD71) is a marker of poor prognosis in breast cancer and can predict response to tamoxifen. *Breast Cancer Res. Treat.* **119**, 283–293 (2010).

225. Konrad, L., Albrecht, M. & Renneberg, H. Transforming growth factor-beta2 mediates mesenchymal-epithelial interactions of testicular somatic cells. *Endocrinology* **141**, 3679–3686 (2000).

226. Schell, C., Albrecht, M., Mayer, C., Schwarzer, J. U. & Frungieri, M. B. Exploring Human Testicular Peritubular Cells : Identification of Secretory Products and Regulation by Tumor Necrosis Factor-a. *Endocrinology* **149**, 1678–1686 (2008).

227. Fujimoto, H. *et al.* Stromal MCP-1 in mammary tumors induces tumor-associated macrophage infiltration and contributes to tumor progression. *Int. J. Cancer* **125**, 1276–1284 (2009).

228. Gerard, C. & Rollins, B. J. Chemokines and disease. *Nat. Immunol.* **2**, 108–115 (2001).

229. Wang, D. Z., Zhou, X. H., Yuan, Y. L. & Zheng, X. M. Optimal dose of busulfan for depleting testicular germ cells of recipient mice before spermatogonial transplantation. *Asian J. Androl.* **12**, 263–270 (2010).

230. Shultz, L. D. *et al.* Human cancer growth and therapy in immunodeficient mouse models. *Cold Spring Harb. Protoc.* **2014**, 694–708 (2014).

231. Cao, X. *et al.* Defective lymphoid development in mice lacking expression of the common cytokine receptor γ chain. *Immunity* **2**, 223–238 (1995).

232. Shen, W., Bendall, L. J., Gottlieb, D. J. & Bradstock, K. F. The chemokine receptor CXCR4 enhances integrin-mediated in vitro adhesion and facilitates engraftment of leukemic precursor-B cells in the bone marrow. *Exp. Hematol.* **29**, 1439–1447 (2001).

233. Liles, W. C. *et al.* Mobilization of hematopoietic progenitor cells in healthy volunteers by AMD3100, a CXCR4 antagonist. *Blood* **102**, 2728–2730 (2003).

234. Sipkins, D. A. *et al.* In vivo imaging of specialized bone marrow endothelial microdomains for tumour engraftment. *Nature* **435**, 969–973 (2005).

235. Zhang, Y. *et al.* Targeting primary acute myeloid leukemia with a new CXCR4 antagonist IgG1 antibody (PF-06747143). *Sci. Rep.* **7**, 1–13 (2017).

236. Becker, P. *et al.* Targeting the CXCR4 Pathway: Safety, Tolerability and Clinical Activity of Ulocuplumab (BMS-936564), an Anti-CXCR4 Antibody, in Relapsed/Refractory Acute Myeloid Leukemia. *Blood* **124**, 386 (2014).

237. Luecken, M. D. & Theis, F. J. Current best practices in single-cell RNA-seq analysis: a tutorial. *Mol. Syst. Biol.* **15**, e8746 (2019).

238. Arnol, D., Schapiro, D., Bodenmiller, B., Saez-Rodriguez, J. & Stegle, O. Modeling Cell-Cell Interactions from Spatial Molecular Data with Spatial Variance Component Analysis. *Cell Rep.* **29**, 202-211.e6 (2019).

239. Green, C. D. *et al.* A Comprehensive Roadmap of Murine Spermatogenesis Defined by Single-Cell RNA-Seq. *Dev. Cell* **46**, 651–667 (2018).

6 Appendix

Acknowledgements

An dieser Stelle möchte ich mich bei all jenen bedanken, die mich in den letzten Jahren beim Erstellen dieser Arbeit unterstützt und begleitet haben.

Besonders danken möchte ich Dr. Uta Höpken und Dr. Cornelia Eckert, die mich in Ihren Arbeitsgruppen aufgenommen haben. Von Beginn an wurde ich exzellent betreut und konnte stets auf die wissenschaftliche Expertise der beiden bauen. Der intensive Austausch mit Dr. Höpken und Dr. Eckert hat maßgeblich zum Gelingen dieser Arbeit beigetragen.

Ebenfalls bedanken möchte ich mich bei Prof. Dr. Ana Pombo, die meine Arbeit von Seiten der Humboldt-Universität zu Berlin betreute und mir bei den jährlichen Committee Meetings hilfreiche Ratschläge für den weiteren Verlauf der Arbeit geben konnte.

Als dritten Gutachter meiner Arbeit möchte ich auch Prof. Dr. Johannes Schulte für seine Bereitschaft danken, meine Arbeit mit seinem Blick für die klinischen Aspekte des Themas zu bewerten.

Natürlich möchte ich auch allen Kolleg*innen der AG Höpken, AG Rehm und AG Eckert danken. Das gute Arbeitsklima trug dazu bei, dass ich all die Jahre gerne ins Labor kam und sowohl den wissenschaftlichen als auch privaten Austausch genießen konnte. Mein besonderer Dank gilt Madlen Pfau und Kerstin Krüger, die mir besonders zu Beginn neue Methoden beibrachten und mir auch im weiteren Verlauf bei der praktischen Arbeit zur Seite standen. Auch meinen beiden Doktorandinnen-Kolleginnen Janina Pfeilschifter und Maria Zschummel möchte ich für die vielen Gespräche unter Leidensgenossinnen danken. Es war schön, den Weg mit euch gemeinsam zu gehen.

Ebenfalls möchte ich mich bei Yvonne McCabe bedanken, die meine Arbeit auf Grammatik und Rechtschreibung geprüft und ihr Honorar dem Verein KINDerLEBEN (Verein zur Förderung der Klinik für krebskranke Kinder e.V. Berlin) gespendet hat.

Der größte Dank gilt natürlich meiner Familie und meinen Freunden, die mich von Beginn an unterstützt haben. Meiner Mutter, die immer an mich geglaubt hat, und meinem Mann, der auch angesichts meiner zwischenzeitlichen Zweifel überzeugt war, dass alles einen erfolgreichen Abschluss finden würde.